DISSERTATION

Submitted to the Combined Faculties for the Natural Sciences and Mathematics of the Ruperto-Carola University of Heidelberg, Germany, for the degree of Doctor of Natural Sciences

Presented by

M. Sc. Himanshu Soni

Born in Meerut, India

Date of Oral Examination: 11th September, 2019

Deciphering Potential Role of Unfolded Protein Response in Glioblastoma

Referees: Prof. Dr. Karsten Rippe

Dr. Björn Tews

This PhD project has been conducted in two laboratories within the DKFZ. The initial phase of the thesis was done under the supervision of Dr. Björn Tews (Molecular Mechanism of Tumor Invasion; V077) from April, 2015 until September, 2017. The remaining work was conducted under the supervision of Dr. Violaine Goidts (Brain Tumor Translational Targets; B067) from October 2017 until present.

Declaration

I hereby declare that I have written the submitted dissertation “Deciphering Potential Role of Unfolded Protein Response in Glioblastoma” myself and in this process have not used any other sources than those expressly indicated.

I hereby declare that I have not applied to be examined at any other institution, nor have I used the dissertation in this or any other form at any other institution as an examination paper, nor submitted it to any other faculty as a dissertation.

Himanshu Soni

Contents

1. Introduction 1
1.1 Tumors of central nervous system (CNS) 1
1.2 Glioblastoma 4
1.2.1 Major genetic alterations in glioblastoma 4
1.2.2 Subtype classification of glioblastoma 5
1.2.3 Current treatment regimes against gliomas 6
1.3 Unfolded Protein Response 7
1.3.1 Effectors of the UPR 8
1.3.2 Hypoxia-mediated UPR activation 13
1.3.3 UPR and Diseases 15
1.3.4 UPR in cancer 15
1.4 Hallmarks of Cancer 17
1.4.1 Angiogenesis: A major hallmark of glioblastoma 18
1.5 Peptidyl-glycine alpha-amidating monooxygenase 19
1.6 Aim of the Study 22
2. Materials & Methods 23
2.1 Materials 23
2.1.1 Antibodies 23
2.1.2 Buffers 23
2.1.3 Bacterial Culture Media 24
2.1.4 Biochemical Reagents 24
2.1.5 Cell Culture Reagents and Materials 25
2.1.6 *In vivo* Reagents and Materials 26
2.1.7 Mice 26
2.1.8 Cell Lines 26
2.1.9 Other Cell Lines 26
2.1.10 Bacteria 27

2.1.11 Enzymes 27
2.1.12 Databases 27
2.1.13 Equipment 27
2.1.14 Kits 28
2.1.15 Other Material 28
2.1.16 Plasmids 29
2.1.17 Generated Plasmids 29
2.1.18 List of primers and shRNA target sequences 29
2.1.19 Software 30
2.2 Methods 30
2.2.1 Cell culture 30
2.2.2 Lentivirus production 31
2.2.3 pLKO.1 shRNA Cloning 31
2.2.4 Immuno-blotting 31
2.2.5 Real-time PCR 32
2.2.6 Mass spectrometry experiment design 32
2.2.7 Proteomics sample preparation 32
2.2.8 LC-MS/MS analysis 33
2.2.9 Label free data analysis 33
2.2.10 Data availability 34
2.2.11 PHM activity 34
2.2.12 Immunofluorescence 34
2.2.13 Dynabeads immunoprecipitation 35
2.2.14 Extracellular vesicle isolation 35
2.2.15 Electron Microscopy 35
2.2.16 TCA protein precipitation 36
2.2.17 Total binding affinity analysis for PAM promoters 36
2.2.18 Tube formation assay 36
2.2.19 Animal experiments 37

2.2.20 Bioluminescence imaging 37
2.2.21 Statistics 37
3. Results 38
3.1 Methodology to decipher the role of hypoxia-induced UPR in expression of extracellular proteins 38
3.2 Characterization of UPR induction in glioblastoma using artificial ER stress inducers 39
3.2.1 Activation of UPR pathway proteins: IRE1 and PERK 39
3.2.2 Small molecular inhibitors of UPR sensor proteins 41
3.2.3 IRE1-mediated regulation of invasive markers in glioblastoma 42
3.3 Selective activation of UPR sensors under hypoxia in glioblastoma 43
3.3.1 PERK-mediated secretion of proteins in glioblastoma 45
3.3.2 PERK regulates PAM independent of PERK kinase activity 46
3.3.3 PERK is the only eIF2α kinase affecting expression of *PAM* in glioblastoma 48
3.3.4 PERK kinase activity is essential to generate PAM sfCD domain possibly via a physical interaction 50
3.3.5 PERK and HIF1α regulates expression of PAM via AP-1 transcription factor 52
3.3.6 In silico transcription binding affinity (TBA)-based prediction of potential transcription factors regulating PAM mRNA expression 55
3.3.7 Differential expression of PAM in glioblastoma subtypes and its relation to AP-1 transcription factor. 57
3.3.8 PAM regulates angiogenesis *in vitro* 59
3.3.9 PAM regulates tumor progression *in vivo*. 61
4. Discussion 63
5. References 71
6. Publications 97
7. Appendix 98
8. Acknowledgements 100

Figures

Figure 1. Worldwide estimation of number of deaths caused by different types of tumors as a percentage of total number of cancer deaths (2018)[2]. 1
Figure 2 The unfolded protein response (UPR) pathway. 9
Figure 3. Structure of UPR sensor proteins[126]. 13
Figure 4. Hypoxia-regulated pathways. 14
Figure 5. Role of UPR during different stages of tumor development. 17
Figure 6. PAM catalyzes the activation of neuropeptides. 19
Figure 7. PAM splice variants. 20
Figure 8. PAM trafficking through biosynthetic and endocytic pathways. 21
Figure 9. Experimental strategy to determine the UPR-regulated angiogenic targets under hypoxia in glioblastoma cell model. 38
Figure 10. ER stress induced IRE1α activation in glioblastoma cells. 40
Figure 11. ER stress induced PERK activation in LN308 glioblastoma cells. 41
Figure 12. Small molecule inhibitors of UPR pathway. 42
Figure 13. IRE1α-mediated regulation of extracellular proteins in LN308 glioblastoma cells. 43
Figure 14. Activation of PERK and ATF6α branch of UPR in glioblastoma cells under hypoxia. 44
Figure 15. Reduced activation of IRE1 under hypoxia in glioblastoma. 44
Figure 16. Volcano plot representing the regulated secretory proteins from LN308 glioblastoma cells under hypoxic conditions for 72 hours without (left) and with GSK2606414 (right). 45
Figure 17. PERK regulates PAM at mRNA level independent of PERK kinase activity. 47
Figure 18. PERK regulates PAM activity under hypoxia. 48
Figure 19. PERK is the only eIF2α kinase affecting expression of PAM in glioblastoma under hypoxia. 49
Figure 20. *PAM* mRNA increase under hypoxia is NRF2-independent. 50
Figure 21. PERK activation causes accumulation of the PAM sfCD fragment, possibly via a physical interaction. 51
Figure 22. PERK does not phosphorylate PAM at Serine 937 and Serine 949 residue. 52
Figure 23. *PAM* mRNA increases under hypoxia in glioblastoma. 53
Figure 24. PAM is also secreted in extracellular vesicles from LN308 glioblastoma cells under hypoxia. 54
Figure 25. *PAM* mRNA increase under hypoxia is HIF1α dependent. 55
Figure 26. Total binding affinities of the PAM promoter. 57
Figure 27. Differential expression of PAM in glioblastoma subtypes and its relation to AP-1 transcription factor. 58
Figure 28. 4P3BA does not effectively reduce PHM activity in LN308 glioblastoma cells. 59
Figure 29. PERK and PAM support blood vessel formation in glioblastoma *in vitro*. 60

FIGURES

Figure 30. Active ADM increases number of junctions and meshes formed by HUVECs *in vitro*. 61
Figure 31. PAM expression is necessary for progression of glioblastoma *in vivo*. 62
Figure 32. PERK is necessary for the expression of PAM in glioblastoma. 68

Tables

Table 1 Major glioma entities according to 2016 WHO classification of CNS tumors including the major genetic alterations they bear. 3
Table 2. List of proteins found to be significantly regulated by PERK under hypoxia. 46
Table 3. Log2- and z-transformed TBAs, for 579 TF binding motifs from JASPAR, for the promoter of PAM transcripts (NM_138821). 56

Summary

The unfolded protein response (UPR) plays a significant role in reducing the burden of protein from the endoplasmic reticulum (ER) of cells by enhancing the expression of factors which facilitate protein folding, such as chaperones and isomerases, while simultaneously reducing translation and initiating ER-associated degradation pathways. When confronted with adverse conditions in their microenvironment, tumor cells need to adapt their proteomes by producing and secreting factors which support their survival and growth. This results in the generation of ER stress conditions that leads to activation of the UPR pathway. UPR has been linked to almost every type of cancer including grade IV glioma, glioblastoma, a devastating disease with patients surviving on average only 15 months after diagnosis. One of the reasons for this poor prognosis is the ability of glioblastoma to induce early angiogenesis followed by invasion of the normal brain parenchyma. This PhD thesis focuses on understanding how UPR is regulated in glioblastoma and how this contributes to tumor angiogenesis. To this end, the UPR pathway in glioblastoma cell lines was first characterized using artificial ER stress inducers. As hypoxia is the leading physiological inducer of UPR while also regulating the early events of glioblastoma progression, the UPR branches that are activated under hypoxia were investigated. PKR-like kinase (PERK), a UPR sensor protein which controls the translation machinery of tumor cells under ER stress was examined in detail, and it was determined whether this protein is involved in the regulation of expression and secretion of any angiogenic proteins in glioblastoma. For this purpose, proteomic analysis of the conditioned media of LN308 glioblastoma cells with and without PERK inhibition was performed and PERK-regulated secretory factors were identified. Among the hits was Peptidyl-glycine alpha-amidating monooxygenase (PAM), a transmembrane protein which plays a role in the rate-limiting final step of the activation of various neuropeptides, including the angiogenic peptide adrenomedullin (ADM). PAM was validated as a pro-angiogenic factor for glioblastoma, its regulation by hypoxia (HIF1α) was characterized, and the importance of PERK kinase activity for the generation of a small soluble cytosolic cleaved product of PAM (PAM-sfCD), which has the ability to induce potential gene expression changes favoring glioblastoma progression, was shown. PAM was also found to have mesenchymal-subtype specific expression in glioblastoma, where AP-1 was found to be the leading transcription factor regulating *PAM* transcripts. The *in vivo* study in this thesis illustrates the importance of PAM for glioblastoma growth kinetics in an orthotopic xenotransplanted mouse model, revealing an increased overall survival of animals upon PAM knockdown. Supporting this, clinical data suggest better survival of glioblastoma patients with lower expression of *PAM*.

Thus, this work reveals the importance of the PERK-mediated expression and post-translational modification of PAM for angiogenesis and tumor progression in glioblastoma, introducing the protein as a novel anti-angiogenic therapeutic target in this deadly disease.

Zusammenfassung

Die Reaktion auf entfaltete Proteine (engl. Unfolded protein response, UPR) spielt eine bedeutende Rolle bei der Verringerung der Proteinausschüttung aus dem endoplasmatischen Retikulum (ER), indem unter anderem die Expression von Chaperonen und Isomerasen verstärkt wird, während gleichzeitig die Translation reduziert und ER-assoziierte Abbau Wege initiiert werden.

Aufgrund veränderter Bedingungen in der unmittelbaren Umgebung, passen Tumorzellen ihr Proteom durch die Produktion und Sekretion bestimmter Faktoren, die das Überleben und das Wachstum unterstützen, an. Hierzu zählt beispielweise die Bildung eines Stresszustands des ER, der zur Aktivierung des UPR-Signalwegs führt. Die Aktivierung des UPR lässt sich bei fast jeder Krebsart, einschließlich dem Glioblastom, einem Gliom Grad IV, dessen Standardtherapie aus Tumorresektion gefolgt von Chemo- und Radiotherapie besteht, finden. Die schlechte Prognose des Glioblastoms lässt sich durch den frühen Beginn der Angiogenese, die zur Invasion in das gesunde Gehirnparenchym führt, erklären.

Die vorliegende Doktorarbeit beschäftigt sich mit der Fragestellung, wie UPR-Aktivierung im Glioblastom reguliert wird und diese zur Tumorangiogenese beiträgt. Hierzu wurde zunächst der UPR-Signalweg in verschiedenen Glioblastomzelllinien mit ER-Stress induzierenden Reagenzien charakterisiert. Mittels Hypoxie, welches zu den stärksten physiologischen UPR-Auslösern zählt und zusätzlich die frühen Ereignisse der Glioblastomentwicklung reguliert, wurden die aktivierten UPR-Signalwege identifiziert. In diesem Zusammenhang wurde das UPR-Sensorprotein PKR-like Kinase (PERK), welches die Translation in Tumorzellen unter ER-Stress steuert, charaktisiert und der Effekt auf die Regulierung eines angiogenen Proteins in Glioblastomen untersucht. Um dies herauszufinden, wurde eine Proteomanalyse des konditionierten Mediums von LN308-Glioblastomzellen mit bzw. ohne PERK-Inhibierung durchgeführt und die von PERK regulierten sekretorische Faktoren identifiziert. Dabei wurde das Transmembranprotein Peptidyl-Glycin-alpha-amidierende Monooxygenase (PAM), das eine signifikante Rolle im geschwindigkeitsbestimmenden letzten Schritt der Aktivierung von Neuropeptiden und Adrenomedullin (ADM) spielt sowie an der Angiogenese beteiligt ist, gefunden. PAM wurde als pro-angiogener Faktor in Glioblastomen validiert, dessen Regulierung durch Hypoxie (HIF1α) charakterisiert und die Bedeutung der PERK-Kinase-Aktivität für die Entstehung eines löslichen Spaltprodukts von PAM (PAM-sfCD) im Cytosol gezeigt. PAM-sfCD trägt zu einer Veränderung der Genexpression zugunsten der Entwicklung von Glioblastomen bei. Zusätzlich weist PAM eine erhöhte Proteinexpression im mesenchymalen Subtyp von Glioblastomen auf, wobei AP-1 der ausschlaggebende Faktor bei der Regulierung der Transkription von PAM ist. Eine in vivo Studie veranschaulicht die Bedeutung von PAM für das Glioblastomwachstum an Hand eines orthotopisch, xenotransplantierten Mausmodell und zeigt ein verlängertes Überleben von Tieren mit PAM-Knockdown. Dies wird von klinischen Daten, welche das

verlängerte Überleben von Glioblastompatienten mit niedrigerer PAM Expression in Verbindung bringen, unterstützt.

Die vorliegende Doktorarbeit hebt daher die Bedeutung der PERK-vermittelte Expression und der posttranslationalen Modifikation von PAM mit einem Fokus auf die angiogenen Vorteile hinsichtlich der Tumorentwicklung, hervor und unterstreicht somit die Relevanz von PAM als anti-angiogenes Ziel für die Therapie von Glioblastomen.

Abbreviations

4EBP1	Eukaryotic translation initiation factor 4E binding protein 1
ADM	Adrenomedullin
AIM-2	Absent in melanoma 2
ALS	Amyotrophic lateral sclerosis
AP-1	Activator protein 1
AP-1i	AP-1 inhibitor
AQP1	Aquaporin 1
ARE	Antioxidant response elements
ASK	Apoptosis signal-regulating kinase
ATF6	Cyclic AMP-dependent transcription factor 6
ATRX	Alpha-thalassemia syndrome gene
BCA	Bicinchoninic acid
BLAST	Basic Local Alignment Search Tool
bZIP	Basic leucine zipper domain
Ca2+	Calcium
CA9	Carbonic anhydrase 9
CAM1	L1 cell adhesion molecule
CAR-T	Chimeric antigen receptor T-cell
CCT020312	PERK-selective activator
CD	Cluster of differentiation
CDKN2A	Cyclin dependent kinase inhibitor 2A
CHI3L1	Chitinase 3 like 1
CHOP	C/EBP-homologous protein
CL	Classical
CNS	Central nervous system
CRT2	Calreticulin 2
CSCs	Cancer–stem cells
CTGF	Connective Tissue Growth Factor
CYR61	Cysteine Rich Angiogenic Inducer 61
DAG	Lipid diacylglycerol
DAMPs	Damage Associated Molecular Patterns
DIPG	Diffuse intrinsic pontine glioma
DMSO	Dimethyl sulphoxide
DNAJC3/P58IPK	DNAJ homolog subfamily C member 3
DTT	Dithiotreitol

EDEM	ER degradation-enhancing alpha-mannosidase-like protein 1
EDTA	Ethylendiaminetetracetate
EGFR	Epidermal growth factor receptor
eIF2α	Eukaryotic elongation factor 2α
EMT	Epithelial to mesenchymal transition
ER	Endoplasmic Reticulum
ERAD	ER-associated degradation
ERDJ	Endoplasmic reticulum DNA J domain-containing protein
ERK	Extracellular signal-regulated kinase
ERO1	Endoplasmic oxidoreductin-1-like protein
ERSE	ER stress response element
FAK	Focal adhesion kinase
FCS	Fetal calf serum
FDA	Food and Drug Administration
FGF	Fibroblast Growth Factor
FKBPs	FK506 binding proteins
FOSL-1	Fos-related antigen 1
FOXO1	Forkhead box protein O1
GADD34	Protein phosphatase 1 regulatory subunit 15A
G-CIMP	Glioma-CpG island methylator phenotype
GCLC	Glutamate-cysteine ligase catalytic subunit
GCN2	General Control Nonderepressible 2
G-CSF	Granulocyte colony-stimulating factor
GLOBOCAN	Global cancer statistics 2018
GLS	Golgi translocation signal
GP100	Glycoprotein 100
GRB2	Growth factor receptor-bound protein 2
GRP78/BIP/HSPA5	ER-resident chaperone 78 kDa glucose-regulated protein
GSCs	Glioblastoma stem-like cells
GSK2606414	PERK-specific inhibitor
GTP	Guanosine-5'-triphosphate
H&E	Hematoxylin and eosin
H3F3A	H3 Histone Family Member 3A
HER2	Human epidermal growth factor receptor 2
HERPUD1	Homocysteine Inducible ER Protein With Ubiquitin Like Domain 1
HIF1α	Hypoxia-inducible factor 1α
HIST1H3B	Histone Cluster 1 H3 Family Member B

HRI	Heme-Regulated Inhibitor
HRP	Horse-reddish peroxidase
HSP40	Heat shock protein 40
HUVECs	Human umbilical vein endothelial cell
HYOU1	Hypoxia up-regulated protein 1
IDH	Isocitrate dehydrogenase
IGF-1	Insulin-like growth factor 1
IL	Interleukin
IRE1α	Serine/threonine-protein kinase/endoribonuclease 1α
JNK	Mitogen-activated protein kinase 8
KEAP1	Kelch-like ECH-associated protein 1
LB	Luria-Bertani Medium
LRRC4	Leucine-rich repeat C4
MAGE-1	Melanoma-associated antigen 1
MAPKK6	Mitogen-activated protein kinase kinase 6
MDM2	Double minute 2 protein
MEFs	Mouse embryonic fibroblasts
MES	Mesenchymal
MGMT	O-6-methylguanine-DNA methyltransferase
MHC	Major histocompatibility complex
MICA/B	MHC class I and Natural killer cell-activating receptor ligands
MMP	Matrix-metallo proteinase
mTOR	Mammalian target of rapamycin
NEB	New England Biolabs
NF1	Neurofibromin
NF-Y	Nuclear transcription factor Y
NK	Natural killer
NOD-SCID	Nonobese diabetic/severe combined immunodeficiency
NRF2	Nuclear factor erythroid 2-related factor 2
PAM	Peptidyl-glycine alpha-amidating monooxygenase
PAM-sfCD	PAM soluble fragment Cytosolic Domain
PBS	Phosphate buffered saline
PDGFRA	Platelet-derived growth factor receptor alpha
PDIA	Protein disulfide-isomerase A
PERK	PKR-like kinase
PFA	Paraformaldehyde
PI3K	Phosphatidylinositol 3-kinase

PIGF	Phosphatidylinositol-glycan biosynthesis class F protein
PKR	Protein Kinase R
PML	Promyelocytic leukaemia tumour suppressor
PN	Proneural
PPIases	Peptidyl prolyl isomerases
Ppp1r15b/CReP	Protein phosphatase 1 regulatory subunit 15B
PTEN	Phosphatase And Tensin Homolog
PTP1B	Protein-tyrosine phosphatase 1B
RELA	Reticuloendotheliosis Viral Oncogene Homolog A
RHEB	Ras homolog enriched in brain
RIDD	Regulated IRE1-Dependent Decay
S1P	Site-1 protease
S2P	Site-2 protease
SDF1	Stromal cell-derived factor 1
SDS	Sodium dodecyl sulfate
SERCA2	Sarcoplasmic/endoplasmic reticulum calcium ATPase2
sfCD	Soluble fragment cytosolic domain
SHH	Sonic hedgehog
SLPI	Secretory leukocyte peptidase inhibitor
SRC	Src homology 2 domain-containing-transforming protein C
SREBP	Sterol-regulatory element-binding protein
SS	Signal peptide
Syn-1	Syndecan-1
TAAs	Tumor associated antigens
TAMs	Tumor-associated macrophages
TBE	TRIS-Borat-EDTA
TBS	TRIS buffered saline
TCF3	Transcription factor 7-like 1-A
TCGA	The Cancer Genome Atlas consortium
TF	Transcription factor
THBS4	Thrombospondin-4
TM	Transmembrane
TP53	Tumor protein p53
TRAF	TNF receptor-associated factor
TRES	Transmissible ER stress
TRIO	Triple functional domain protein
TRIS	Tris-(hydroxymethyl)-aminomethan

TRP2	Tyrosinase-related protein 2
TSAs	Tumor-specific antigens
TSC1–TSC2	Tuberous sclerosis protein complex
UHMK1	U2AF homology motif kinase 1
UPR	Unfolded protein Response
VEGF	Vascular endothelial growth factor
WFS1	Wolfram syndrome 1
WHO	World health organization
XBP1	X-box binding protein 1
ZEB	Zinc finger E-box-binding homeobox

1. Introduction

1.1 Tumors of central nervous system (CNS)

Chronic diseases for example cancer, cardiovascular diseases, etc, are the leading cause of deaths in the world leaving cancer as the second biggest reason of deaths worldwide. A new report submitted by the global cancer statistics 2018 (GLOBOCAN) estimated 18.1 million new cases of cancer and 9.6 million cancer-related deaths in the year 2018 worldwide. Out of all cancer-types, central nervous system (CNS) tumor accounts for almost 2.5% of the total deaths (Figure 1)[1]. Brain tumors have been classified for past centuries on the basis of microscopic evaluation of expression markers and assigned to different putative group of origin on the basis of similarities.

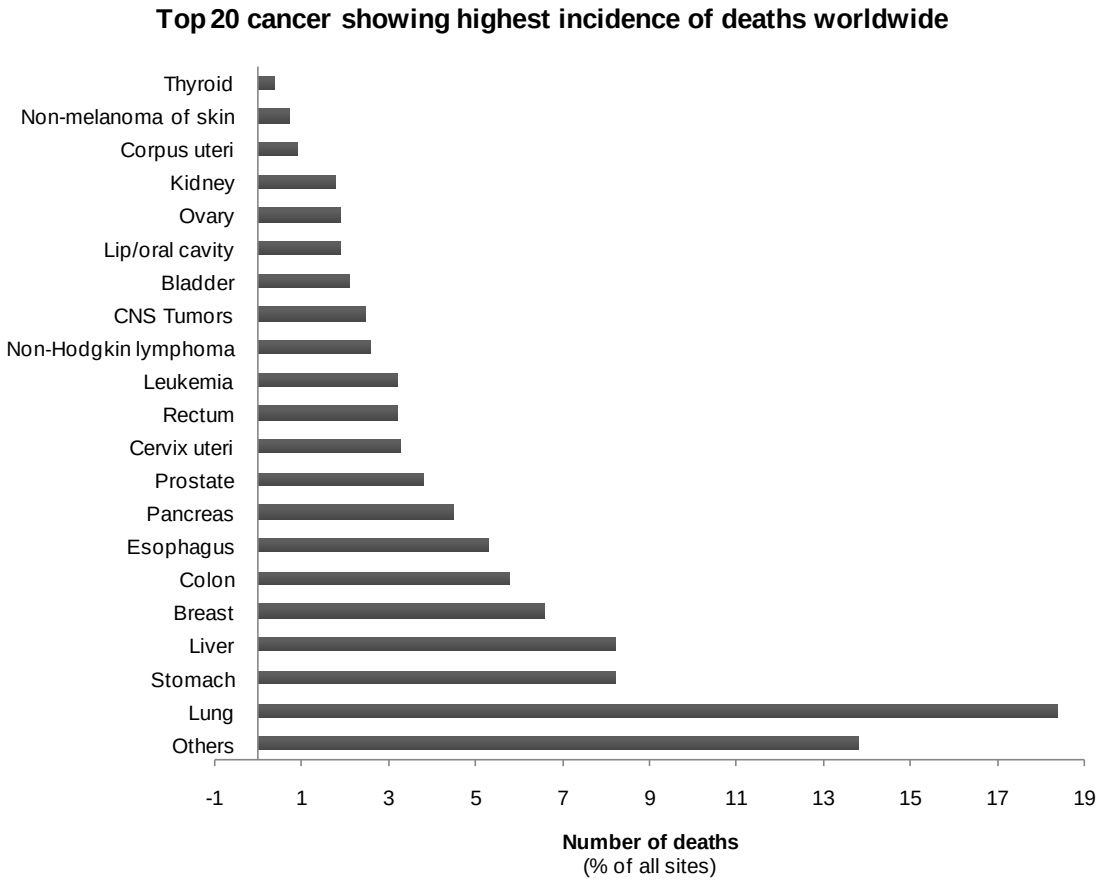

Figure 1. Worldwide estimation of number of deaths caused by different types of tumors as a percentage of total number of cancer deaths (2018)[2].

This type of classification was based on the cell of origin namely, astrocytes, oligodendrocytes and ependymal cells classifying the tumor into astrocytoma, oligoastrocytoma/oligodendroglioma and ependymoma by using hematoxylin and eosin staining (H&E staining), immuno-histochemical analysis of different biomarkers and characterization of tissue ultrastructures whereas the clinical relevance was mostly ignored in the process[3]. These were further classified on the basis of their malignancy. Continuous research in the field at genetic level has brought up the significance genetics of tumors hold in the process of tumorigenesis. This has led to the recent updates in 2016 of the WHO classification of brain tumors published in 2007. This updated classification takes into account the phenotypic and genotypic parameters which in turn provide robust diagnostics, increased accuracy of prognosis and treatment response, the best example of which is oligoastrocytoma[4,5]. It includes new tumor entities based on both histological and molecular parameters. The new classification contain entities like glioblastoma with isocitrate dehydrogenase (IDH)-wildtype and glioblastoma with IDH-mutant; diffuse midline glioma with H3 K27M-mutation; *RELA* fusion-positive ependymoma; wingless (WNT)-activated medulloblastoma and sonic hedgehog (SHH)-activated medulloblastoma; and embryonal tumor with multilayered rosettes, C19MC-altered. Diffuse glioma, medulloblastomas and other embryonal tumors have obtained a major restructuring in this updated version. Louis et al (2016) can be referred for a detailed version of the new update of the 2007 WHO classification of the brain tumor[4]. The 2016 WHO classification of glioma has grouped this tumor type in different categories on the basis of histological-pathological markers together with genetic alterations they have. This classification has been quoted with the statement “genotype trumps phenotype” which goes in terms with the diagnosis of the tumor type. The major changes to glioma (astrocytoma, oligodendroglioma and ependymoma) classification in the new version of WHO (2016) has been linked to genetic alterations like 1p/19q co-deletion, IDH mutations, tumor protein 53, alpha-thalassemia syndrome gene (*ATRX*), the gain of 7 and loss of 10q genotype, EGFR amplification and mutations, PTEN mutations, BRAF-KIAA fusion genes and BRAF mutations in glial tumors and histone H3F3A and HIST1H3B mutations. Table 1 enlists the major changes in the classification of the glioma.

	Genetic aberrations	Type of glioma
Diffuse astrocytic/ oligodendroglial tumors	IDH wild-type, IDH mutant	Glioblastoma
	IDH mutant	Diffuse astrocytoma
		Anaplastic astrocytoma
	IDH mutant, 1p/19q co-deleted	Oligodendroglioma
		Anaplastic Oligodendroglioma
	H3-K27M mutant	Diffuse midline glioma
	MYBL rearrangement	Well differentiated pediatric diffuse glioma
Ependymomal tumors	RELA-fusion	Ependymoma, RELA-fusion positive
	YAP1 gene fusions	Ependymoma
	NF2 mutations	Spinal intramedullary ependymal tumours
	Unidentified aberrations	Posterior fossa (PF) ependymal tumours
Other gliomas	BRAF-V600E mutation	Pilocytic astrocytoma
		Pleomorphic xanthoastrocytoma
	TSC1 or TSC2 mutation	Subependymal giant-cell astrocytoma
	MYB-QK1 gene fusions	Angiocentric glioma

Table 1 Major glioma entities according to 2016 WHO classification of CNS tumors including the major genetic alterations they bear.

1.2 Glioblastoma

Glioblastoma are the most common, highly aggressive, grade IV gliomas, of which almost two-third are primary in nature thus leaving patients with little or no clinical history. Primary glioblastoma shows a rapid development of tumor in course of less than 3 months with highly infiltrative growth and mostly occur in older age (>60 years). On the other hand, secondary glioblastoma develop from low-grade gliomas and mostly occur in patients with less than 45 years of age. Both the glioblastoma types differ in their genetic background, as primary glioblastoma primarily show *EGFR* amplifications/mutations, homozygous deletion of the *CDKN2A-p16*$^{INK4\alpha}$ and deletion of *PTEN,* while secondary glioblastoma shows alterations/mutations in *IDH1/2* or *TP53*[6].

1.2.1 Major genetic alterations in glioblastoma

Tumor Protein 53 (*TP53*)

TP53, present on chromosome 17, acts as a major player in the cell cycle, DNA damage response and cellular differentiation mechanisms. TP53 arrests the cell cycle and renders cell to apoptosis in case of excessive damage to DNA under various stress conditions by regulating the expression of p21. p21 protein binds to cyclin-dependent kinases (CDKs) and inhibits the cell cycle progression from G1 phase. Another protein, MDM2 acts as a negative regulator of TP53 by directly binding to and inhibiting its activity, whereas CDKN2A-p14^{ARF} acts as a negative regulator of MDM2 thereby activating TP53. Any genetic alterations in this pathway can lead to the inhibition of TP53-mediated restriction of cell cycle progression under conditions of oncogenic transformation thereby supporting neoplastic growth[6]. *TP53* mutation is usually found in 90% of *IDH* mutant cases with no 1p/19q co-deletion, but does not hold diagnostic significance as it is found in many different kind of gliomas including glioblastoma, medulloblastoma and pediatric gliomas.

***EGFR* amplifications and mutations**

Even when 40-50% of glioblastoma cases show either mutation or amplification (occurring because of chromosome 7 trisomy or polysomy) or both in the *EGFR* gene specifically *EGFRvIII* (leading to the mutations in the extracellular domain of the protein), no diagnostic or prognostic relevance has been seen so far. *EGFRvIII* acts as a constitutively active protein ensuring continuous signaling through SHC–GRB2–RAS and class I PI3K supporting tumorigenicity, cell proliferation and resistence to apoptosis[7]. Steps are being taken in exploiting the mutated *EGFR* conditions and many clinical trials are on the run.

***PTEN* mutation**

Phosphatase and Tensin Homolog (PTEN) acts as a tumor suppressor by inactivating PI3K/AKT signaling pathway. Mutations in the gene can lead to continuous activation of PI3K/AKT signaling which further enhances cellular proliferation and survival while inhibiting apoptosis[6]. *PTEN* mutation occurs in 20-30% of glioblastoma cases and is accompanied with 10q loss of heterozygosity inactivating PTEN function. This genetic alteration has little diagnostic value and by far no prognostic outcome.

RB* or *CDKN2A-p16$^{INK4\alpha}$

Active RB, retinoblastoma protein, attenuates the progression of cycle by directly binding to E2F (transcription factor) and inhibiting transcription of growth-promoting genes. Growth-factor signaling leads to the expression of cyclins and CDKs which together phosphorylate and inhibit the activity of RB protein. This enhances the E2F-mediated expression of genes necessary for mitosis. Moreover, INK4 family members, including CDKN2A-p16$^{INK4\alpha}$ acts as positive regulators of RB-mediated inhibition of E2F transcription factor by reducing its cyclins-CDKs-mediated inhibitory phosphorylation. Inactivation of RB pathway can occur because of mutations in either of the genes; *RB* (mutations, deletions or promoter methylation) or *CDKN2A-p16$^{INK4\alpha}$* (homologous deletion or mutation), and is found in almost 75% of all primary glioblastoma patients.

***IDH* mutations**

IDH mutations have been found in both *IDH1* and *IDH2* genes and have been constantly used now days for diagnostic purposes. It is a somatic, missense and heterozygous mutation that affects codons 132 and 172 in *IDH1* and *IDH2* genes respectively. Out of these, around 90% of the cases show *IDH1* R132H mutations occurring during the start of the tumorigenesis and remains until the end of tumor progression. They are more common in grade II-IV diffuse gliomas but are not present in primary brain tumors. The mutation in this enzyme leads to alterations in the enzyme activities leading to increased level of 2-hydroxyglutarate and lower levels of α-ketoglutarate. This has also been correlated with increased methylation of CpG islands across the genome including *MGMT* gene promoter which might be a reason of better outcome of *IDH* mutant gliomas when combined with chemotherapy along with radiotherapy. O-6-methylguanine-DNA methyltransferase (MGMT) promoter methylation reduces the expression of this protein resulting in better outcome from therapies including alkylating agents[8,9].

1.2.2 Subtype classification of glioblastoma

The presence of high degree of genomic heterogeneity within glioblastoma patients led the researchers to establish The Cancer Genome Atlas consortium (TCGA) wherein around 600 patient-derived tumors were

profiled for whole transcriptome expression patterns and classified on the basis of major clusters thus obtained with commonly found mutations in *TP53*, *EGFR*, *IDH1* and *PTEN* [10,11]. These clusters include proneural (PN), mesenchymal (MES) and classical (CL) subtype of glioblastoma, including abnormalities in *IDH1*, *EGFR* and *NF1* respectively, with mesenchymal subtype having the worst prognosis for all glioblastoma patients[12–14]. Also, many studies have concluded and indicated a proneural to mesenchymal switch upon application of current therapies as the main reason behind tumor recurrence [15,16]. Moreover, MES subtype of glioblastoma is found associated with microglia/tumor-associated macrophages (TAMs) which support the growth and progression of glioblastoma and are responsible for the poor prognosis. This MES glioblastoma phenotype is associated with the deactivation of NF-1 expression in glioblastoma which was postulated to act on gene expression changes and thus chemotactic towards TAMs and microglia[11,16]. Furthermore, a study based on global methylation pattern of glioblastoma has shown a distinct glioma-CpG island methylator phenotype (G-CIMP) and has led to the inclusion of three new categories while having the other three categories falling into the already existing transcriptome-based glioblastoma subtypes[17]. According to this classification, 30-40% of adult/pediatric glioblastoma has exclusive mutations in either *H3F3A* (K27), *H3F3A* (G34) or *IDH1* genes thereby taking them as major alteration for the three distinct methylation-based glioblastoma categories. The other three categories in this classification includes glioblastoma with *PDGFRA* mutations (RTK-I; proneural expression signature), *EGFR* mutations (RTK-II; classical expression signature) and *NF1* alteration (Mesenchymal expression signature)[17,18].

1.2.3 Current treatment regimes against gliomas

Normal treatment regime for glioma involves surgical resection of the tumor followed by radiotherapy and chemotherapy. Efforts are being made to enhance the overall effect of the current therapies and thus overall survival. Research in the field has helped us understand and better target the aggressive disorder. Scientists have expanded their knowledge and incites in understanding and exploiting the latest technological advances to invent new strategies which includes targeted-gene and small molecule inhibitor therapies, and immunotherapies in order to reduce gliomas burden and increase progression-free survival[19]. One such example of intra-tumoral gene therapy is via retroviral-based gene transfer, where cytosine deaminase gene containing reterovirus is directly injected within tumor cells, an effort by Tocagen company. The drug converts an extracellular substrate flucytosine to its active agent 5-flourouracil killing the cancer cell. The drug is going through phase II/III trials in order to analyze its efficacy. Multiple pathways which get modulated in gliomas as explained above are being exploited to find targeted therapies. Bevacizumab, a homogenized VEGF antibody found suitable for recurrent glioblastoma in a study published in 2009 and thus approved by FDA, had no benefits for overall survival to patients having newly diagnosed glioblastoma[20–25]. This has led to understand the possibility of new

angiogenic pathways in glioblastoma. A sudden boom in the field of immuno-oncology has opened new ways to tackle the disease. Immuno-suppression is one of the most prominent features of glioma that has been exploited recently in order to curb the disease. Pathways like PI3K mediated activation of AKT/mTOR (activated in low grade gliomas) are also being targeted. Everolimus, an inhibitor of mTOR has shown promising preliminary results with increased progression-free survival of patients. Immuno-suppression has been one of the major hallmarks of gliomas[26,27]. Immuno-therapies like, cellular therapies, vaccinations and immuno-modulatory therapies targeting immuno-checkpoints are also under clinical trials and have shown major advantages to the patients. Adoptive T cell transfer therapy includes patients T cell stimulation against patient tumor cells *in vitro* and transferring them back in the patients to target gliomas. One such example of this therapy is upcoming chimeric antigen receptor (CAR) T-cell therapy. Vaccination therapies against tumor specific- (TSAs) or tumor associated antigens (TAAs) like HER2, TRP2, GP100, MAGE-1, IL13Rα2, AIM-2 and EGFRvIII, are also under clinical trials for validation of their use to treat glioma patients[28–31].

1.3 Unfolded Protein Response

Every cell tightly regulates the mechanism behind synthesis, proper folding and maturation of polypeptide chains. This helps the cell in maintaining intracellular protein homeostasis and also the tissue microenvironment. The plasma membrane and secretory proteins constitute upto 42% of the protein load within eukaryotic cells that needs to be processed within the endoplasmic reticulum (ER) (the primary site of protein synthesis). ER is also important for lipid biosynthesis[32], Ca2+ handling[33,34], and intraorganellar trafficking[35]. Certain conditions like nutrient deprivation, hypoxia or redox changes within a cell lead to imbalance of the proteome of the cell. Such conditions influence the gene expression profile and changes the way the new proteome has to be dealt with. Unfolded protein response is one such pathway which makes sure that the change in the proteome of the cell does not get affected at the step of synthesis and processing of polypeptide chains. Unfolded protein response enhances the protein folding capacity of the ER by increasing the expression of chaperones, enzymes for post-translational modifications and ER-associated degradation (ERAD) pathway proteins[36]. Under acute ER stress conditions, the UPR leads to apoptosis[37]. UPR comprises of three effector proteins (Figure 2) residing on the membrane of the ER: the serine/threonine-protein kinase/endoribonuclease IRE1 (IRE1α), the protein kinase R-like ER kinase or eukaryotic translation initiation factor 2α kinase 3 (PERK/EIF2AK3) and the cyclic AMP-dependent transcription factor 6 (ATF6). These effector proteins detect the misfolded protein in the ER lumen and mitigate the ER stress by regulating the transcription and translational machinery of the cell through the cytosolic domain. IRE1α and ATF6α change the transcriptome of the cell while PERK protein regulates the translation initiation. The ER-resident chaperone 78 kDa glucose-regulated protein

(GRP78/BIP/HSPA5) binds to the inactive IRE1α, PERK and ATF6 monomeric units under physiological conditions. Upon activation of the UPR, GRP78 is displaced by misfolded proteins activating all the three effectors[38]. The effector function of the UPR can be both pro-survival or pro-apoptotic depending upon the continuity of the ER stress. Diseases like neurodegenerative[39], inflammation[40], diabetes[41], metabolic disorders[42] and cancer[43–45], are all associated with UPR.

1.3.1 Effectors of the UPR

IRE1α

IRE1α is one of the three effector proteins of the UPR. It is a type-I ER membrane protein comprising of 977 amino acids (aa) with an ER-lumen domain (aa 19-443), a transmembrane domain (aa 444-464) and a cytoplasmic tail (465-977; Figure 3A). ER lumenal domain contains MHC-like motif which binds to either misfolded proteins or the chaperones present in the ER[46,47]. GRP78 binds to the hydrophobic amino acids present in the ER lumenal domain of IRE1α. During accumulation of misfolded proteins, GRP78 switch its binding partner from UPR effectors to the misfolded proteins, rendering the UPR effector proteins ready to get activated[38]. This interaction causes conformational changes in the cytosolic domain of IRE1α and brings its two monomeric units in close proximity. The cytosolic domain of IRE1α contains two enzymatic subunits i.e. a kinase domain and an RNase domain. The kinase domain of IRE1α trans-autophosphorylates itself at serine 724 residue leaving the enzyme in an active state. This also leads to the activation of the RNase domain of IRE1α. Activated IRE1α cleaves off the 26 nucleotide intron from the *XBP1u* (X-box binding protein 1-unspliced) mRNA, leaving two arms ready to be ligated by RTCB Ligase enzyme generating *XBP1s* (XBP1 spliced) mRNA[48]. The *XBP1s* mRNA thus has a frameshift which translates to XBP1s transcription factor. XBP1u protein, translated under normal physiological condition, regulates the splicing event of *XBP1u* mRNA to generate *XBP1s* mRNA and also mediates

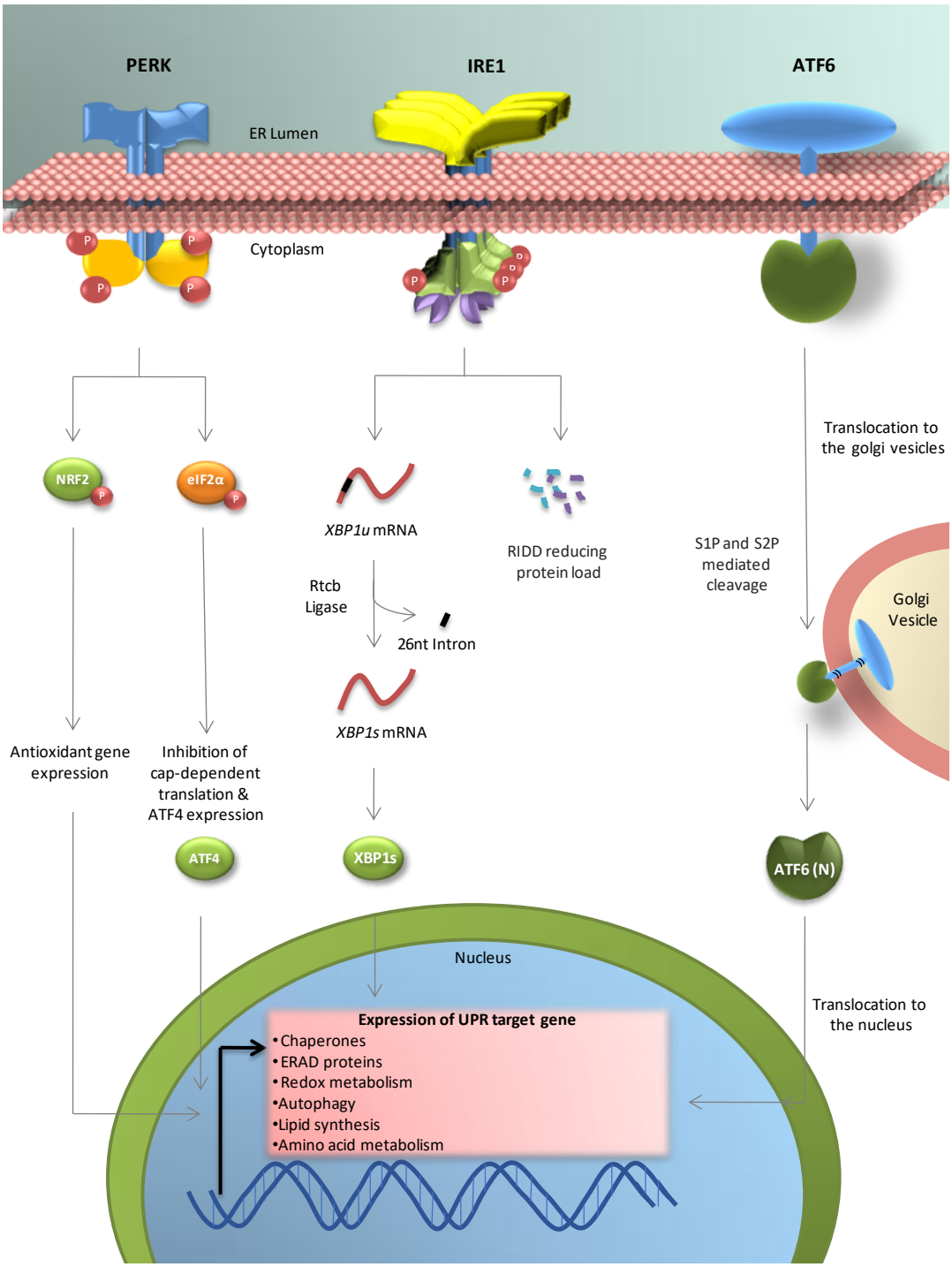

Figure 2 The unfolded protein response (UPR) pathway.
The three branches of the UPR get activated upon detection of misfolded proteins in the endoplasmic reticulum. PERK activation induces translation inhibition and expression of anti-oxidant genes. IRE1 regulates expression of XBP1s transcription factor regulating expression of ERAD pathway proteins. ATF6 on the other hand is localized to the nucleus upon UPR induction and cleaved by Golgi-resident SIP and S2P protease enzymes and cleaved ATF6(N) acts as a transcription factor responsible for the expression of several UPR genes. All three branches regulated proteins at levels of transcription, translation and post-translation in order to reduce ER protein load and maintain protein homeostasis.

XBP1s protein to degradation machinery[49–51]. Moreover, IRE1α degrades ER-localized mRNAs, ribosomal RNAs and microRNAs via its RNase domain. This activity of IRE1α is termed as Regulated IRE1-Dependent Decay (RIDD). IRE1α has been shown to preferentially splice *XBP1u* mRNA under dimerized state while oligomerized state is essential for the RIDD activity of IRE1α[52–55]. There are literature evidences showing a basal level of RIDD activity of IRE1α under normal physiological condition -within a cell whereas the *XBP1u* mRNA splicing is only active under oligomerized state of IRE1α. IRE1α branch cross-talks with the ATF6α via XBP1s transcription factor[56]. XBP1s is involved in the expression of protein chaperones like GRP78 and ERAD pathway protein like EDEM1, ERDJ3 and ERDJ4[57–59]. XBP1s also increases the expression of proteins playing a role in secretory pathway and lipid biosynthesis[60–63]. The phospho-state of IRE1α has been shown to be reversed by two different phosphatase namely PP2A and PPM[64,65]. The pro-survival phenotype of IRE1α activation is termed as adaptive ER stress response. Under severe stress conditions, IRE1α effector protein activates JNK signaling pathway which leads the cell to apoptosis[66]. IRE1α has many interacting partners which modulates its activity depending on the physiological state of the cell.

PERK

PKR-like kinase (PERK) is a type-I transmembrane protein kinase having a lumenal domain, a transmembrane domain and a cytosolic kinase domain (Figure 3B). It comprises of 1116 amino acid with a total molecular weight of 125 kDa. The lumenal domain of PERK has 20% identity to the lumenal domain of IRE1α protein while its cytosolic domain shares 40% similarity to the PKR kinase enzyme[67,68]. Like IRE1α, the lumenal domain of PERK is bound to GRP78 under normal physiological conditions. ER stress leads to dissociation of GRP78 from the PERK which leads to dimerization and trans-autophosphorylation of PERK at threonine 980 residue in the kinase domain leading to its activation[68]. PERK can be dephosphorylated and inactivated by the enzyme protein-tyrosine phosphatase 1B (PTP1B)[69]. Among the protein which can regulate the inhibition of PERK are DNAJ homolog subfamily C member 3 (DNAJC3/P58IPK), which is a member of the HSP40 family and Nck1[70–72]. Active PERK phosphorylates its downstream target eIF2α at serine 51 residue blocking the first step of translation initiation[73]. eIF2α is a component of EIF2 heterotrimeric complex (subunits α, β, γ; genes:EIF2B1, EIF2B2, and EIF2B3). This complex regulates the initial step of translation where methionyl-tRNA binds to the ribosome in an αGTP-dependent manner. The phosphorylation of eIF2α increases its affinity towards eIF2B which follows the inhibition of the exchange of GDP to GTP thereby leading to translation inhibition[74]. But there are certain UPR target mRNAs which are still translated like ATF4[75], the basic zipper transcriptional regulator ATF5[76], pro-apoptotic protein CHOP[77], and GADD34[78] due to the presence of upstream open reading frames at the 5'untranslated region (5'UTR). ATF4 is a transcriptional factor regulating pro-survival genes like ATF3 during early ER stress as well as the pro-apoptotic gene

CHOP under continuous UPR activation. Effect of PERK on eIF2α can be reversed by two ER stress regulated proteins namely GADD34 (PPP1R15A) and the constitutively expressed CReP (PPP1R15B) by negatively regulating the eIF2α phosphorylation status. eIF2α can also be phosphorylated at serine 51 residue by three other kinases depending upon the stress conditions a cell is confronting.

These are GCN2 activated under amino acid starvation, PKR activated under viral infection, and Heme-regulated inhibitor (HRI) activated under heme-deprivation, and oxidative stress conditions[79]. Nuclear factor erythroid 2-related factor 2 (NRF2) was found to be another very important transcription factor being activated by PERK. NRF2 acts as a master regulator of redox homeostasis within a cell. It transcribes anti-oxidant genes (e.g. glutamate-cysteine ligase catalytic subunit (GCLC), hemeoxygenase-1) in order to reduce the damaging effect of reactive oxygen species within a cell. PERK-mediated phosphorylation of NRF2 leads to disruption of NRF2-KeapN1 interaction and NRF2 nuclear localization which otherwise leads to degradation of this transcription factor[80–82]. PERK also phosphorylates and induce nuclear localization of FOXO1 transcription factor. PERK-mediated phosphorylation of lipid diacylglycerol (DAG), an important second messenger and also precursor for phosphatidic acid (PA), regulates the activation of Akt and ERK1/2 signaling downstream of RAS. This triggers activation of the mTOR signaling and supports tumorigenesis[83].

ATF6

ATF6α/β is the third effector branch of the UPR which does not require any transcription or translation step to get activated. It is a type-II transmembrane protein having a C-terminus ER luminal domain, a transmembrane domain and an N-terminus cytosolic domain (Figure 3C). The ER-lumen domain contains a Golgi translocation signal (GLS). Both the isoforms differs with respect to their function in the UPR signaling. The ATF6α isoform acts a transcriptional activator with two GLS on the N-terminus, whereas ATF6β acts as a transcriptional repressor protein with only one GLS on the N-terminus[84]. Thus the activity of ATF6α depends on the amount of ATF6β expressed within a cell[85]. The cytosolic domain of ATF6α contains the basic leucine zipper domain (bZIP) relevant for the transcriptional signaling of the UPR[86]. Under normal physiological conditions, both the isoforms can make homo or heteromers of their mono-, di- or oligomer units with di-sulphide bridges on their cytosolic domains. It is only under UPR activation that GRP78 is displaced from their GLS domain on the ER-lumen side which is now available to translocate ATF6 to the golgi vesicle[87]. Several factors have been shown to influence the activation of ATF6α/β. Higa and coworkers reported protein disulfide-isomerase A5 (PDIA5) to regulate translocation and transcriptional activity of ATF6α/β which might be a reason for chemotherapy resistance to Imatinib in patient-derived leukemia cells[88]. Calreticulin, a co-chaperone was also found bound to the GLS domain of the ATF6α/β. Thrombospondin-4 (THBS4) also binds to the ER-lumenal domain of ATF6α/β inducing its pro-survival signaling[89]. ATF6α/β was also shown to be influenced by the dual specificity mitogen-

activated protein kinase kinase 6 (MAPKK6)- mitogen-activated protein kinase P38 α/β (P38α/β)- pathway in dormant human squamous carcinoma cells[90]. The exposure of the GLS domain directs ATF6α/β packaging into the COPII vesicles[91]. Wolfram syndrome 1 (WFS1), a responder of the IRE1α branch, can influence this process and retain ATF6 in the ER[92]. The two Golgi membrane residing serine protease enzymes; membrane-bound transcription factor site-1 protease (S1P) and membrane-bound transcription factor site-2 protease (S2P) cleaves ATF6α/β intra-membranously, thereby releasing a 50 kDa fragment (ATF6α/β-f), containing the bZIP motive[93]. This step is of vital importance for the activation and transcription activity of ATF6α. The ATF6α/β-f thus generated translocates into the nucleus where it binds to the ER stress response element (ERSE) in tandem with nuclear transcription factor Y (NF-Y)[94,95]. The ATF6α/β-f can also be subjected to ubiquitination and subsequent proteasomal degradation limiting its activity in the UPR[96]. The ATF6α/β-f transcription factor binds not only to the NF-Y but also with XBP1s, transcriptional repressor protein YY1 (YY1), and TATA-binding protein which regulates the expression of various target genes like *XBP1, NF-Y, interleukin-10* (*IL-10*), as well as its own *ATF6α* and *ATF6β*[97–99]. The ATF6/XBP1s heterodimer transcribes the growth arrest and DNA damage inducible 45a (GADD45A) inhibiting S-phase transition of the cell cycle and stimulating DNA excision repair[100]. ATF6 also increases the expression of DNAJ homolog subfamily C member 3 (DNAJC3/P58IPK) which binds to and inhibits the kinase domain of PERK. ATF6 increases the expression of enzymes essential for the post-translational modifications of newly synthesized polypeptide chains like Protein disulfide- isomerase A4 (PDIA4) and ERO1. It also leads to the enhancement in the expression of the chaperones GRP78, GRP94, Homocysteine-responsive endoplasmic reticulum-resident ubiquitin-like domain member 1 protein (HERPUD1), Calreticulin 2 (CRT2), and Hypoxia up-regulated protein 1(HYOU1) which are all essential for maintaining protein homeostasis. In addition, ATF6α also increases ERAD pathway proteins OS9, and SEL1 pro-apoptotic proteins CHOP and BCL-2, as well as the sarcoplasmic/endoplasmic reticulum calcium ATPase2 (SERCA2) and GTP-binding protein RHEB (Ras homolog enriched in brain)[101–104].

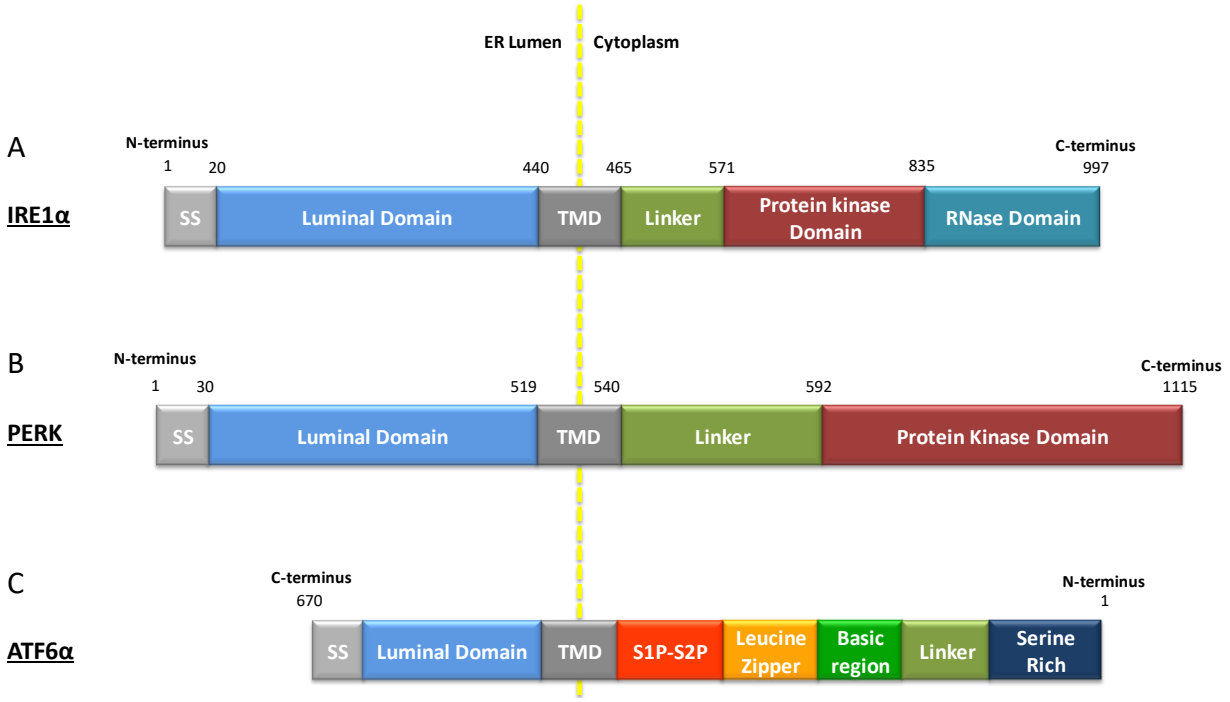

Figure 3. Structure of UPR sensor proteins[105].
SS (signal peptide), TMD (transmembrane domain), S1P-S2P (cleavage site)

1.3.2 Hypoxia-mediated UPR activation

Extreme heterogenic nature of the tumor microenvironment in terms of nutrient supply, oxygen and pH alters the metabolic and proliferative status of the tumors. Indeed, tumor microenvironment has been a major contributor of changes in gene expression leading to aggressive tumor phenotypes including proliferation, angiogenesis, metastasis and chemoresistance. Hypoxia, one of the most influencing microenvironment conditions within tumor alters the gene expression and cellular functions mostly through stabilization of hypoxia-inducible factor HIF1α. The other pathways known to be regulated by hypoxia are mTOR signaling and unfolded protein response (Figure 4). Hypoxia leads to the inhibition of mTOR signaling reducing phosphorylation of 4EBP1 and thereby inhibiting translation [106]. It does this by activating tuberous sclerosis protein complex (TSC1–TSC2) through different mechanism or via the promyelocytic leukaemia tumour suppressor (PML) which binds to and inactivate mTOR by sequestering it within nuclear bodies. Although, this can be reversed in advanced stage tumors bearing mutation or loss of function in TSC2 and PTEN genes where tumor cells can benefit from active protein translation, pro-survival autophagy, energy metabolism and apoptosis inhibition[106–109]. One such example is the hypoxia-induced inhibition of mTORC1 in immortalized breast epithelial cells whereas continuous activation of mTORC1 in cells derived from advanced stage breast cancer samples under similar

conditions[110]. On the other hand, UPR helps tumor cells in adapting to increased ER stress due to changes in different signaling pathways during tumorigenesis. It enhances the protein folding capacity of the ER and thus contributes to the different phenotypic changes a cancer cell bears under hypoxia like angiogenesis and invasion, among others. All the three pathways cross-talk between each other in order to regulate cellular metabolism, autophagy, ER stress and thus supporting tumor growth under harsh hypoxic conditions[106].

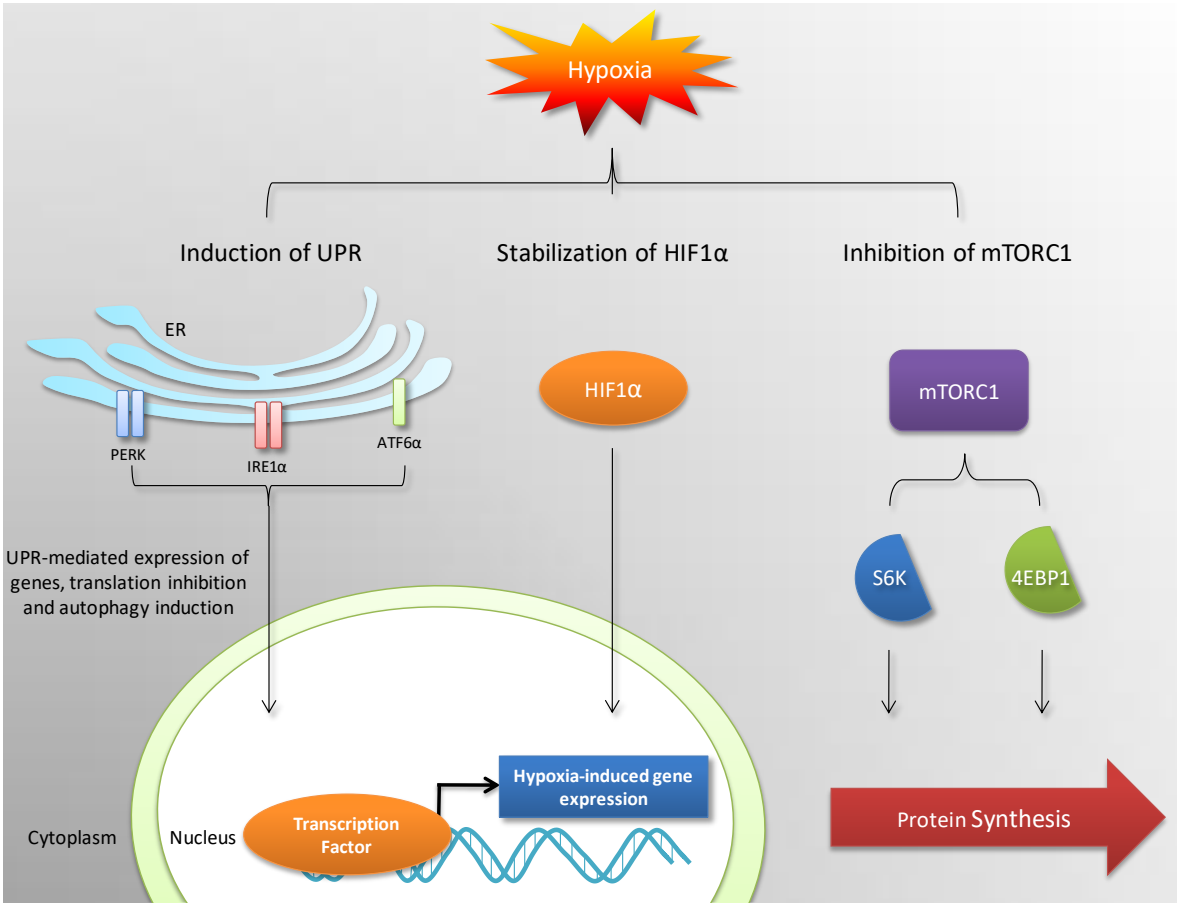

Figure 4. Hypoxia-regulated pathways.
In normal cells, induction of hypoxia leads to activation of UPR, stabilization of HIF1α protein and inhibition of mTOR kinase signaling. Tumor cells with mutation in the pathways necessary for inhibiting mTORC1 signaling gather pro-survival benefits from the mTORC1-mediated translation, energy metabolism and autophagy regulation. UPR increases the protein folding capacity of the cell while HIF1α leads to expression of factors necessary of angiogenesis, invasion and other hallmarks of cancer.

1.3.3 UPR and Diseases

UPR has been found active in several health disorders related to the central nervous system (CNS), lung, kidney, heart and liver diseases, aging, cancer and metabolic disorders like diabetes, having both protective or deteriorating role depending upon the extent of its activation [111,112,121–124,113–120]. UPR activation has been linked to different outcomes in neurodegenerative disorders. For example IRE1/XBP1 has been found active and responsible for deleterious effects in Epilepsy, amyotrophic lateral sclerosis (ALS), and Huntington's disease, whereas in acute neuronal injury like spinal cord lesions, XBP1s protein administration locally enhanced the survival of the cells [125–129]. Similar phenomenon was seen in Alzheimer's disease where XBP1 activation decreased amyloid-β accumulation and improved neuronal function.[130] Interestingly, in Parkinson's disease model, XBP1 deletion gives different phenotypic outcome at different stage of the disease[131]. The PERK branch of UPR enhances neuro-protection in Parkinson's and ALS disease by P-eIF2α-mediated translation halt [132–134], although reduction in PERK–mediated increase in P-eIF2α improved memory and synaptic functions in case of Alzheimer's and prion-diseases respectively [135–137]. In diabetes, inactive IRE1 and PERK branch has been found responsible for altered insulin secretion, less β-cell viability and increased resistance to insulin during diabetes due to accumulation of misfolded insulin and lipotoxicity during the disease [138–142]. XBP1s mediates expression of VEGFα, ATF6α reduces the oxidative stress, ischemia and reperfusion injuries in cardiomyocytes, thereby playing a significant role in restoring heart functioning[143–146,147]. PERK normally stays inactive possibly to maintain low level of ER stress in injured heart[148].

1.3.4 UPR in cancer

UPR activation has been related with almost every stage of a tumor progression, including transformation and proliferation of cells, angiogenesis, invasion and tumor metastasis. Cancerous transformation of cells requires activation or inactivation of oncogenes and tumor-suppressor genes like *BRAFv600E*, *c-MYC* and *H-RAS*, or *p53*, respectively. This leads to an increased proliferation which further enhances the burden on the ER of the cell leading to UPR activation[149–151]. On the other hand, cancer cells try to circumvent the potential apoptosis which comes along with the UPR activation by reducing the expression of apoptotic protein, for example, H-RAS decreases *CHOP* mRNA levels in order to reduce the apoptotic signaling in mouse embryonic fibroblasts (MEFs)[151]. Active c-MYC was also shown to reduce apoptosis by inducing PERK-mediated autophagy[150]. P58IPK, responsible for reducing PERK and PKR activation has been implicated in reducing UPR-mediated cell death[70]. This whole process is effective in selecting those transformed cells which have optimum ER stress required for pro-survival or adaptive UPR response supporting growth and proliferation of cancer cells and circumventing the apoptotic signaling. Different branches of UPR have shown differential functioning in regard to proliferation. IRE1-XBP1s

branch has been linked with G1 arrest, whereas PERK activation showed reduction in β-catenin-mediated cyclinD1 expression reducing proliferation of the cancer cells[152–154]. UPR activation has many benefits under stress like hypoxia and nutrient deprivation. IRE1α-XBP1s axis enhances cell survival under hypoxic conditions. In certain cancer types like breast cancer, XBP1s has been found to interact with HIF1α and thus increase its transcription efficiency[155]. PERK branch induces autophagy via eIF2α-ATF4 signaling under hypoxia enabling cancer cells to self sustain under condition of nutrient deprivation[156]. Activation of ER stress in cancer cells also changes the secretome and several of these soluble factors can induce ER stress in immune system of the host, known as Transmissible ER stress (TRES). In a study, TRES has been shown to induce expression of cytokines in dendritic cells providing pro-survival benefits to tumor cells both *in vitro* and *in vivo*[157,158]*.* Another study showed reduced expression of MHC class I and Natural killer cell-activating receptor ligands MICA/B, due to UPR signaling which thus reduced CD8+ T cell and NK cell-mediated cytoxicity[159–161]. Another very important hallmark of cancer, i.e. angiogenesis, has also been found regulated by the UPR pathway. All three effector proteins of the UPR (IRE1α, PERK, ATF6α) has been shown in different studies regulating angiogenic factors like VEGF-A. XBP1s was found directly interacting with HIF1α to enhance its DNA-binding efficiency in triple-negative breast cancer[155]. PERK also regulates VEGF-A, IL6 and FGF expression via ATF4 transcription factor and ATF6α was also found binding to VEGF-A promoter region regulating its expression[162–164]. UPR signaling influences the transition of cancer cells under stress from epithelial to mesenchymal phenotype both directly and indirectly. IRE1α signaling via XBP1s was shown regulating the expression of transcription factors necessary for migration and invasion of cancer cells like Snail1, Snail2, Zeb2 and TCF3 transcription factors[165]. One study found a strong association between EMT markers and ATF4 expression in 792 breast, colon and gastric tumours[166]. Cancer stem-like cells (CSCs) are a sub-population within tumor which bear the ability to self-renew and also give rise to all different kind of cells of the tumor bulk. Moreover, they carry the potency to withstand the cancer therapeutic stress and, enhance tumor progression and metastasis. UPR signaling has also been implicated in providing resistance to current chemotherapies, which might acts as a process of selecting the most aggressive but chemo-resistant cancer–stem cells (Figure 5)[153,155,167].

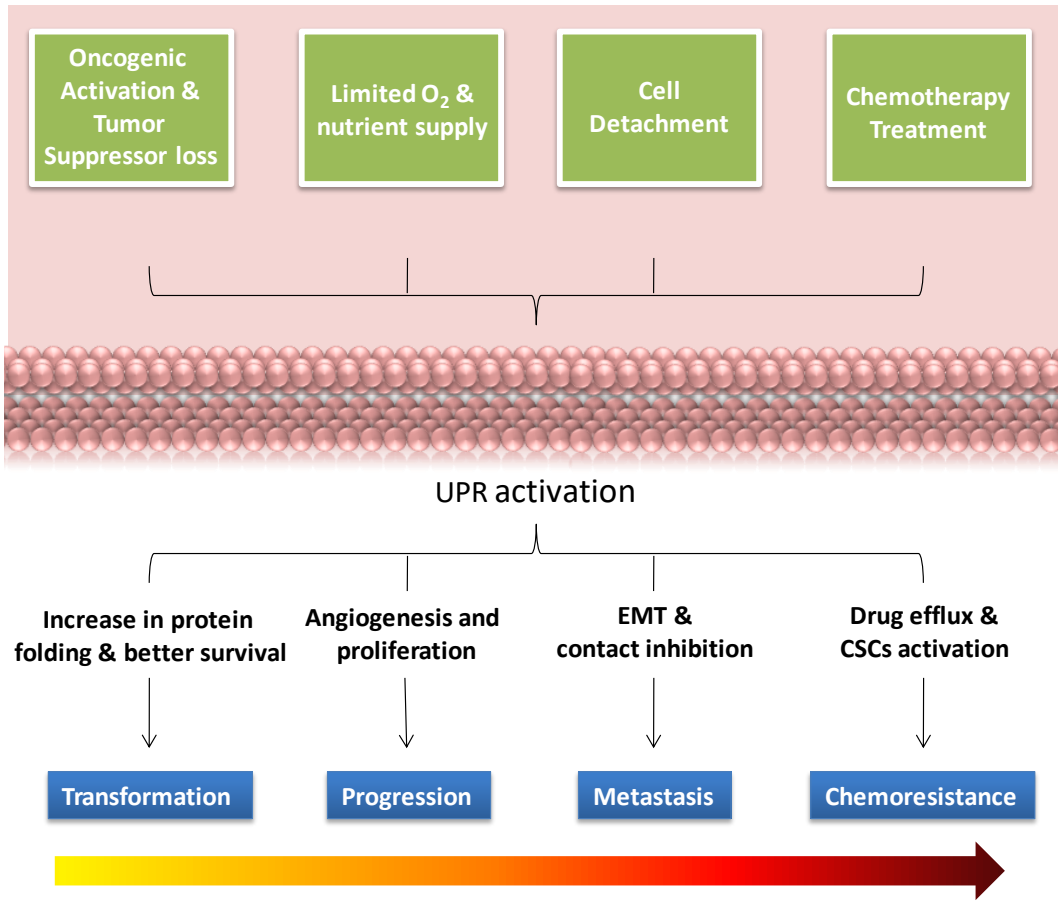

Figure 5. Role of UPR during different stages of tumor development.
UPR activation contributes to tumor progression at almost every stage. This happens due to the fact that every stage during tumor development brings forward a change in the gene expression profile of the cancer cell, putting forward new challenges for the protein folding machinery. In order to maintain protein homeostasis, cancer cell balances the optimum activation of all three branches of the UPR and gain from the pro-survival benefits.

1.4 Hallmarks of Cancer

Tumorigenesis is a multistep process where normal cells evolve to transform into a neoplastic growth by successively acquiring different hallmarks of cancer. These hallmarks, as described by Hanahan and Weinberg et al (2000), includes sustained proliferative signaling, evasion of growth suppressors, induction of angiogenesis, activation of invasion and metastasis, replicative immortality, and resistance to cell death[168]. The revised version of cancer hallmarks, published in 2011 introduced two new characteristic traits to this list; reprogramming cellular metabolism to support continuous proliferation and growth, and avoidance of immune destruction. They also brought in two major characteristics that are responsible for the acquisition of these traits. These characteristics include genomic instability (involving both genetic mutations as well as chromosome rearrangements) and inflammatory state of the neoplastic tissue where certain immune cell tends to support malignant nature of the tumor[169].

Tumor mass not just includes cancer cells but also normal cells which are recruited and reprogrammed to support tumor cells in attaining these key hallmarks of cancer, including angiogenesis.

1.4.1 Angiogenesis: A major hallmark of glioblastoma

Angiogenesis is the sprouting of new blood vessels from the existing ones. As the tumor grows, it requires constant nutrient and oxygen supply for its well being. This enforces tumor to attain an angiogenic switch whereby it regulates the formation of neo-vasculature in its surrounding[170]. Glioblastoma achieves this by maintaining a balance between the secretion of pro- and anti-angiogenic factors, like VEGF-A and TSP-1, respectively [171], where even the tumor stromal cells play significant role.[172,173] Few of the angiogenic inducers in glioblastoma include YKL-40 (chitinase 3 like 1, CHI3L1), a glycoprotein which induces the expression of VEGFA via Syndecan-1 (Syn-1) and integrin αvβ5-induced activation of focal adhesion kinase (FAK) and extracellular-regulated kinase (ERK) signaling pathways[174]. CD147 (Cluster of differentiation 147) is one of the other proangiogenic factors which can induce neo-vasculature formation via both insulin-like growth factor 1 (IGF-1) and HIF1α.[175,176] On the other hand, LRRC4 (Leucine-rich repeat C4) inhibits the induction of angiogenesis by reducing VEGFA expression thereby acting as an anti-angiogenic factor in glioblastoma[177]. Advances in the understanding of the role of microRNAs have revealed their significant influence in regulating angiogenesis in glioblastoma. Studies have found overexpression of miR-210-3p, miR-21 and miR-296 microRNAs as a favorable event for neo-blood vessel formation while overexpression of miR-15b and miR-299 has been evidenced as anti-angiogenic in glioblastoma[178]. VEGF-A ligands (regulated by both hypoxia and Oncogenic signaling) binds to VEGF (1-3) receptors present on endothelial cell surface in order to activate endothelial cell proliferation and migration towards the tumor [179,180]. The neo-vasculature thus formed, shows prematurely developed capillary sprouting, tangled vessel branching, twisted and out of shape vessels and uneven blood circulation [181]. Angiogenic phenomenon is an early event during premalignant neoplastic growth which also supports the invasive phenotype of glioblastoma[182]. Glioblastoma stem-like cells (GSCs), which contribute to the tumor heterogeneity and also the reason of chemo-resistance, are equipped with the ability to differentiate into endothelial and pericyte-like cells forming a pseudo-vasculature, a phenomenon known as “vasculature mimicry”.[183–186] It was found that these endothelial-like tumor cells bear similar mutations as is found in the adjacent tumor bulk surrounding the vasculature and was more prevalent in the tumor core rather than the tumor edges. Furthermore, immune system of the host also plays significant role in enhancing nutrient supply to the growing glioblastoma via induction of angiogenesis. The fact that the immune cell infiltration to the tumor microenvironment depends on the vessel normalization, application of anti-angiogenic therapies modulate this aspect of tumor vasculature leading to recruitment of bone-marrow derived myeloid cells whereas the tumor and stromal secreted factors changes the phenotypes of these cells to more tumor–supportive (for example M2 phenotype of macrophages) leading to resistence against current anti-angiogenic therapies[187]. These secretory factors

include VEGF which suppresses T-cell immune response by inhibiting dendritic cell maturation, granulocyte colony-stimulating factor (G-CSF) and interleukin-17 (IL-17) promoting refractoriness of glioblastoma to anti-angiogenic therapies[188–190]. Such a complex regulation of angiogenesis requires proper stratification of patient cohorts in order to effectively examine the effect of anti-angiogenic therapies targeting various angiogenic factors in glioblastoma. Thus there is an urge for a better understanding and identification of reliable biomarkers of angiogenesis in glioblastoma. Some of the biomarkers that have been taken into consideration are tissue biomarkers including, VEGF, CA9, CD68 & CD11 (tumor-associated macrophages); blood biomarkers like VEGF and sVEGFR2, SDF-1α, PIGF, and MMPs, and imaging biomarkers[187].

1.5 Peptidyl-glycine alpha-amidating monooxygenase

Peptidyl-glycine alpha-amidating monooxygenase (PAM) is the only bi-functional enzyme which activates neuro-peptides. PAM, a type-I integral membrane protein, catalyzes the amidation of the C-terminus glycine residue with its hydroxylating monooxygenase domain (PHM) which is then identified and cleaved off by its lyase enzymatic domain (PAL) in a ascorbate, copper and oxygen dependent manner (Figure 6)[191–194]. Both the hydroxylating monooxygenase and lyase domain has optimum activity under low pH of the secretory pathway lumen[195]. PHM domain is made up of two core domains each having eight anti-parallel β-strands having hydrophobic core joined by disulphide linkages. Both the domains are linked with a single polypeptide chain and each has a copper binding site separated by an 11 A° cleft, a site where peptidyl-glycine substrate binds[196,197]. On the other hand, PAL catalytic domain has a six-bladed β-propeller also held together by disulphide linkages. The cavity in the center of the domain has a calcium binding site for structural integrity and a zinc-binding site for catalytic function of the domain[198].

Figure 6. PAM catalyzes the activation of neuropeptides.
PHM domain of PAM hydroxylates the c-terminus glycine residue which is then identified and cleaved off by PAL domain leading to activation of the neuropeptides, for example, ADM[199].

The longest isoform of PAM i.e. PAM-1 consists of the two enzymatic domains having endoprotease-sensitve linker region between them, the transmembrane domain and the cytosolic domain. PAM-2 isoform lacks this linker region while PAM-3 isoform lack both the transmembrane domain, in addition to the linker region between the enzymatic domains and thus is expressed as a soluble isoform (Figure 7).

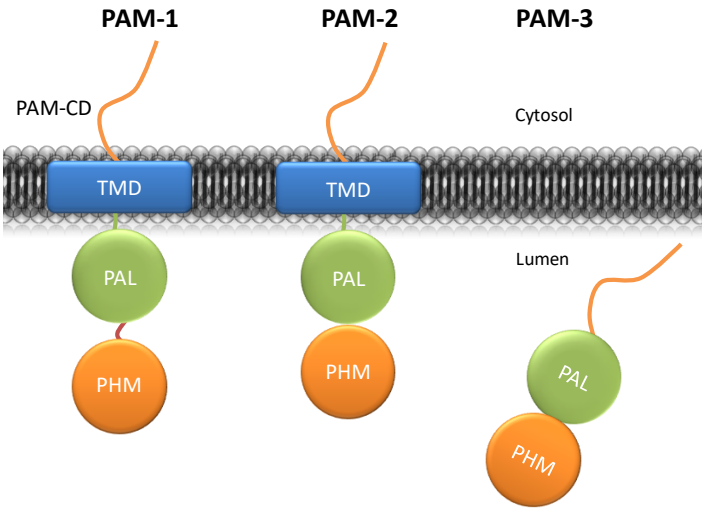

Figure 7. PAM splice variants.
PAM consists of a hydroxylating domain (PHM), a lyse domain (PAL), a linker region between these catalytic domain, a transmembrane domain and a cytoplasmic unstructured tail. The figure shows different isoforms of PAM depending upon presence and absence of linker region between the catalytic domains and the transmembrane domain of PAM[199].

PAM is expressed in different tissues at varied levels and has been found in endocrine tissues, airway epithelium, ependymal cells in the brain, endothelial cells, and adult atrium as well as the brain and pituitary. Heart and neuronal tissues have specifically shown tissue-specific expression of different isoforms of PAM indicating their distinct roles[200,201]. Soluble forms of PAM have also been found in serum and cerebrospinal fluid[202,203]. Apart from the catalytic domains of PAM, another very significant component of PAM is the unstructured cytosolic domain (86 amino acids long) sensitive to endo-proteolytic cleavage. This domain contains few hydrophobic patches and is essential for interaction with different proteins including kinases that phosphorylates and regulates PAM trafficking through the secretory pathway[204]. KALIRIN and TRIO (Rho GDP/GTP exchange factor (Rho-GEF) family) which are essential for cytoskeleton control and the maintenance of synapses, and Rassf9, a member of the Ras-association domain family (important for epidermal homeostasis) have been found interacting with PAM. A Ser/Thr kinase, Uhmk1, phosphorylates the C-terminus of PAM[205,206]. Adaptor protein-1 (member of endosomal and secretory granule coat prtoeins) responsible for linking cargo proteins to clathrin, interacts with PAM along with Atp7a (the P-type ATPase necessary for copper transport to golgi-vesicle)[207]. Various phosphorylation sites have been detected in the cytosolic domain of PAM using mass spectrometry and assigned specific roles in its trafficking through the secretory and endocytic pathway using phosphomimetic mutants[204]. The cytosolic domain of PAM can be cleaved off by different enzymes like γ-secretase which generates a short-lived 16 kDa soluble protein fragment (sf-CD) also shown to localize to the nucleus and act as a signaling molecule[208]. Increased expression of PAM-1 changes the cell morphology and modulates expression of certain proteins like copper chaperones, aquaproin 1 and Slpi protease inhibitor which might be due to the sf-CD-mediated alteration of gene expression[209]. PAM

has been correlated with maintenance of copper homeostasis and termed as a copper sensing protein. Studies involving PAM heterozygous mice show defects like increased adiposity, behavioral defects like body temperature disbalance, increased anxiety and seizures as observed in copper restricted diet in normal mice[210–212]. PAM has also been implicated as a rapid sensor of oxygen availability as the PHM activity is completely dependent on the presence of oxygen[213]. On the other hand the linker region between the PHM and PAL domain of PAM with a cluster of histidine residues (His–Gly–His–His), has been shown to act as a pH sensor determining the fate of PAM-1 after being internalized from plasma membrane[214]. PAM is expressed in many different cancer types like prostrate, breast, glioblastoma, lung, pituitary and colon cancer, and relates with the phenotypic changes brought forward by the downstream activated neuropeptides like adrenomedullin[215–222]. Knowing the numerous other functions of PAM protein, it will be quiet essential to understand different mechanism with which PAM regulates phenotypic changes in cancer in general (Figure 8).

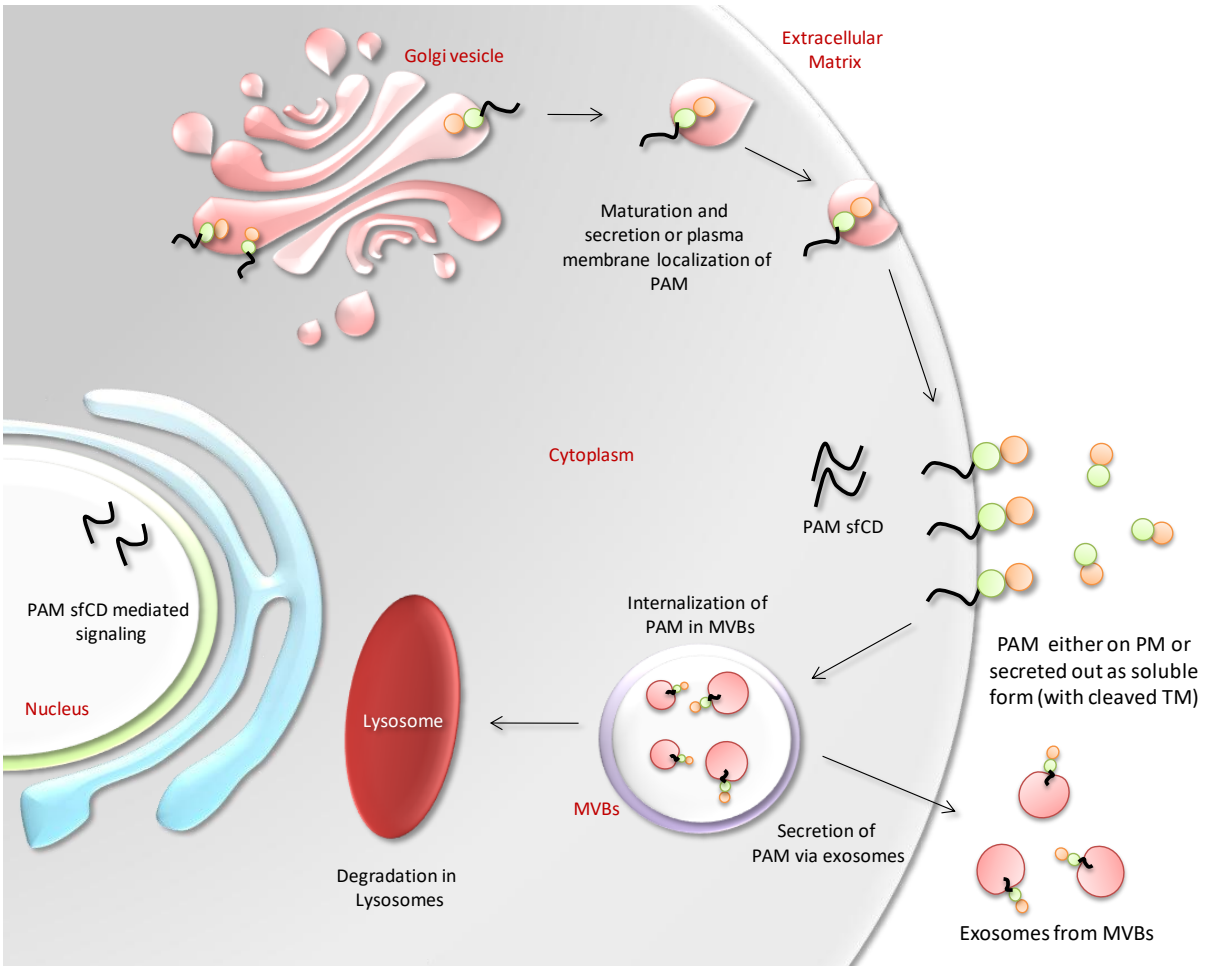

Figure 8. PAM trafficking through biosynthetic and endocytic pathways.
PAM isoforms are effectively secreted or expressed on the surface of the cell. Post-translational modification of the cytosolic domain of PAM regulates its trafficking within different membranous system in the cell. PAM present in multi-vesicular bodies can either be subjected to degradation in lysosomes or secreted out of the cell in the form of exosomes[199].

1.6 Aim of the Study

Glioblastoma is the most aggressive form of primary brain tumor with less than 15 months of median patient survival. The main reason behind this poor prognosis is its intra-tumoral genetic heterogeneity which leads to a highly resistant phenotype showing a high rate of neo-vasculature formation, diffused growth and modulation of the tumor microenvironment jeopardizing the current therapy regimen. This aggressive phenotype renders the tumor cells with high level of ER stress activating unfolded protein response (UPR) which supports them at almost every stage of tumor progression starting from the transformation and proliferation to their invasion to distant locations thus becoming one of the leading pathways promoting tumor growth. In order to better understand the role of the UPR in glioblastoma to target it effectively, the main theme of the PhD thesis is to determine hypoxia-led regulation of UPR in the tumor progression and identify potential therapeutic targets against its different hallmarks. To address these questions, we first characterized the activation of UPR in glioblastoma cells under artificial (Tunicamycin or thapsigargin) and a physiological (hypoxia) ER stress inducer, in regulating different UPR branches. UPR-mediated changes in the secretome of hypoxia treated glioblastoma cells was analyzed later using mass spectrometry based on specific UPR sensor protein. A potential hit thus identified was validated and characterized for its regulation with the specific UPR sensor and its role in regard to angiogenesis in glioblastoma. Pro-tumorigenic benefits of the target protein were studied in xenograft mouse model.

2. Materials & Methods

2.1 Materials

2.1.1 Antibodies

Antibody	Product Number
Anti-PERK	Cell Signaling (3192S)
Anti-Goat, HRP couple	Santa Cruz Biotech, Heidelberg, Germany
Anti-Guinea pig, HRP coupled	Santa Cruz Biotech, Heidelberg, Germany
Anti-eIF2α	Cell signaling (9722S)
Anti-eIF2S1	Abcam (ab32157)
Anti-mouse, HRP coupled	Cell Signaling Technology, Danvers, USA
Anti-ATF6α	Novus Biologicals (NBP1-40256)
Anti-IRE1α	Santa Cruz (sc-20790)
Anti-P-IRE1α	Thermo Scientific (PA1-16927)
Anti-EEF2	Santa Cruz (sc-166415)
Anti-PAM	Abcam (ab109175)
Anti-ATF4	Cell Signaling (11815S)
Anti-rabbit, HRP coupled	Cell signaling Technology, Danvers, USA
Anti-CHOP	Cell Signaling (2895S)
Rabbit anti-human IgG Control	Jackson's Immuno Research (309-005-008)
Mouse IgG Control	Santa Cruz, Heidelberg, Germany
Anti-α-HIF1α	Cell Signaling (3716S)
Anti-FOSL1	Santa Cruz (sc-605)
Anti-c-JUN	Santa Cruz (sc-1694)
Anti-P-c-Jun	Santa Cruz (sc-16311R)
Anti-Hevin	Santa Cruz (sc-165539)
Anti-CTGF	Santa Cruz (sc-14939)
Anti-CYR61	Santa Cruz (sc-13100)
Anti-XBP1s	Biolegend (619502)
Anti-GRP78 (BIP)	Santa Cruz (sc-1050)

2.1.2 Buffers

Buffers	Composition
1x Phosphate buffered saline (PBS)	137 mM NaCl, 2.7 mM KCl, 9.2 mM Na2HPO4, 1.8 mM KH2 PO4, pH 7.4
1x Transfer buffer	25 mM Tris, 200 mM glycine, 20 % methanol, pH 8.8
1x TRIS buffered saline (TBS)	150 mM NaCl, 10 mM Tris, pH 7.5
1x TRIS-Borat-EDTA (TBE)	0.445 M Tris-Borat, 10 mM EDTA, pH 8

Blocking buffer	5 % milk powder or 5 % BSA in TBS-T
Loading buffer (6x)	30 % Glycerine, 0.25 % Bromophenol blue

2.1.3 Bacterial Culture Media

Medium	Composition
LB (Luria-Bertani)	0.5 % (w/v) NaCl, 1 % (w/v) Tryptone, 0.5 % (w/v) Yeast extract
LB Agar	0.5 % (w/v) NaCl, 1 % (w/v) Tryptone, 0.5 % (w/v) Yeast extract, 1.6 % (w/v) Agarose

2.1.4 Biochemical Reagents

Reagent	Product Number
Agarose	Sigma-Aldrich, Munich, Germany
Ampicillin	Roche Diagnostics, Mannheim, Germany
Bicinchoninic acid (BCA)	Sigma-Aldrich, Munich, Germany
Bovine serum albumin	New England Biolabs (NEB), Ipswich, USA
Bromophenol blue	Waldeck GmbH, Münster, Germany
Complete mini protease inhibitors	Roche Diagnostics, Mannheim, Germany
cOmplete™, EDTA free protease inhibitor cocktail	Roche Diagnostics, Mannheim, Germany
Dithiotreitol (DTT) (0.1 M)	Thermo Fischer Scientific, Langenselbold, Germany
DNA loading dye (6x)	Thermo Fischer Scientific, Langenselbold, Germany
DNA marker (1kb)	Fermentas, St Leon-Rot, Germany
dNTP mix (100 µM each)	Thermo Fischer Scientific, Langenselbold, Germany
Ethanol	Merck Millipore, Darmstadt, Germany
Ethidium bromide	Sigma-Aldrich, Munich, Germany
Ethyl acetate, 99.7 %	Sigma-Aldrich, Buchs SG, Switzerland
Ethylendiaminetetracetate (EDTA) (25 mM)	Thermo Fischer Scientific, Langenselbold, Germany
Glycerol	Carl Roth, Karlsruhe, Germany
Hardset antifade mounting medium with DAPI	Vector Laboratories, Burlingame, USA
Histoplast parafin	Thermo Fischer Scientific, Langenselbold, Germany
IP lysis buffer	Thermo Fischer Scientific, Langenselbold, Germany
Methanol	Sigma-Aldrich, Munich, Germany
Nuclease-free water	Ambion, Austin, USA
NuPAGE® LDS sample buffer (4x)	Life Technologies, Darmstadt, Germany
NuPAGE® SDS running buffer (20x)	Life Technologies, Darmstadt, Germany

Oligo-d(T) nucleotides	Thermo Fischer Scientific, Langenselbold, Germany
Paraformaldehyde (PFA)	Sigma-Aldrich, Munich, Germany
PCR nucleotide mix	Roche Diagnostics, Mannheim, Germany
Pierce ECL Western blotting substrate	Thermo Fischer Scientific, Langenselbold, Germany
Random primer mix	New England Biolabs NEB), Ipswich, USA
RIPA-lysis buffer	Sigma-Aldrich, Munich, Germany
Sodium dodecyl sulfate (SDS)	Sigma-Aldrich, Munich, Germany
Sodium fluoride (NaF)	Carl Roth, Karlsruhe, Germany
Sodium orthovanadate (Na_3VO_4)	Carl Roth, Karlsruhe, Germany
Spectra multicolor broad range protein ladder	Fermentas, St Leon-Rot, Germany
Tris-(hydroxymethyl)-aminomethan (TRIS)	Carl Roth, Karlsruhe, Germany
Triton X-100	Sigma-Aldrich, Munich, Germany
Tween-20	Sigma-Aldrich, Munich, Germany
Whole milk powder	Carl Roth, Karlsruhe, Germany

2.1.5 Cell Culture Reagents and Materials

Article	Company
2-Mercaptoethanol, 98 %	Sigma-Aldrich, Munich, Germany
96-well plates (white, non-binding with clear bottom)	Greiner/Sigma-Aldrich, Munich, Germany
Accutase solution	Sigma-Aldrich, Munich, Germany
Cryo tubes	Nunc, Wiesbaden, Germany
Dimethyl sulphoxide (DMSO)	Sigma-Aldrich, Munich, Germany
DMEM (Dulbecco's modified eagle medium)	Sigma-Aldrich, Munich, Germany
Fetal calf serum (FCS)	Merck Millipore, Darmstadt, Germany
Horse serum	Merck Millipore, Darmstadt, Germany
L-Glutamine	Thermo Fischer Scientific, Langenselbold, Germany
Opti-MEM I reduced serum medium	Thermo Fischer Scientific, Langenselbold, Germany
PBS	Thermo Fischer Scientific, Langenselbold, Germany
Penicillin/Streptomycin (10000 U/ml, 100 µg/ml)	Thermo Fischer Scientific, Langenselbold, Germany
Puromycin	VWR International, Darmstadt, Germany
Reservoir (sterile)	Corning inc., Corning, USA
Syringe filters (0.45 µm)	Merck Millipore, Darmstadt, Germany
TransIT®-LT1 transfection reagent	Mirus Bio, Madison, USA
Trypsin EDTA solution (0.5 %)	Sigma-Aldrich, Munich, Germany

2.1.6 *In vivo* Reagents and Materials

Article	Company
Isoflurane	Abbott, Wiesbaden, Germany
Nanofil needle with syringe	World Precision Instruments, Sarasota, USA
Small animal stereotaxic instrument, model 900	David Kopf Instruments, Tujunga, USA
VivoGlo™ luciferin	Promega, Madison, USA

2.1.7 Mice

Strain	Source
Nonobese diabetic/severe combined immunodeficiency (NOD-SCID)®	In-house breeding facility of the DKFZ, Heidelberg, Germany

2.1.8 Cell Lines

Glioblastoma Stem-like Cell Lines

GSC lines were obtained from Christel Herold-Mende at the Division of Experimental Neurosurgery in the University of Heidelberg.

Cell Line	Sex	Age (Years)	OS** (Months)
NCH421k	M	66	34
NCH711d	M	20.4	N/A*
NCH644	F	67	30
NCH705	N/A*	78	24

N/A* not available

2.1.9 Other Cell Lines

Cell Line	Origin	Source
LN308	Human glioblastoma	(Bady et al., 2012)
LN229	Human glioblastoma	(Weiler et al., 2014)
HEK293T	Human Embryonic Kidney	ATCC, Wesel, Germany
Normal Human Astrocytes	Human Brain	Kindly provided by Andreas von Deimling, Department of Neuropathology, DKFZ, Heidelberg, Germany
NCH82	Human glioblastoma	(Karcher et al., 2006)

2.1.10 Bacteria

Cells	Supplier
OneShot® STABL3 chemically competent *E.coli*	Thermo Fischer Scientific, Langenselbold, Germany

2.1.11 Enzymes

Enzyme	**Company**
Age I (10 U/µl)	Thermo Fischer Scientific, Langenselbold, Germany
DNase I (1 U/µl)	Thermo Fischer Scientific, Langenselbold, Germany
EcoRI (10 U/µl)	Thermo Fischer Scientific, Langenselbold, Germany
PRECISOR High-Fidelity DNA Polymerase	BioCat, Heidleberg, Germany
RNase I (1 U/µl)	Thermo Fischer Scientific, Langenselbold, Germany
SuperScript II Reverse Transcriptase	Thermo Fischer Scientific, Langenselbold, Germany
Xbal (10 U/µl)	Thermo Fischer Scientific, Langenselbold, Germany

2.1.12 Databases

Databases	**Address**
cBioPortal for Cancer Genomics	www.cbioportal.org/
Ensembl	www.ensembl.org
Gene Cards (Human Genes Database)	www.genecards.org/
OligoCalc	www.basic.northwestern.edu/biotools/oligocalc.html
--PubMed	www.ncbi.nim.nih.gov/PubMed/
Universal Protein Resource	www.uniprot.org
R2: Genomics Analysis and Visualization Platform	https://hgserver1.amc.nl/cgi-bin/r2/main.cgi

2.1.13 Equipment

Equipment	**Company**
Axioplan 2 microscope	Carl Zeiss Microscopy, Jena, Germany
Biofuge Fresco table top centrifuge	Haraeus Instruments, Hanau, Germany
Cytospin3-centrifuge	Thermo Fischer Scientific, Langenselbold, Germany
Dynamag™ magnet	Thermo Fischer Scientific, Langenselbold, Germany
Heating block QBT	Grant Instruments, Cambridge, UK
HistoCore Arcadia embedding system	Leica Biosystems, Wetzlar, Germany

Incubator HERA cell 150	Thermo Fischer Scientific, Langenselbold, Germany
L8-M ultracentrifuge	Beckmann Coulter, Krefeld, Germany
Leica TCS SP5 confocal microscope	Leica Biosystems, Wetzlar, Germany
Mini Trans-Blot® cell	Bio-Rad, Munich, Germany
Mithras LB 940 plate reader	Berthold Technologies, Bad Wilbad, Germany
NanoDrop®ND-1000 spectrometer	NanoDrop, Wilmington, USA
QuickPoint electrophoresis cell	Novex, Sandiego, USA
Vortex Genie 2	Scientific Industries Inc., New York, USA
Water bath B-480	Büchi, Flawil, Switzerland
XCell SureLock™ Mini-Cell electrophoresis system	Thermo Fischer Scientific, Langenselbold, Germany

2.1.14 Kits

Kit	Company
ABsolute SYBR® Green ROX mix	Thermo Fischer Scientific, Langenselbold, Germany
CellTiter-Glo® luminescent cell viability assay	Promega, Madison, USA
Maxi preparation DNA kit	Qiagen, Hilden, Germany
Mini preparation DNA kit	Qiagen, Hilden, Germany
Rapid DNA dephos and ligation kit	Roche Diagnostics, Mannheim, Germany
RNeasy® Mini kit	Qiagen, Hilden, Germany

2.1.15 Other Material

Article	Supplier
96-well low profile PVS plate (skirted)	Thermo Fischer Scientific, Langenselbold, Germany
ABgene™ adhesive PCR plate seals	ABgene, Epsom, UK
Cover slips (10 mm round)	Thermo Fischer Scientific Gerhard Menzel, Braunschweig, Germany
Cover slips (26 x 76 mm)	Thermo Fischer Scientific Gerhard Menzel, Braunschweig, Germany
Dynabeads® Protein G	Thermo Fischer Scientific, Langenselbold, Germany
Glass slides	Sigma Aldrich, Munich, Germany
Glass vials	Mikrolab Aarhus A/S, Viby, Denmark
NuPAGE® antioxidant	Life Technologies, Darmstadt, Germany
NuPAGE® Bis-Tris precast gels (15 or 10 well; 1.5 or 1 mm)	Life Technologies, Darmstadt, Germany
PCR tubes (0.2 ml)	Molecular BioProducts, San Diego, USA
Pipette tips (10 µl, 20 µl, 100 µl, 200 µl, 1000 µl)	Starlab, Ahrensburg, Germany

Polyvinylidene fluoride (PVDF) membrane	Sigma Aldrich, Munich, Germany
Reaction tubes (1.5 ml and 2 ml)	Eppendorf, Hamburg, Germany
X-ray films, Super RX	FUJIFilm, Tokyo, Japan

2.1.16 Plasmids

Commercially Available Plasmids (Plasmid maps are provided in the Appendix section)

Plasmid	Company
pLKO.1 puro	Addgene, Cambridge, USA
pLVX-Puro	Clontech, Mountain View, USA
pMD2.G	Addgene, Cambridge, USA
psPAX2	Addgene, Cambridge, USA

2.1.17 Generated Plasmids

pLVX-tGFP

pLVX-PAM

pLKO-puro-shNT

pLKO-puro-shPERK

pLKO-puro-shPERK-2

pLKO-puro-shPAM

pLKO-puro-shGCN2

pLKO-puro-shPKR

pLKO-puro-shHRI

pLKO.1-shNT-GFP-fLUC

2.1.18 List of primers and shRNA target sequences

List of primers used for quantitative PCR

Name	**Forward Primer**	**Reverse Primer**
XBP1s	TGAGTCCGCAGCAGGTGCA	CTGGGTCCTTCTGGGTAGACCTC
NDRG1	GTTTCCTGGCGTCGTCTC	ATGTCCCTGCTGTCACCTG

XBP1-EP	CCTGGTTGCTGAAGAGGAGG	CCATGGGGAGATGTTCTGGAG
PAM	TTACACCTCACACGTCTGCC	ATCAACTGGATGCCCCACAG
VEGF-A	GGCCTCCGAAACCATGAACT	TGGGACTTCTGCTCTCCTTCT
HIF1α	TCCATGTGACCATGAGGAAA	CCAAGCAGGTCATAGGTGGT
PERK	GCCAATGACAGTAGCTGGAATG	GTGTTCAAGCTTGGCTAAGGCTT
EEF2	CTGGAGATCTGCCTGAAGGA	GAGACGACCGGGTCAGATT
RPS13	CCCAGTCGGCTTTACCCTAT	GCCCTTCTTGGCCAGTTTGT

List of shRNA target sequences

Target Gene	**Target sequence**
PERK-1	GGCAACCATTGTGCTAATAAA
PERK-2	GCCACTTTGAACTTCGGTATA
HIF1α	CCGCTGGAGACACAATCATAT
PAM	GCCTTTAATTGCTGGCATGTA
Non-Target (NT)	CAACAAGATGAAGAGCACCAA

2.1.19 Software

Software	**Company**
Basic Local Alignment Search Tool (BLAST)	blast.ncbi.nlm.nih.gov
GraphPad Prism 7	GraphPad, San Diego, USA
ImageJ	rsbweb.nih.gov/ij
Microsoft Excel 2010	Microsoft, Redmond, USA
PlasMapper Version 2.0	wishart.biology.ualberta.ca

2.2 Methods

2.2.1 Cell culture

LN308, LN229, NCH82 glioblastoma cells were cultured in DMEM (Sigma-Aldrich, Munich, Germany) with 10% FCS (Merck Millipore, Darmstadt, Germany) and Penicillin/Streptomycin (10000 U/ml, 100 µg/ml; Thermo Fischer Scientific, Langenselbold, Germany). HUVECs cells were cultured in dishes pre-coated with 0.2% gelatin in dH_2O. Endopan 3 medium (PAN biotech-P04-0010k) along with provided supplements was used to culture HUVECs and accutase (Sigma-Aldrich, Munich, Germany) was used to split these cells. Cells were regularly checked for mycoplasma contamination as per the recommendations of the German Collection of Microorganisms and Cells (Germany). Glioblastoma cell lines were authenticated using single nucleotide polymorphism profiling. GSCs were isolated from primary

GBM tumors resected from patients as per legal guidelines approved by Institutional Review board at the Medical Faculty of Heidelberg. Tumor samples were dissociated enzymatically to isolate cells which were cultured as neurospheres. The cells were grown in standard culture conditions (37°C, 95 % humidity and 5 % CO_2) in serum-free stem cell medium (DMEM/F-12 medium, 20 % (v/v) BIT-admixture and 20 ng/ml each of basal fibroblast growth factor (bFGF) and epidermal growth factor (EGF)).

2.2.2 Lentivirus production

Lentivirus was produced in HEK-293T cells using TransIT®-LT1 by transfecting a lentiviral construct of interest along with pMD2.G (Addgene, USA), psPAX2 (Addgene, USA). Conditioned media with the virus particles was pre-cleared via centrifugation for 5 min at 2000 rpm and filtered through 0.45 µm cellulose acetate filters (Merck-Millipore, Germany). Lenti-viral particles were harvested by centrifuging the cleared conditioned media for 90 min at 25000 rpm at 4°C using SW41 swing-out rotor in a L8-M ultracentrifuge. The virus particles were resuspended in PBS and stored at -80 °C. The virus titer was determined by infecting target cells using dilutions which resulted in linear relationship between the dilution and percentage of GFP-positive cells.

2.2.3 pLKO.1 shRNA Cloning

shRNA oligos (section 2.2.18) were primed at 95°C for 4 min using hybridization buffer (Tris HCl (pH 7.8), 100 mM, NaCl 1M, and EDTA 10 mM). The primed oligos were then ligated into pLKO.1 vector digested with EcoRI and AgeI restriction enzymes using T4 DNA ligase (EL0011) overnight. The ligation mix was transformed in *E. Coli* DH5α competent cells and colonies were confirmed for the presence of shRNA oligos first using colony screening PCR and later sequencing.

2.2.4 Immuno-blotting

Cells were lysed in 100 µl RIPA-lysis buffer (R0278-50ML) supplemented with 10 mM NaF, 10 mM Na_3VO_4 and complete mini protease inhibitor cocktail (Roche #11836170001). The lysed cells were centrifuged for 20 minutes at 13000 rpm. Protein extracts were stored at -80°C. Bicinchoninic assay was used to measure protein concentration. Protein samples were prepared using LDS sample buffer (Novex #NP0007) and equal amount of protein was loaded onto 4-12 % Bis-Tris Gels (40 µg from cell pellet and 3 µg from conditioned media). Electrophoresis was performed at 250 V and 170 mA for 45 minutes in MOPS running buffer. Protein was later transferred on a PVDF membrane using a protocol having

subsequent increase in current every 10 minutes for 50 minutes (100, 200, 300, 400, 500 mA). The membrane was blocked, incubated with primary and subsequently with respective secondary antibody. The protein detection was done on X-ray films.

2.2.5 Real-time PCR

RNA isolation was performed using Qiagen RNA isolation kit (#74106) as per the product manual. 1 ug of RNA was used to synthesize cDNA using ProtoScript® II Reverse Transcriptase, NEB (#M0368L). Real time PCR was performed by mixing 10 ng of cDNA, 0.5 µM of forward & reverse primer each (final concentration; Appendix Table S2) and Qiagen SyBr green dye (#204057). LightCycler 480 instrument was used to perform the RT-PCR.

2.2.6 Mass spectrometry experiment design

$1x10^6$ LN308 glioma cells were seeded and were allowed to grow until 70-80 percent confluency (2 days). The cells were washed and incubated in serum-free-DMEM. Overnight incubation of GSK2606414 (1 µM) was given as a PERK negative control. The next day, cells were incubated under hypoxic condition of 1% O_2. After 72 hours incubation, the conditioned media was collected in 50 ml falcon and spin down at 2000 rpm for 3 min. The conditioned media (free of debris) was collected in a new 50 ml falcon tube after filtering the content through a 0.45 µm filter. The filtered conditioned media was emptied in an Amicon Ultra-15 (PLGC Ultracel-PL Membrane, 10 kDa, UFC901008, EMD Millipore). The conditioned media was concentrated by centrifuging the filter at 4000 rpm for 15 min at 4 °C. The concentrated media content was collected in a 2 ml tube and snap frozen.

2.2.7 Proteomics sample preparation

Each sample type was prepared in three biological replicates. For the protein precipitation, 2.25 ml of ice cold ethanol was added to 250 µl of cell secretome samples. After ~16 hour of precipitation at -80°C, the protein pellets were collected by centrifugation at 18.000 g, 4 °C for 30 min. 20 µl of 6M Guanidine-Hydrochloride (Gu-HCl, Sigma-Aldrich, USA) was used to dissolve the protein pellets. 50 mM of NH_4HCO_3 (pH 7.8, Sigma-Aldrich, USA) was added to dilute the concentration of Gu-HCl to 0.6 M for the protein amount determination using bicinchoninic acid assay (Pierce™ BCA Protein Assay Kit, ThermoFisher Scientific™ Hamburg Germany).The samples were then reduced with 10 mM final concentration of Tris (2-carboxyethyl) phosphine hydrochloride (TCEP, Sigma-Aldrich, USA) at 56 °C for

30 min, alkylated with 30 mM Iodoacetamide (IAA, Sigma-Aldrich, USA) at 25 °C in dark chamber for 30 min and diluted to 0.2 M Gu-HCl with 50 mM of NH_4HCO_3 (pH 7.8) for Trypsin digestion. Trypsin (Trypsin Gold, Promega, USA) was added at a ratio of 1:50 (w/w, protease to substrate) for the enzymatic digestion. The digestion was performed for maximum 15 hours at 37 °C. The digestion was stopped by acidifying with 10% trifluoroacetic acid (TFA) until pH <2. The peptide samples were desalted using solid phase extraction method utilizing SepPak C18 cartridges (100 mg sorbent per cartridge, Waters, USA). The cartridges were preconditioned twice with 1 ml methanol each time and then equilibrated three times with 0.1% TFA. The peptide samples were loaded onto the cartridges. After washing three times with 1 ml 0.1% TFA, they were eluted with 80% acetonitrile (ACN), 0.1% formic acid (FA) and dried under vacuum. The dried peptides were dissolved in 0.1% TFA and stored at -80°C for further analysis. The digestion quality was checked by monolithic reverse phase separation as described in Burkhart et al. 2012.

2.2.8 LC-MS/MS analysis

1µg of peptide was used per injection on an Ultimate 3000 Rapid Separation Liquid Chromatography (RSLC) nano system coupled to a Q-ExactivePlus mass spectrometer (both ThermoFisher Scientific, Germany). Peptides were trapped on a pre-column (Acclaim C18 PepMap100, 100 µm 2 cm, ThermoFisher Scientific, Germany) using 0.1% TFA at a flowrate of 20 µl/min and subsequently separated on a reverse phase main-column (Acclaim C18 PepMap100, 75 µm-50 cm, Thermo Scientific, Germany) using a binary gradient consisted of A: 0.1% formic acid (FA) and B: 84% acetonitrile, 0.1% FA at a flow rate of 250 nl/min. The linear gradient was run from 3 to 42% for 180min at a flow rate of 250 nl/min. For the mass spectrometry (MS) analysis, full MS scans were acquired at a resolution of 70.000 full width at half maximum (FWHM), target value of 3e6, maximum injection time of 120 ms. Data dependent MS scans were acquired using high-energy collisional dissociation (HCD) on 15 most abundant ions (top15) at normalized collision energy of 27%, resolution of 17.500 FWHM, isolation window of 1.2 m/z, target value of 5e4 and maximum injection time of 250 ms. Only precursor ions with charge states between 2 and 4 will be fragmented.

2.2.9 Label free data analysis

For the data analysis, Progenesis QI for Proteomics software (version 3.0 Non-Linear Dynamics) was used. The peptide identification was done using two search algorithms: X!Tandem [224] via SearchGUI interface version 2.5.0 [225] and Mascot 2.4 (Matrix Science). The Uniprot human database (downloaded on 22sd of July 2015) was used with the following search parameters: Trypsin as protease (maximum 2 miss cleavages), fixed modification: carbamidomethylation at cysteine, variable modification: oxidation at

methionine, 10 ppm as MS1 tolerance and 0.02 Da as MS2 tolerance. To combine search results from X!Tandem and Mascot, PeptideShaker version 1.9.0 [226] was used at a false discovery rate of 1 %. Only proteins identified with at least 2 unique peptides were considered for the final analysis. The statistical data analysis was performed using R version 3.3.1 (codename "Bug in Your Hair"). For the calculation and data formatting, packages *reshape2* were used and for the graphical illustrations *ggplot2*and*gridExtra* packages were used. The significance P-value was calculated using function t-test (Student's t-test, two-sided, true variance equality, confidence level at 0.95). Proteins were considered to be differentially regulated, if their P-value was below 0.05 and the fold change was greater than 2 (up-regulated) or less than 0.5 (down-regulated). The mass spectrometry proteomics data have been deposited to the ProteomeXchange Consortium via the PRIDE [227] partner repository with the dataset identifier PXD012523 and 10.6019/PXD012523.

2.2.10 Data availability

Mass spectrometry dataset generated and analyzed in this study is available on ProteomeXchange: PRIDE PXD012523
(https://www.ebi.ac.uk/pride/archive/projects/PXD012523)

2.2.11 PHM activity

Cells were lysed in 10 volumes of buffer containing NaTES–mannitol–Triton X-100 (TMT) (pH 7.4) and protease inhibitors, as previously described[228]. Protein concentrations were determined using BCA reagent (Pierce). Samples were diluted 10-fold in PHM diluent (TMT containing 1 mg/ml bovine serum albumin) and incubated at 37°C for 1 h in the presence of 125I-Acetyl-Tyr-Val-Gly, $CuSO_4$ and ascorbate (for PHM assays) or 125I-Acetyl-Tyr-Val-(OH)-Gly (for PAL assays)[228]. Uncharged amidated product was extracted with ethyl acetate and counted. Data were converted to picomoles of the product per microgram of protein per hour (pmol/µg protein/h) and analyzed with unpaired *t* tests. Each sample was assayed in triplicate.

2.2.12 Immunofluorescence

The coverslips were washed with PBS twice and the cells were fixed using 4% formaldehyde overnight, washed thrice in PBS and blocked in blocking buffer (1X PBS/5% normal serum/0.3% Triton™ X-100) for 60 min. The coverslips were incubated with antibody dilution (diluted in 1X PBS/1% BSA/0.3% Triton™ X-100) for overnight at 4°C (PERK ab (AF3999-SP)), rinsed thrice with PBS and incubated with

Fluorochrome-conjugated secondary antibody for 1–2 hr at room temperature in the dark and humid environment. ab150089 and ab150132 secondary antibodies were used having Alexa488 and Alexa594 labels respectively. After secondary antibody incubation the coverslips were mounted with Vectorsheild DAPI-mount (#H-1200) onto a glass slide. The images were taken using Leica SP5 confocal microscope.

2.2.13 Dynabeads immunoprecipitation

Cells were lysed using Pierce IP-lysis buffer (#87787). The supernatant was collected in new tubes and pre-cleared using 25 µl of Dynabeads Protein G (Invitrogen #10003D) for an hour at 4°C. In parallel, 25 µl of Dynabeads were washed with PBS-Tween20 (0.1%) and incubated with 1 µg of antibody for 20 min at room temperature on a rocker in 200 µl PBS-Tween20 (0.1%). Later, 500 µg of protein from the pre-cleared lysate was incubated with the Dynabeads-Antibody complex making a final volume of 500 µl in IP-lysis buffer for overnight at 4°C. The Dynabeads were washed with 500 µl PBS-Tween20 (0.1%) thrice and boiled at 95°C for 4 min after resuspending in 5x Laemmli buffer and loaded onto SDS-PAGE gel.

2.2.14 Extracellular vesicle isolation

The conditioned media was collected and taken through sequential centrifugation steps in order to obtain clean extracellular vesicle fraction. The conditioned media was first centrifuged at 1500 rpm for 10 min to remove cell debris. Supernatant was collected and centrifuged at 2500 rpm for 10 min and 4000 rpm for 30 min. The supernatant was used in each step for further processing. The final step involved the centrifugation of collected supernatant at 25000 rpm for 3 hours to obtain extracellular vesicles. The supernatant was discarded and pellet obtained was either resuspended in RIPA for western blotting or reconstituted in PBS overnight at 4°C for electron microscopy imaging.

2.2.15 Electron Microscopy

For electron microscopy (EM) extracellular vesicles from purified preparations were adsorbed onto glow discharged carbon coated formvar grids, washed in buffer and negatively stained with 2% aqueous uranyl acetate. For immuno-EM, the immuno reaction was performed after buffer wash including incubation with blocking agent (Aurion, Wageningen, The Netherlands), dilution series of primary antibody and Protein A-Au reporter (CMC, UMC Utrecht, The Netherlands). Micrographs were taken with a Zeiss EM 910 at 100kV (Carl Zeiss, Oberkochen, Germany) using a slow scan CCD camera (TRS, Moorenweis, Germany).

2.2.16 TCA protein precipitation

Conditioned media was collected and spun down to remove cell debris. The supernatant was then mixed with trichloroacetic acid (TCA) making a final concentration of 10%, and kept at 4°C overnight on ice. The tubes were centrifuged at 13000 rpm for 30 min to pellet down the precipitated protein. Supernatant was discarded and the pellets were washed twice with acetone (kept at -20°C) by centrifuging at 13000 rpm for 30 min. Later, the pellet was dried for two minutes to remove excess of acetone and re-suspended in RIPA buffer. Equal amount of protein was loaded for SDS-PAGE.

2.2.17 Total binding affinity analysis for PAM promoters

Genome-wide total binding affinities (TBA) for transcription factors of all promoters of protein-coding genes was performed as follows: Curated gene transcript annotation was downloaded (December 20, 2018) from the RefSeq track of the UCSC Genome Browser (human reference genome GRCh38/hg38) [229] and filtered for transcripts which contain coding sequences. A promoter was defined as the region spanning from 1500 bases upstream to 500 bases downstream (with respect to the transcription strand) of the transcription start site (TSS). For genes with multiple TSS, all promoters were considered individually, resulting in a total of 25,387 promoters of 19,301 protein-coding genes. Position frequency matrices (PFM) were obtained from JASPAR (release 7, 2018) [230]for core matrices of a total of 579 vertebrate TF, using the R package JASPAR2018 (version 1.1.1) (https://bioconductor.org/packages/release/data/annotation/html/JASPAR20). For each promoter and each TF, we computed the binding affinity using the R package MatrixRider (version 1.12.0) (https://bioconductor.org/packages/release/bioc/html/MatrixRider.html) with a cutoff of zero for *getSeqOccupancy()*, corresponding to the TBA, i.e., the binding affinity summed over the entire promoter rather than over individual TF binding sites [231]. The resulting set of 25,387 TBA obtained for each TF was transformed first by taking the logarithm (base 2) and then by computing the corresponding z-score (i.e., the number of standard deviations it is above or below the mean log2-transformed TBA for that TF). This transformation allows for better comparability between TBA of different TF because the raw TBA scores highly depend on both the length and the information content of the different binding motifs.

2.2.18 Tube formation assay

As described previously, the tube formation assay was performed by coating wells of a 48-well plate with 150 µl of growth factor reduced matrigel (Product #356230; Corning) and allowed to polymerize for 10

min at 37°C [232]. HUVECs were detached using accutase and resuspended in a concentration of 80,000 cells per 800 µl. 250 µl of cell suspension was added to each well coated with matrigel and the plate was incubated at Incubate plate at 37°C and 5%CO_2. The tubes formed by HUVECs were imaged using Axio Vert.A1microscope. The quantification was done manually. A junction is identified as a point where more than 2 segments meet whereas a mesh is identified as a closed network formed by the segments. A segment is a tube formed between two different junctions. The measurement was done manually.

2.2.19 Animal experiments

Anesthetized male NSG mice (NOD SCIDγ Jackson, USA), 10-12 weeks of age, were given an analgesic and xenografted with 8×10^4 LN308 glioma cells expressing GFP and luciferase (stably integrated in the cells using a pLKO lentiviral backbone), at a position 1 mm lateral and 2 mm posterior from the *bregma*. Mice with neurological symptoms or a weight loss of >20% were euthanized. All animal procedures were conducted in accordance with the institutional animal research guidelines after obtaining approval from the regional commission of Karlsruhe, Baden-Wuerttemberg, Germany (file number G127-16). Survival was compared using the log-rank test.

2.2.20 Bioluminescence imaging

All mice were imaged at day 7 and 14 post tumor cell injection. D-luciferin was injected at a concentration of 150 mg/kg body weight (Biomol, Germany). Mice were anaesthetized using 1.5 % of isoflurane (Abbott, Germany). After 10 min incubation, images were acquired using an IVIS Lumina II system (Caliper Life Science, USA) with exposure times of 1, 3 and 5 min. Total bioluminescence flux signals (photons/sec) were quantified with LivingImage 4.4 (PerkinElmer, USA) as a measure of tumor burden.

2.2.21 Statistics

Excel 2010 and GraphPad Prism 7 were used to carry out statistical testing. Experiments were performed in biological triplicate (unless otherwise mentioned) and data provided in the manuscript represents the mean ± standard error. Unpaired two sided student's t-test was used to determine level of significance. Log rank (Cox-Mantel) test was used to calculate the difference in the distribution of survival data in Kaplan Meier analysis.

3. Results

Identification of extracellular matrix proteins regulated by UPR under in glioblastoma

The text and the figures in this section have been adapted from Soni et al., submitted, and correspond to my PhD research project.

3.1 Methodology to decipher the role of hypoxia-induced UPR in expression of extracellular proteins

To understand the role of UPR in modulating the secretome of glioblastoma, we first characterized UPR in LN308 glioblastoma cell model using artificial ER stress inducers. We then identified the activation status of different sensors of the UPR under hypoxic condition (Figure 9) and determined extracellular matrix proteins which the hypoxia-activated UPR branch, already known to regulate angiogenesis, might induce, using proteomics approach. Later, we validated and characterized the potential target. We also studied the phenotypic role of the target in glioblastoma context and subsequently validated the phenotype *in vivo*.

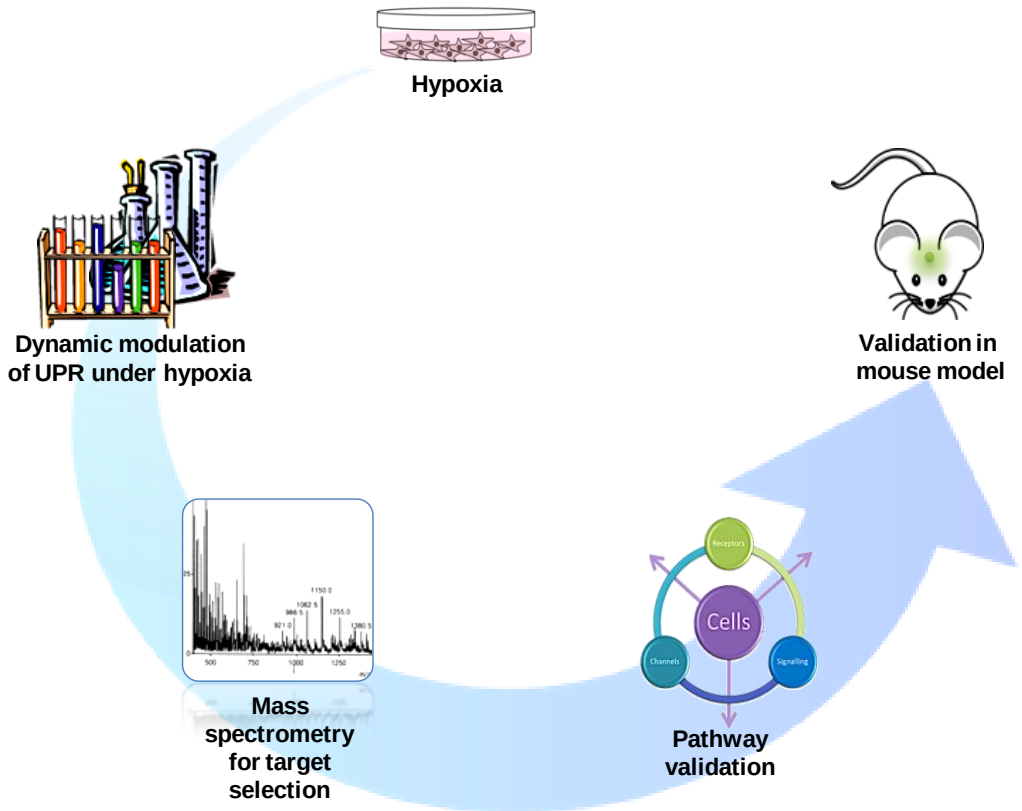

Figure 9. Experimental strategy to determine the UPR-regulated angiogenic targets under hypoxia in glioblastoma cell model.

3.2 Characterization of UPR induction in glioblastoma using artificial ER stress inducers

3.2.1 Activation of UPR pathway proteins: IRE1 and PERK

To understand the dynamics of signaling of different UPR sensors in glioblastoma, we first characterized IRE1α branch of the UPR in glioblastoma cells using artificial ER stress inducers. We examined the phospho-state of IRE1α at Serine 724 residue under tunicamycin treatment. For this, we treated LN308 cells with tunicamycin for 4 hours and harvested the cells, and later immuno-precipitated P-IRE1α population. Figure 10A shows a prominent increase in the P-IRE1α levels under tunicamycin treatment as compared to the vehicle control suggesting an activation of IRE1α by autophosphorylation at Serine 724 residue. Next, we treated the glioblastoma cell lines (LN229 and LN308) and HEK293 cells (a non glioblastoma model) with 2.5 µg/ml of tunicamycin for different time points and analyzed the splicing activity of its RNase domain towards *XBP1* mRNA. Tunicamycin is a nucleoside antibiotic that inhibits N-linked glycosylation of newly synthesized polypeptide chains, specifically inhibiting protein folding and secretion via Golgi vesicles. The accumulation of misfolded proteins in the ER leads to UPR activation. All three cell lines showed activation of *XBP1* splicing within 4 hours of tunicamycin treatment (Figure 10B-D). While both HEK293 and LN308 cells showed an oscillatory pattern of *XBP1s* mRNA generation with time under ER stress, we observed a comparatively reduced IRE1α RNase activity in LN308 cells during the second cycle after 16 hours of tunicamycin treatment in comparison to HEK293 cells suggesting a better adaptation of LN308 cells to ER stress. We also compared the effect of tunicamycin with another artificial inducer of UPR, thapsigargin. Thapsigargin is a non-competitive inhibitor of calcium transport via sarco/endoplasmic calcium ATPases (SERCAs) which causes an increase of cytosolic calcium levels. This reduces the availability of calcium for ER chaperones and leads to accumulation of miss-folded proteins within the ER. Both tunicamycin and thapsigargin showed similar induction of *Hspa5*, a well known ER chaperone expressed under UPR activation, and *XBP1s* mRNA (Figure 10E). This suggests a simultaneous phosphorylation of IRE1α and generation of *XBP1s* in LN308 cells under artificially induced ER stress condition. The data also postulates a dynamic nature of IRE1α during UPR where its activation reduces gradually with time to possibly maintain a pro-survival effect, but is increased again potentially due to inability of the UPR to cope with accumulating ER stress.

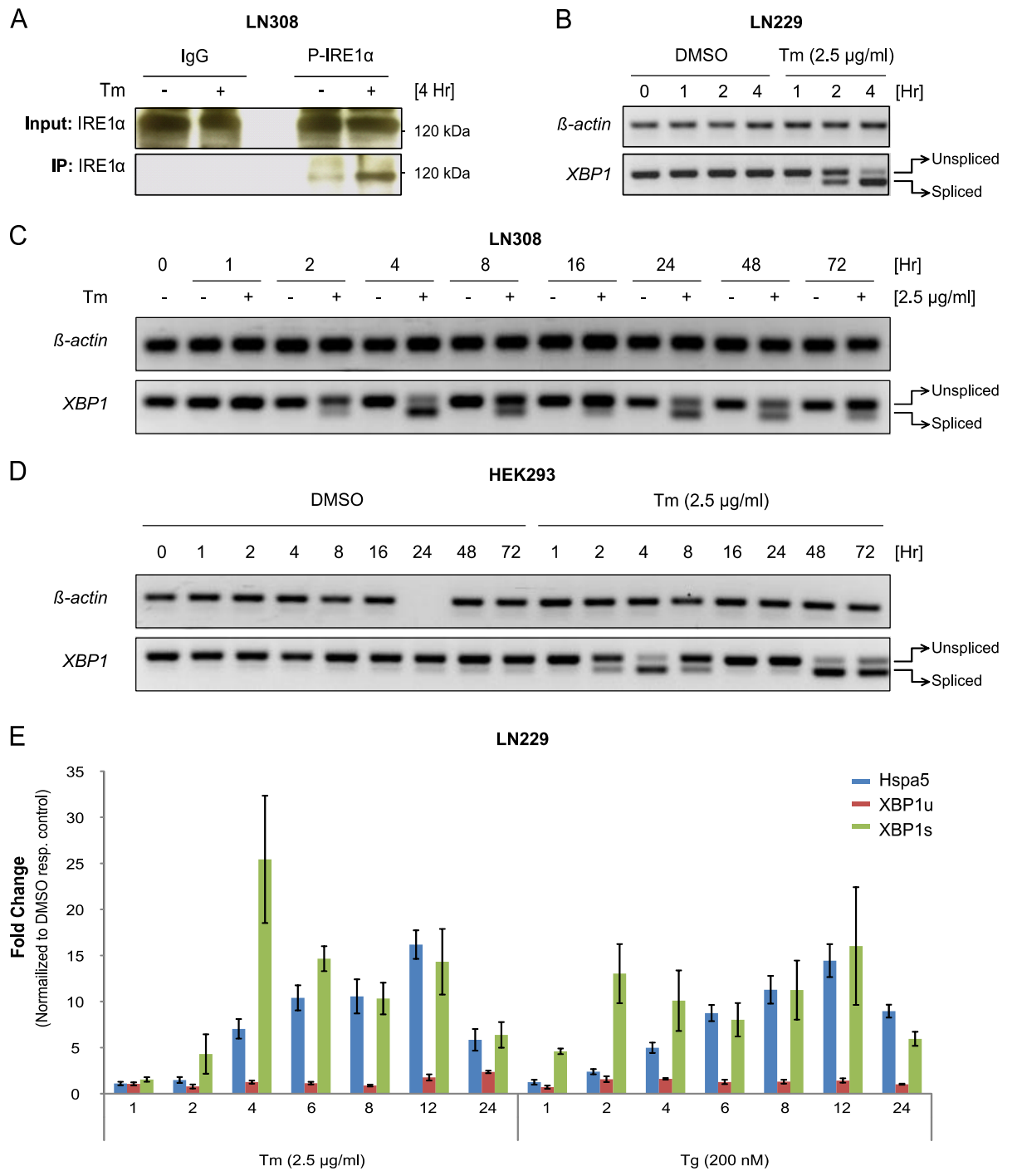

Figure 10. ER stress induced IRE1α activation in glioblastoma cells.
A) Level of immuno-precipitated P-Ser724 IRE1α in LN308 cells treated with tunicamycin (2.5 µg/ml) for 4 hours. Agarose gel showing IRE1α-mediated generation of *XBP1s* in LN229 (B), LN308 (C) and HEK293 (D) cells treated with tunicamycin (Tm) for indicated time-points. *β-actin* was used as a housekeeper. E) LN229 glioblastoma cells were treated with 2.5 µg/ml of tunicamycin and 200 nM of thapsigargin (Tg) for respective time points to determine and quantify the expression pattern of *Hspa5*, *XBP1s* and *XBP1u* mRNA levels. The relative expression of 3 independent biological replicate were averaged and plotted with standard error. *ARF1* was used as a housekeeper. Note: Lane 7 does not show any band for *β-actin* amplification possibly due to technical error.

Next we characterized the activation of PERK branch of UPR in LN308 cells under artificial stress condition. We then treated the cells for 6 and 16 hours with tunicamycin and analyzed the activation of PERK, expression of ATF4 and phosphorylation of eIF2α (Figure 11). The result shows a prominent increase in the expression of ATF4, an upshift in the total PERK protein (indicator of PERK activation) and a slight increase in the P-eIF2α populations after induction of UPR for 6 hours. Interestingly we observed a reduction of PERK downstream effects after 16 hours of tunicamycin treatment in LN308 cells which can be a result of negative feedback loop to reduce the intensity of UPR activation in glioblastoma cells, in the same manner as observed in case of IRE1α and indicate towards adaptation of these cells to the ER stress condition.

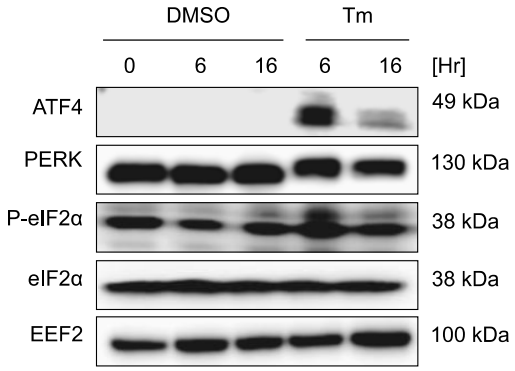

Figure 11. ER stress induced PERK activation in LN308 glioblastoma cells.
Levels of ATF4, P-eIF2α and PERK proteins in LN308 cells treated with tunicamycin treated for indicated time-points.

3.2.2 Small molecular inhibitors of UPR sensor proteins

Understanding branch specific role of UPR in glioblastoma is essential to target it effectively. For this purpose we tested specific inhibitors of IRE1α (STF083010), PERK (GSK2606414) and ATF6α (Ceapin A7) under tunicamycin-induced ER stress condition and determined the optimum concentration of these inhibitors to be further used for proteome analysis using LN308 glioblastoma cell line model. STF083010, a IRE1α RNase specific inhibitor showed maximum efficiency to inhibit *XBP1* splicing at 50 µM (Figure 12A) while GSK2606414 showed maximum inhibition of PERK at 1 µM of concentration (Figure 12B) as seen by the mobility shift in the total PERK protein. For the inhibition of ATF6α branch, we used already known concentration of Ceapin A7 (1µM) which was shown to decrease tunicamycin-induced expression of Bip at both mRNA and protein levels (Figure 12C and D).

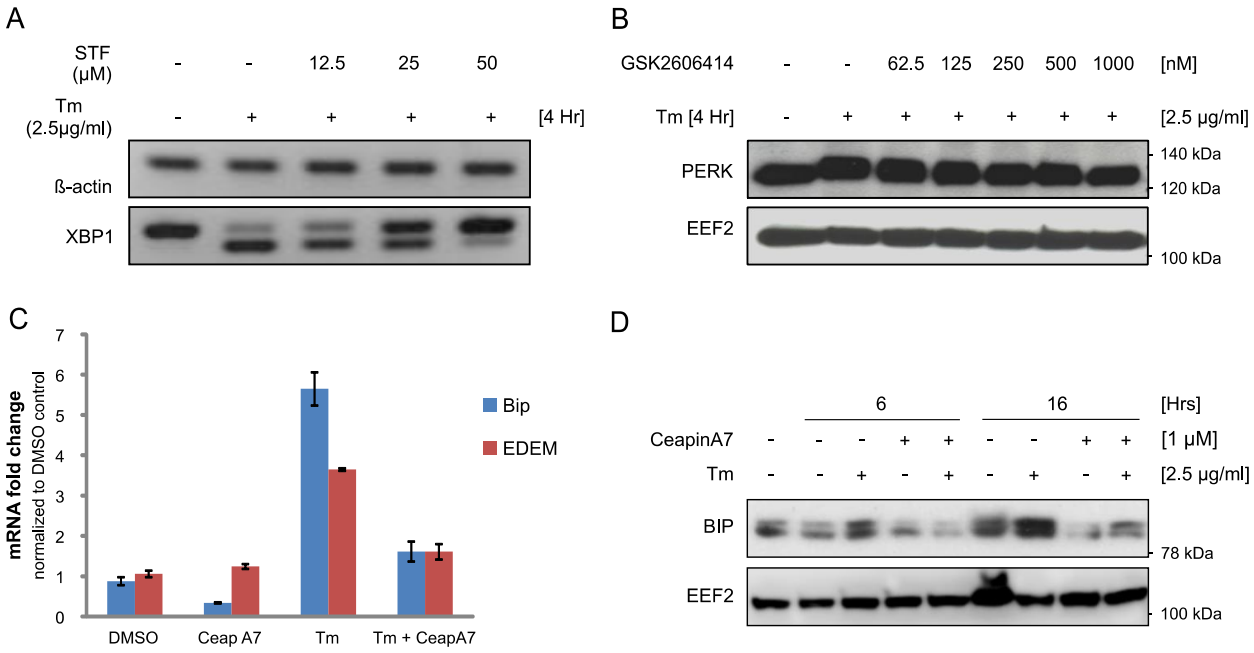

Figure 12. Small molecule inhibitors of UPR pathway.
A) Agarose gel showing reduced splicing of *XBP1* mRNA in LN308 cells under the influence of IRE1α RNase inhibitor, STF083010. B) *β-actin* was used as a housekeeper. GSK2606414-mediated reduction in mobility shift of total-PERK under ER stress condition in LN308 cells. C) Reduced levels of *Bip* and *EDEM* mRNA when ceapin A7 was used to inhibit ATF6α during tunicamycin-induced ER stress in LN308 cells. *RPS13* was used as a housekeeper. D) Effect of Ceapion A7 on Bip protein under tunicamycin-induced UPR. EEF2 was used as a loading control.

3.2.3 IRE1-mediated regulation of invasive markers in glioblastoma

IRE1α is known to negatively regulate the expression of various invasive proteins by targeting and degrading their mRNA, an activity known as Regulated IRE1α Dependent Decay (RIDD). To understand and validate few of the known invasive proteins being regulated by IRE1α we used a specific activator and inactivator of its RNase domain, APY29 and STF083010, respectively (Figure 13). We used nocodazole, an actin cytoskeleton regulator known to regulate SPARC via IRE1α, as a positive control for the experiment known to inhibit IRE1α activity. CYR61, CTGF and Hevin proteins expression increased under nocodazole treatment, a phenomenon which was subsequently inhibited when IRE1α was activated by APY29. STF083010 slightly increased the expression of CTGF among other IRE1 target proteins showcasing basel level activation of IRE1α in LN308 glioblastoma cells. In this respect, we justify that it is of high importance to proceed with the high throughput mass spectrometry screen and identify branch specific role of UPR in glioblastoma secretome.

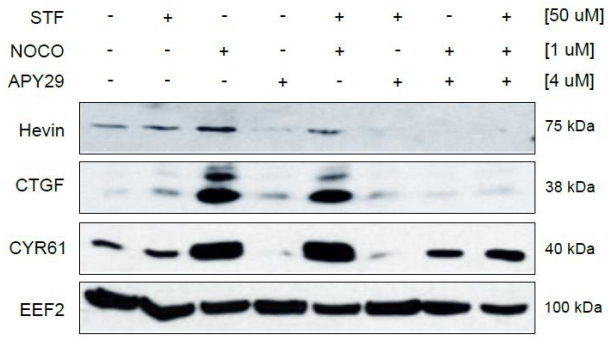

Figure 13. IRE1α-mediated regulation of extracellular proteins in LN308 glioblastoma cells.
Expression of Hevin, CTGF and CYR61 under the influence of IRE1α specific modulators, STF083010 and APY29 in LN308 glioblastoma cells for 24 hours. Nocodazole was used as a known inducer of SPARC.

3.3 Selective activation of UPR sensors under hypoxia in glioblastoma

During tumor progression, the glioblastoma cells confront different stress conditions including mechanical stress, loss of nutrients and hypoxia which activates UPR. As hypoxia is highly potent in selecting cells engaged in inducing angiogenesis, invasion and secretion of factors responsible for modulating tumor microenvironment, we chose to continue our study with this physiological ER stress inducer and determine hypoxia-induced UPR branch-specific regulation of extracellular matrix proteins. In order to understand this, we first analyzed which UPR branch is affected by hypoxic condition in glioblastoma cells. We treated glioblastoma cells with 1% O_2 and checked for the activation of PERK, ATF6α and IRE1α activation status. Activation of PERK (as indicated by mobility shift in total PERK and phosphorylation of eIF2α) was evident in glioblastoma cells under hypoxia, although it was less robust as compared to hypoxia-induced PERK in HEK293 (Figure 14A and B). Hypoxia also resulted in the formation of active cleaved ATF6α (50 kDa) in LN308 glioblastoma cells initially, but this decreased after 48 and 72 hours of hypoxia treatment indicating a potential adaptation to the stress conditions (Figure 14C).

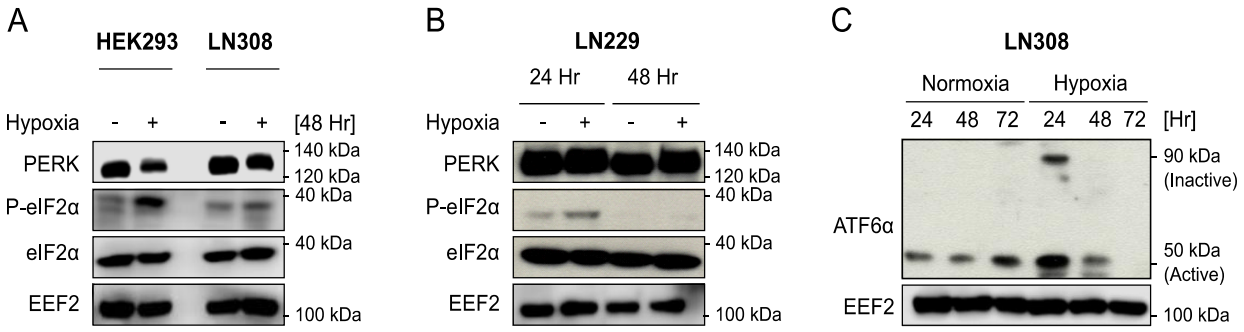

Figure 14. Activation of PERK and ATF6α branch of UPR in glioblastoma cells under hypoxia.
Total PERK, eIF2α and P-eIF2α expression in HEK293, LN308 (A) and LN229 (B) cell lines under normoxia or hypoxia. EEF2 was used as a loading control. B) Active form of ATF6α (50 kDa band) in LN308, under hypoxia for 24, 48 and 72 hours. Adapted from Soni et al., submitted.

Unlike in HEK293 cells, IRE1α was not active in glioblastoma under hypoxia as demonstrated by the absence of *XBP1s* mRNA, a downstream product of the active-IRE1α RNase domain and by the decrease in phosphorylated IRE1α (necessary for the activation of its kinase activity; Figure 15A-F). The data suggests that glioblastoma cells are better equipped to tolerate hypoxia than HEK293 cells, and highlights a possible selective activation of UPR branches under hypoxia in glioblastoma *in vitro*.

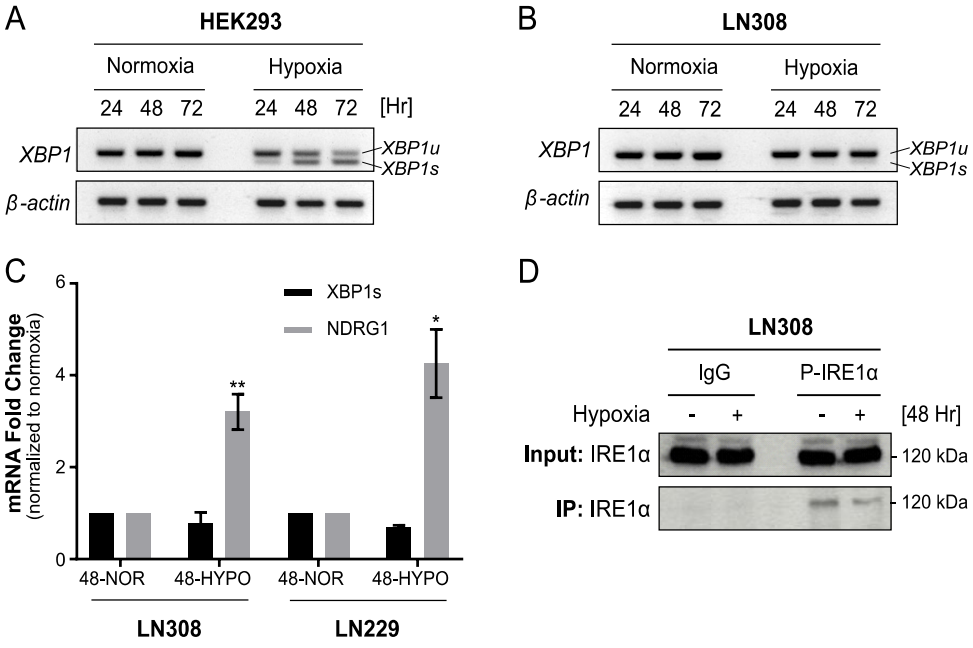

Figure 15. Reduced activation of IRE1 under hypoxia in glioblastoma.
Total amount of *XBP1s* mRNA transcripts in HEK293 (A) and LN308 (B) cells treated with hypoxia for 24, 48, 72 hours. C) *XBP1s* mRNA level as determined by qRT-PCR in LN308 and LN229 cell lines under hypoxia. *NDRG1* was taken as a positive control for hypoxia induction. *RPS13* was used as housekeeping gene. Data are normalized to the respective normoxic conditions and are represented as the mean of three independent experiments ± SEM (T-test: *p-value < 0.05, ** p-value < 0.01). D) Total P-IRE1α species immunoprecipitated using P-IRE1α antibody from LN308 cells treated with hypoxia for 48 hours. NOR-Normoxia, HYPO-Hypoxia. Adapted from Soni et al., submitted.

3.3.1 PERK-mediated secretion of proteins in glioblastoma

To understand how PERK might regulate angiogenesis under low oxygen concentration in glioblastoma, we aimed to identify extracellular matrix proteins which are induced by hypoxia activated PERK. In that respect, LN308 glioblastoma cells were cultivated and treated with GSK2606414 (1 µM), a PERK inhibitor, under normoxic or hypoxic conditions for 72 hours. Proteomics analysis of the conditioned media was performed to identify secreted proteins that are regulated by PERK under hypoxia (Figure 16). Among the identified hits (Table 2), PAM was the only known protein to have its luminal domains secreted outside the cell. Its monooxygenase domains regulate the final step of the activation of neuropeptides for example, ADM, a known angiogenic protein. As PAM addresses both aspects of our study which are secretion of potential hit outside of the cell, as well as ability to regulate neo-blood vessel formation, we chose PAM for further validation and characterization of its involvement in PERK-mediated induction of angiogenesis in glioblastoma.

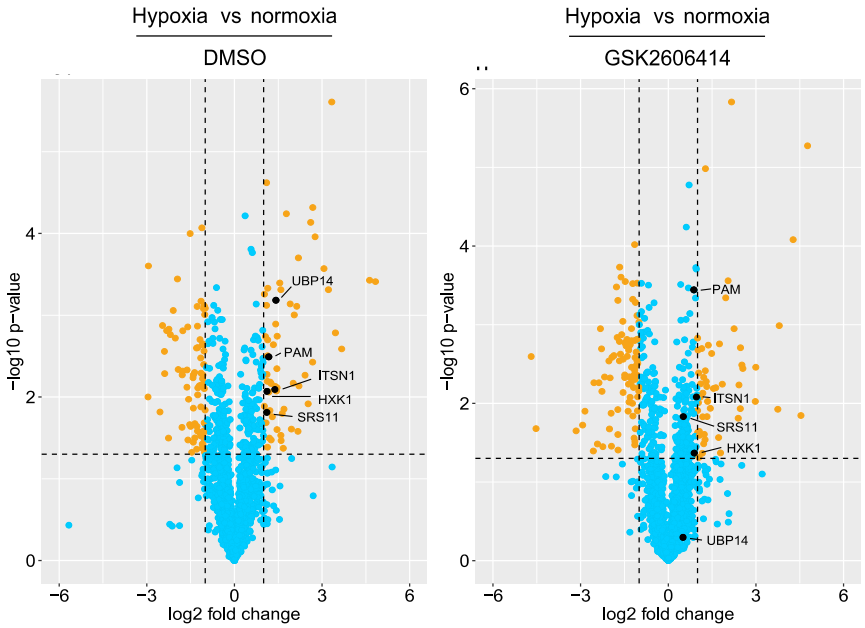

Figure 16. Volcano plot representing the regulated secretory proteins from LN308 glioblastoma cells under hypoxic conditions for 72 hours without (left) and with GSK2606414 (right).
The data are represented as the mean of three independent replicates. The significant P-value cut-off was set at 0.05. Adapted from Soni et al., submitted.

Table 2. List of proteins found to be significantly regulated by PERK under hypoxia.

Accession	Description	Fold change	
		GSK samples	DMSO samples
P19021	Peptidyl-glycine alpha-amidating monooxygenase (AMD_HUMAN)	1.83	2.26
P19367	Hexokinase-1 (HXK1_HUMAN)	1.85	2.17
Q05519	Serine/arginine-rich splicing factor 11 (SRS11_HUMAN)	1.43	2.16
Q15811	Intersectin-1 (ITSN1_HUMAN)	1.95	2.61
Q16666	Gamma-interferon-inducible protein 16 (IF16_HUMAN)	1.97	2.08
Q9NQR4	Omega-amidase NIT2 (NIT2_HUMAN)	1.71	2.19

Adapted from Soni et al., submitted.

3.3.2 PERK regulates PAM independent of PERK kinase activity

In order to verify the involvement of PERK in the regulation of PAM in glioblastoma and thereby validating the mass spectrometry data, we harvested conditioned media from LN308 and LN229 cells upon *PERK* knockdown in hypoxic condition and determined the expression levels of PAM. PAM expression (both mRNA & protein) and secretion increased after 24 or 48 hours under hypoxia and strongly decreased upon silencing of *PERK* (Figure 17A-D). The results were confirmed in a low-passage patient-derived glioblastoma primary cell line (NCH82; Figure 17E). The PERK-mediated reduction of PAM protein was also verified by targeting PERK using a second shRNA in LN308 glioblastoma cells (Figure 17F). Next, we investigated whether PERK kinase activity is necessary for regulating PAM expression by comparing the effect of GSK2606414 (PERK kinase inhibitor) with PERK silencing. While PERK knockdown caused a significant decrease in *PAM* mRNA and protein levels in LN308 and LN229 cells (Figure 17B and D), its kinase inhibition did not show any effect on *PAM* mRNA levels (Figure 17G) or an insignificant reduction on protein level (Figure 17H and I), suggesting that PERK-mediated regulation of PAM is independent of the kinase activity of PERK in glioblastoma.

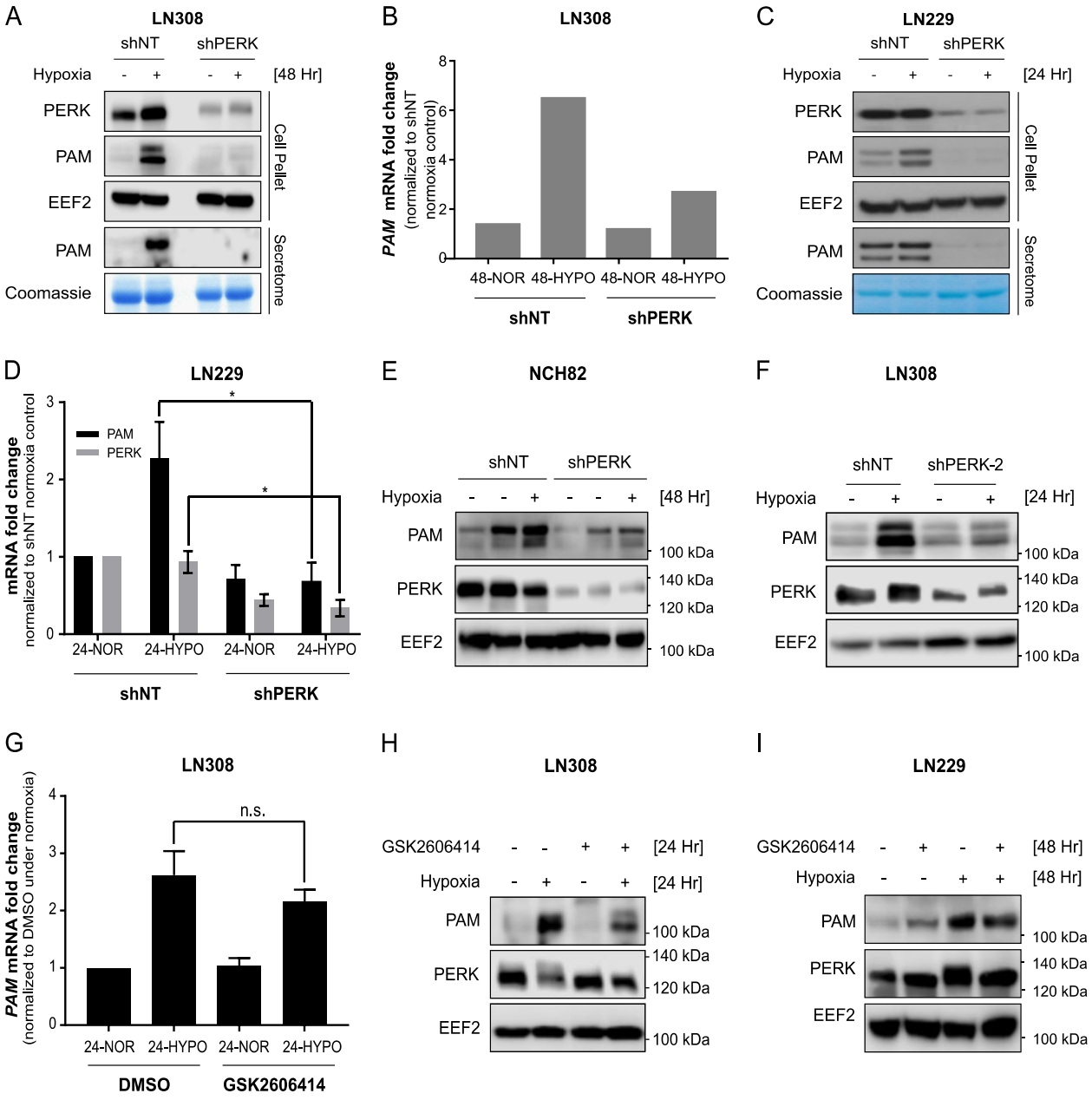

Figure 17. PERK regulates PAM at mRNA level independent of PERK kinase activity.
PAM proteins levels in cells and conditioned media (precipitated using 10% TCA protocol) of LN308 (protein (A) and mRNA (B; single biological replicate)) and LN229 (protein (C) and mRNA (D; mean of five independent replicates ± SEM; t-test with *p-value < 0.05)) glioblastoma cells having either shNT or shPERK. Equal amount of protein was loaded from both the cells and the harvested conditioned media. EEF2 was used as a loading control of proteins isolated from cells whereas coomassie staining was used as a loading control for proteins isolated from conditioned media. *RPS13* was used as housekeeper for RT-PCR. Cells were cultured in serum-free conditions. E) Expression of PAM under *PERK* knockdown in NCH82 low passage patient derived glioblastoma cells under hypoxia for 48 hours. F) Expression of PAM protein under *PERK* knockdown in LN308 glioblastoma cells under 24 hours of hypoxia using shPERK-2. G) *PAM* mRNA levels under PERK kinase inhibitor GSK2606414 in LN308 glioblastoma cells treated with hypoxia for 24 hours. The data is a representation of three independent replicates ± SEM; n.s.: not significant). *RPS13* was used as housekeeper. H) PAM protein levels in LN308 under PERK inhibition using 500 nM GSK2606414. I) PAM protein levels under PERK inhibition using GSK2606414 (500 nM) in LN229 cells under hypoxia for 24 hours. NOR-Normoxia, HYPO-Hypoxia. Adapted from Soni et al., submitted.

PAM consists of to two enzymatic subunits i.e., PHM and PAL, which together amidates neuropeptides at the c-terminus and activates them for regulating different function in the microenvironment. In order to determine whether PERK also affects the activity of PAM, we measured the hydroxylating activity of PAM hydroxylating monooxygenase domain (PHM), which decreased upon *PERK* knockdown (Figure 18A and B). This supports the fact that PERK regulates the expression of *PAM* mRNA thereby also affecting the PHM activity of the glioblastoma.

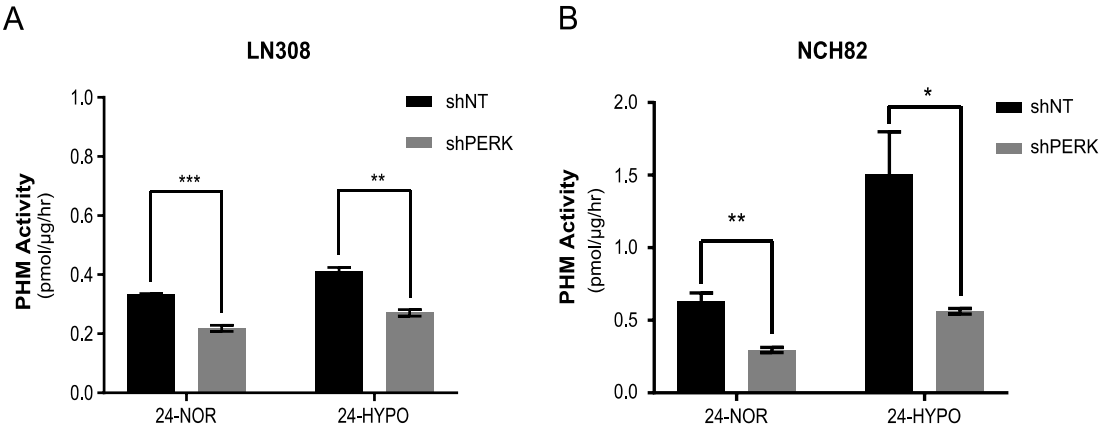

Figure 18. PERK regulates PAM activity under hypoxia.
PHM activity in LN308 (A) and NCH82 (NCH82) cells (B) in hypoxia for 24 hours under *PERK* knockdown conditions. The data are represented as mean of three independent biological replicates ±SEM (t-test with p-value < 0.05* and < 0.01**). NOR-Normoxia, HYPO-Hypoxia. Adapted from Soni et al., submitted.

3.3.3 PERK is the only eIF2α kinase affecting expression of *PAM* in glioblastoma

Our previous observations of hypoxia-mediated increase in phosphorylation of eIF2α and expression of *PAM* mRNA in glioblastoma cells raised two distinct questions. We asked whether PERK regulates the phosphorylation of eIF2α under hypoxic condition in LN229 glioblastoma cells and whether other eIF2α kinases can also regulate expression of *PAM* mRNA (Figure 14B). To determine whether increase in *PAM* mRNA is dependent solely on PERK and whether eIF2α phosphorylation also plays any role in PAM regulation, we knockdown all eIF2α kinases in LN229 cells and checked for PAM expression under hypoxia. Figure 19A shows prominent reduction of PAM protein with *PERK* knockdown elucidating the importance of PERK for its expression. Surprisingly, knockdown of *GCN2*, *PKR* and *HRI* strongly increased the expression of PAM in LN229 glioblastoma cells at both mRNA and protein levels. This suggests a PERK specific increase of *PAM* mRNA in glioblastoma cells under hypoxia (Figure 19A-C). On the other hand, phosphorylation of eIF2α reduces only under *HRI* knockdown condition, which implies dependency of eIF2α phosphorylation on HRI kinase under hypoxia and not on PERK. This also overrules dependency of PAM expression on P-eIF2α levels. Thus, in accordance with these results, the

PERK is suggested to be the only eIF2α kinase increasing *PAM* mRNA expression in glioblastoma under hypoxic condition.

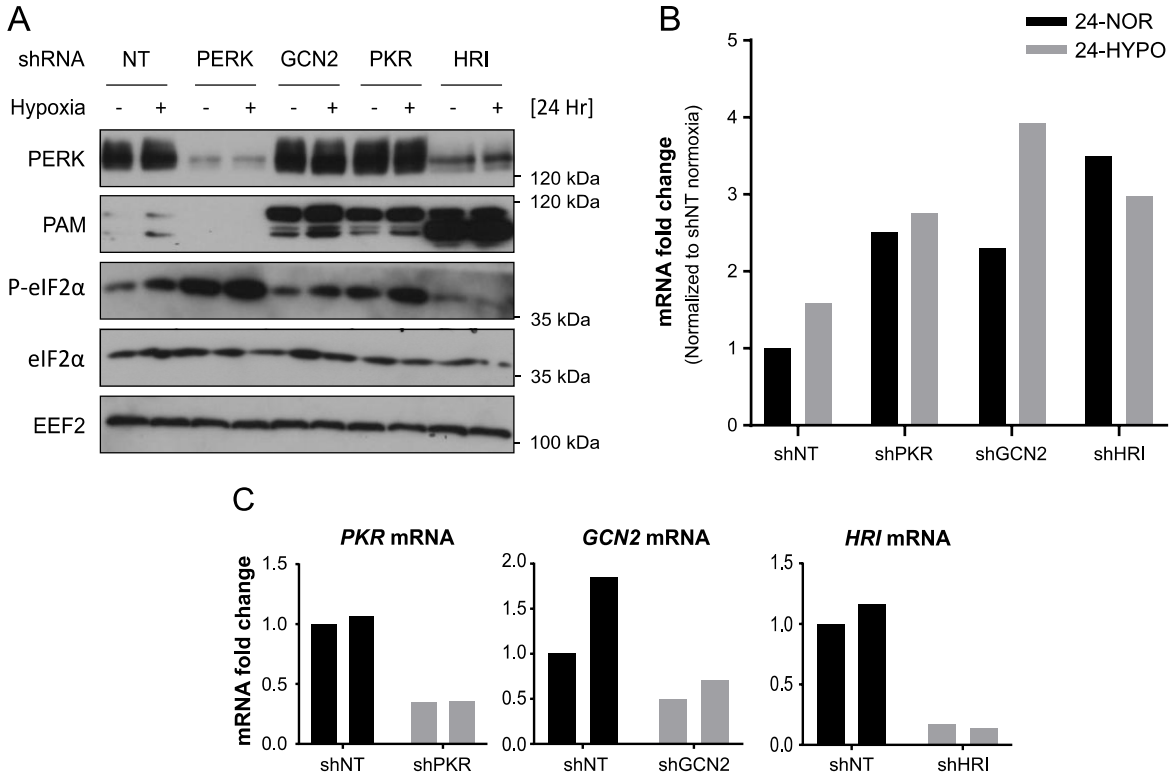

Figure 19. PERK is the only eIF2α kinase affecting expression of PAM in glioblastoma under hypoxia.
PAM protein (A) and (B) mRNA levels under knockdown of *PERK*, *GCN2*, *PKR* and *HRI* in LN229 cells when treated with hypoxia for 24 hours. The mRNA expression data is normalized to shNT normoxia control and is represented as mean of one biological replicate. *RPS13* was used as a housekeeper. C) mRNA fold change of individual eIF2α kinases under knockdown condition normalized to non-target control. NOR-Normoxia, HYPO-Hypoxia.

PERK is also known to show its kinase activity towards NRF2 thereby inducing its nuclear localization. This active NRF2 binds to antioxidant response elements (ARE) on the promoter region of stress and antioxidant genes leading to their expression. As *PERK* knockdown reduced the *PAM* mRNA level, we determined whether PERK regulates *PAM* mRNA expression via NRF2. LN229 cells treated with tBHQ, a selective activator of NRF2 showed increase in NRF2 target genes like *NQO-1* and *HO-1* whereas no increase was observed in *PAM* mRNA expression under these conditions (Figure 20A). In the same direction, we observed no changes in *PAM* mRNA expression under hypoxia treatment when *NRF2* was knocked down in LN229 glioblastoma cells depicting no role of NRF2 in regulating *PAM* mRNA expression (Figure 20B). These observations also supports the fact that PERK kinase activity does not regulate *PAM* mRNA expression in glioblastoma.

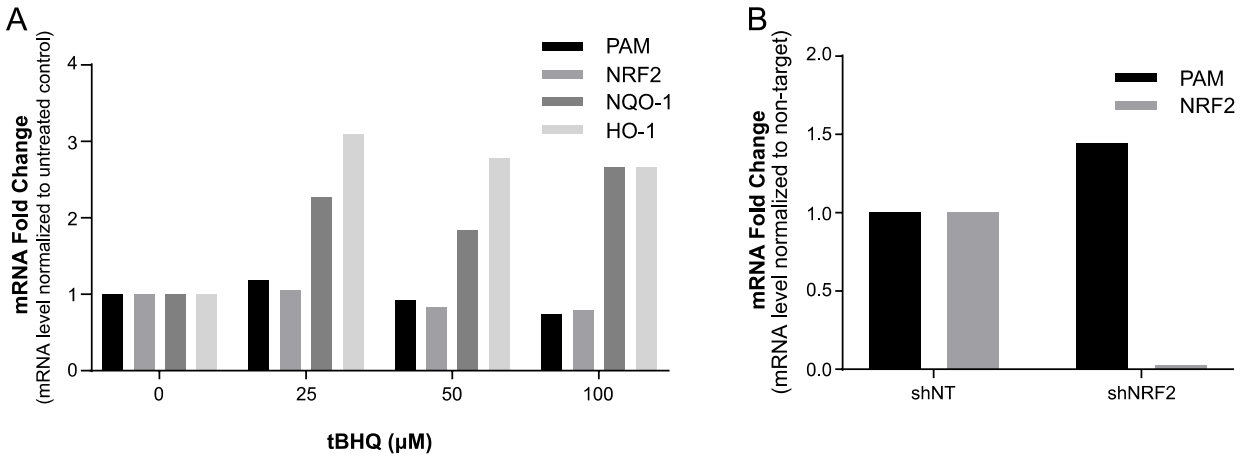

Figure 20. *PAM* mRNA increase under hypoxia is NRF2-independent.
A) *PAM* mRNA expression in LN229 cells under NRF2 activation using tBHQ. *NQO-1* and *HO-1* were used as positive controls for tBHQ-mediated activation of NRF2 target genes. *RPS13* was used as housekeeping gene. Data are normalized to the untreated control and is represented as single biological replicate. B) *PAM* mRNA expression in LN229 cells under *NRF2* knockdown. The experiment was performed as single biological replicate. *RPS13* was used as housekeeping gene.

3.3.4 PERK kinase activity is essential to generate PAM sfCD domain possibly via a physical interaction

As PERK kinase activity does not seem to be necessary for the regulation of PAM at the mRNA level, we asked ourselves whether active PERK is involved in the post-translational modification of PAM. PAM is composed of several domains which also include the unstructured cytosolic domain that can be cleaved to generate sfCD (soluble fragment-cytosolic domain). PAM sfCD has been previously shown to be localized to the nuclei and suggested to be involved in the regulation of gene expression. LN229 cells with PAM over-expression or knockdown were treated with PERK activator CCT020312 under hypoxia. Interestingly, we observed an increased amount of the 16 kDa PAM sfCD (Figure 21A), a phenomenon that occurs in a concentration dependent manner and happens independently of the oxygen level (Figure 21B and C). Indeed, we found a reduction in PAM sfCD when hypoxia-activated PERK was inhibited using GSK2606414 in LN229 cells (Figure 21D) which strongly supports that the activity of CCT020312 towards PAM sfCD was PERK-specific. Our data highlight the importance of PERK kinase activity in regulating the generation of PAM sfCD without inducing any changes at *PAM* mRNA level (Figure 21E).

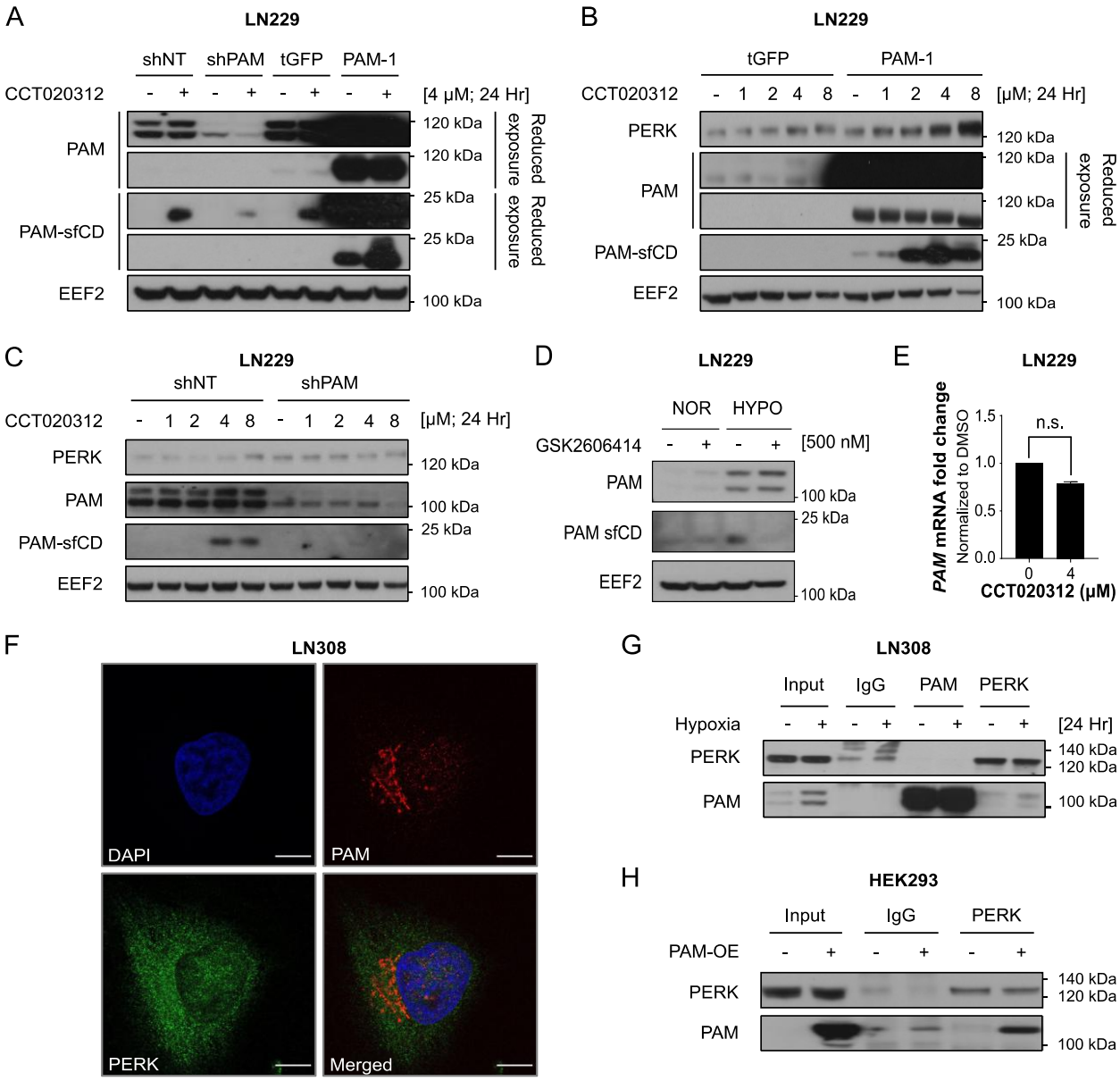

Figure 21. PERK activation causes accumulation of the PAM sfCD fragment, possibly via a physical interaction.
A) sfCD PAM levels in LN229 cells with *PAM* knockdown or with PAM overexpression treated with 4 μM CCT020312 under 24 hour hypoxia. Plasmid overexpressing turboGFP (tGFP) was used as negative control. sfCD PAM levels in LN229 cells having either PAM overexpression (B) or knockdown (C) were treated with different concentrations of CCT020312 under normal oxygen concentration. Plasmid overexpressing turboGFP (tGFP) was used as negative control. D) PAM sfCD levels under hypoxia with and without inhibition of PERK kinase activity using GSK2606414 in LN229 cells under 24 hours of hypoxia. E) *PAM* mRNA levels from LN229 cells treated with 4 μM of CCT020312 under hypoxia. Data were normalized to the housekeeper *RPS13* and are represented as the mean of three independent experiments ± SEM (t-test with n.s.: not significant). F) PAM and PERK immunofluorescence images from LN308 cells treated with hypoxia for 24 hours. DAPI was used as nuclear stain. Scale bars: 10 μm. G) Levels of PAM and PERK in co-IP experiments using respective antibodies in LN308 cells. H) PAM co-IP with PERK antibody from HEK293 cells over-expressing PAM protein. NOR-Normoxia, HYPO-Hypoxia. Adapted from Soni et al., submitted.

As both proteins localize to the cytoplasm (Figure 21F), we determined whether PERK interacts with PAM by co-immunoprecipitation in LN308 cells as well as in HEK293 cells over-expressing PAM (Figure 21G and H). The data indicate that the proteins bind to each other which might be important for the generation of PAM sfCD. The fact that PERK interacts with *PAM* and regulates the generation of PAM sfCD led us to ask whether PERK can also phosphorylate PAM protein. PAM cytosolic domain consists of multiple phosphorylation sites of which two most studied residues, serine 937 and serine 949 are shown to regulate its trafficking through endocytic pathway. To address the same question and determine whether PERK can phosphorylate PAM at Ser937 and Ser949, we treated the LN229 cells with CCT020312 (4 µM) for 24 hours and immunoprecipitated PAM protein. To analyze P-Ser937 and P-Ser949 PAM populations, we used phospho-specific antibodies. Figure 22 shows no significant increase in any of the phosphorylation states of PAM or PAM sfCD when treated with CCT020312 suggesting that PERK does not phosphorylate PAM and thus there might be a possible indirect regulation of PAM sfCD by PERK kinase domain.

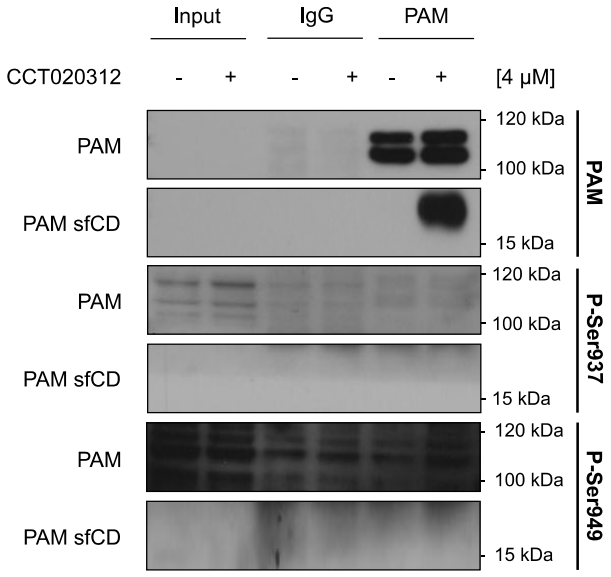

Figure 22. PERK does not phosphorylate PAM at Serine 937 and Serine 949 residue.
Levels of P-Ser937 and P-Ser949 in LN229 cells treated with/without CCT020312 (4µM) for 24 hours under hypoxia observed after immunoprecipitating total PAM protein.

3.3.5 PERK and HIF1α regulates expression of PAM via AP-1 transcription factor

Hypoxia regulates the expression of PAM in different glioblastoma cell lines both at mRNA (Figure 23A) and protein levels (Figure 23B-D) which also affects its PHM activity and secretion (Figure 23E-F). As PAM has also been identified in purified exosomes, we prepared a crude extracellular fraction from the conditioned media of LN308 cells treated with hypoxia and observed the expression of PAM by immuno-electron microscopy (Figure 24A and B). Next, we determined whether Hypoxia inducible factor 1α

(HIF1α) was responsible for the increased level of PAM expression under hypoxia. LN308 cells were transduced with shNT or shHIF1α and cultivated under low oxygen conditions. *HIF1α* knockdown significantly reduced the level of PAM at mRNA and protein level. Taken together, the data demonstrates that HIF1α stabilization is required for *PAM* mRNA increase under hypoxia in glioblastoma (Figure 25A and B).

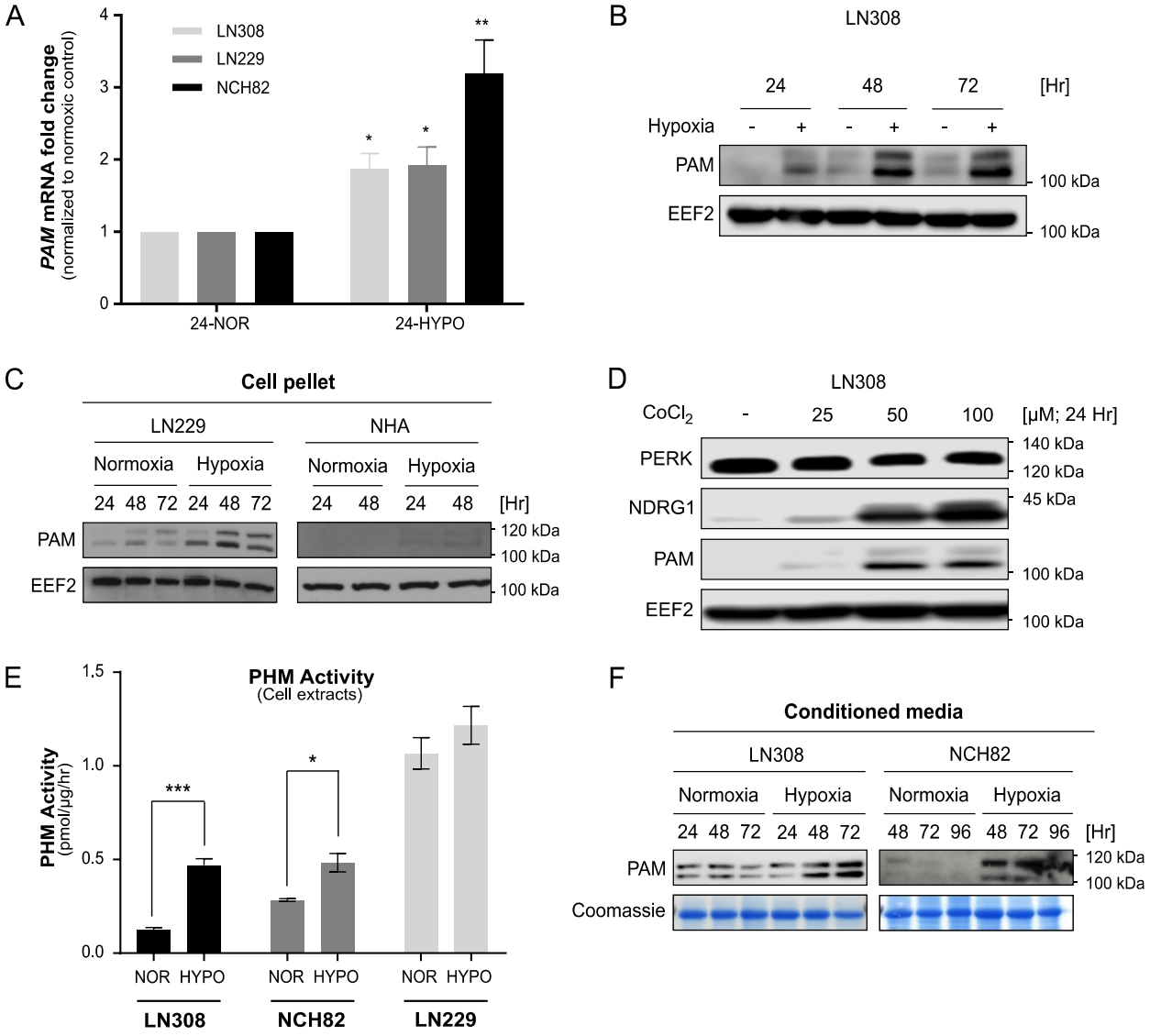

Figure 23. *PAM* mRNA increases under hypoxia in glioblastoma.
A) *PAM* mRNA levels under hypoxia in different glioblastoma cell lines. *EEF2* was used as housekeeping gene. Data are normalized to the respective normoxic conditions and are represented as the mean of three independent biological experiments ± SEM (t-test: p-value < 0.05* and< 0.01**). B) Time course increase in expression of PAM in LN308 glioblastoma cell line. C) Expression of PAM under hypoxic conditions in LN229 and human astrocytes (NHA). D) PAM protein levels under $CoCl_2$ treatment in LN308 cells. E) PHM activity in different glioblastoma cell lines under 24 hours of hypoxia. The experiments were performed in three independent biological replicates ± SEM (t-test: p-value < 0.05* and < 0.001***). F) Secretion of PAM protein in conditioned media from LN308 and NCH82 cells. NOR-Normoxia, HYPO-Hypoxia. Adapted from Soni et al., submitted.

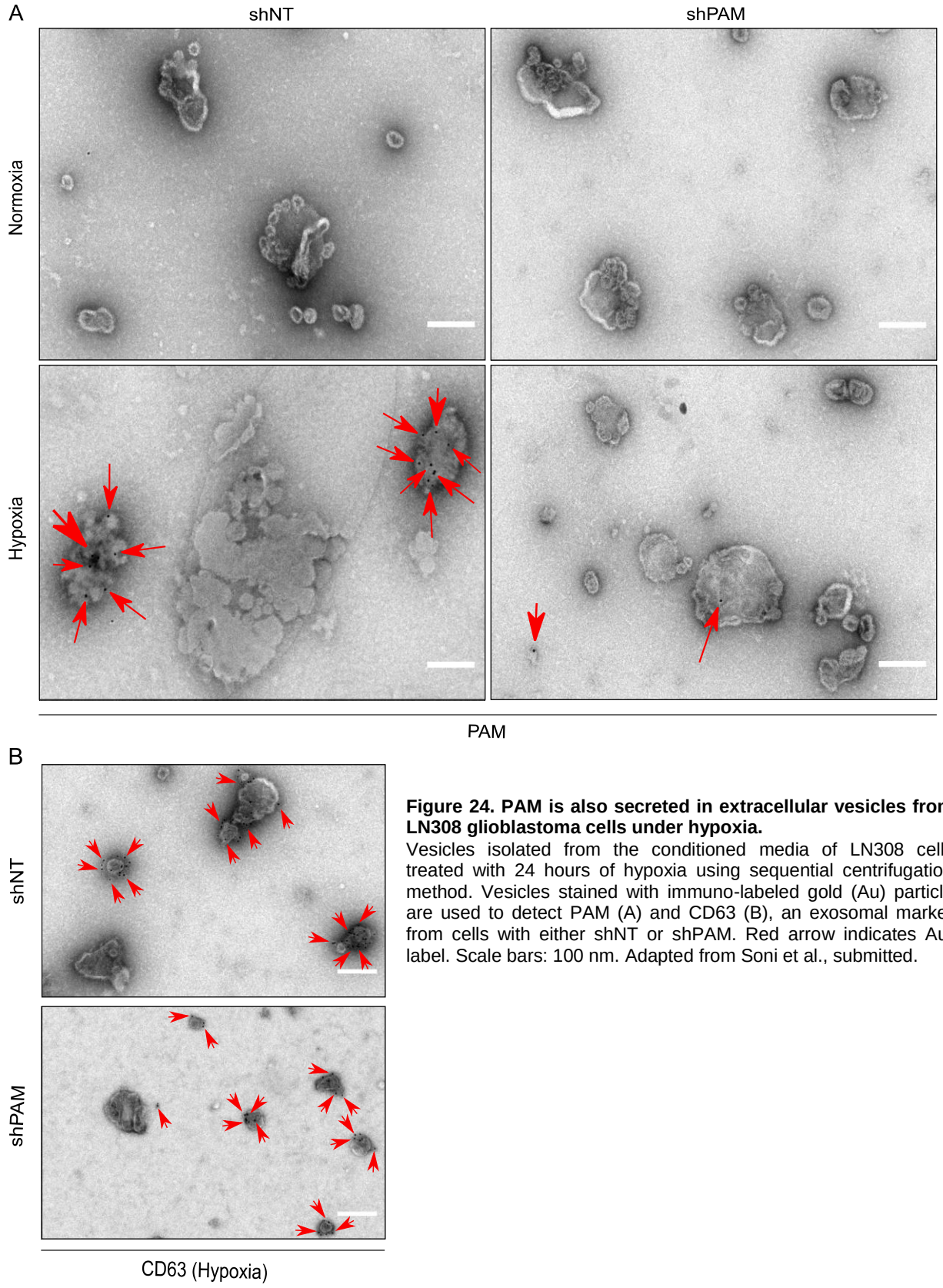

Figure 24. PAM is also secreted in extracellular vesicles from LN308 glioblastoma cells under hypoxia.
Vesicles isolated from the conditioned media of LN308 cells treated with 24 hours of hypoxia using sequential centrifugation method. Vesicles stained with immuno-labeled gold (Au) particle are used to detect PAM (A) and CD63 (B), an exosomal marker from cells with either shNT or shPAM. Red arrow indicates Au-label. Scale bars: 100 nm. Adapted from Soni et al., submitted.

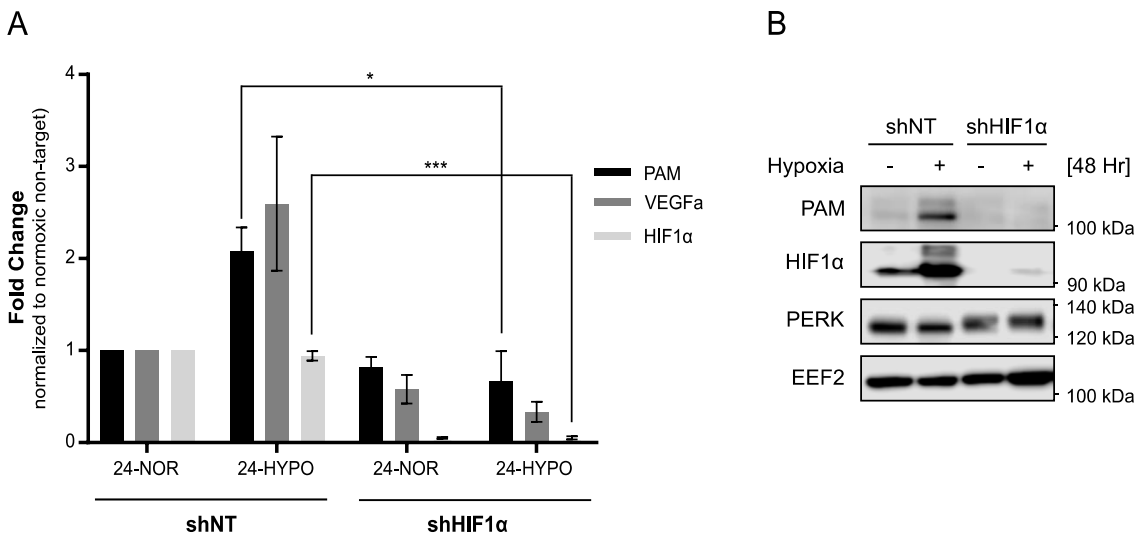

Figure 25. *PAM* mRNA increase under hypoxia is HIF1α dependent.
mRNA (A) (mean of three independent biological replicates ± SEM; t-test with p-value < 0.05* and < 0.001***) and protein (B) levels of PAM under non-target or *HIF1α* knockdown in LN308 cells. *RPS13* was used as housekeeping gene. NOR-Normoxia, HYPO-Hypoxia. Adapted from Soni et al., submitted.

3.3.6 In silico transcription binding affinity (TBA)-based prediction of potential transcription factors regulating PAM mRNA expression

As PERK and HIF1α both regulates *PAM* mRNA levels we took an *in silico* approach in order to identify potential transcription factors (TFs) of PAM that might be regulated by PERK. We performed comparative analysis of transcription binding affinities (TBAs) of all TFs and generated a list with TFs having the highest TBAs for the PAM promoter (NM_138821) defined as -1500 bases to +500 base pairs from the transcription start site (Table 3). From the putative transcription factors identified, several members of the AP-1 transcription complex such as FOSL1, JUND and JUNB were among the top hits (Figure 26A-C).

Table 3. Log2- and z-transformed TBAs, for 579 TF binding motifs from JASPAR, for the promoter of PAM transcripts (NM_138821).

Only motifs with scores >= 1.5 are reported. Adapted from Soni et al., submitted.

ID	Name	z-Score
MA0665.1	MSC	2.68
MA0784.1	POU1F1	2.42
MA0787.1	POU3F2	2.36
MA0786.1	POU3F1	2.27
MA0866.1	SOX21	2.21
MA0735.1	GLIS1	2.10
MA0737.1	GLIS3	2.03
MA0795.1	SMAD3	2.01
MA0667.1	MYF6	2.01
MA0031.1	FOXD1	1.82
MA0157.2	FOXO3	1.81
MA0080.4	SPI1	1.80
MA0845.1	FOXB1	1.77
MA0785.1	POU2F1	1.73
MA0842.1	NRL	1.72
MA1103.1	FOXK2	1.70
MA1152.1	SOX15	1.67
MA0032.2	FOXC1	1.63
MA0788.1	POU3F3	1.61
MA0852.2	FOXK1	1.61
MA0089.1	MAFG::NFE2L1	1.60
MA0751.1	ZIC4	1.57
MA1137.1	FOSL1::JUNB	1.57
MA0789.1	POU3F4	1.55
MA1128.1	FOSL1::JUN	1.55
MA1141.1	FOS::JUND	1.54
MA0792.1	POU5F1B	1.52
MA0613.1	FOXG1	1.51

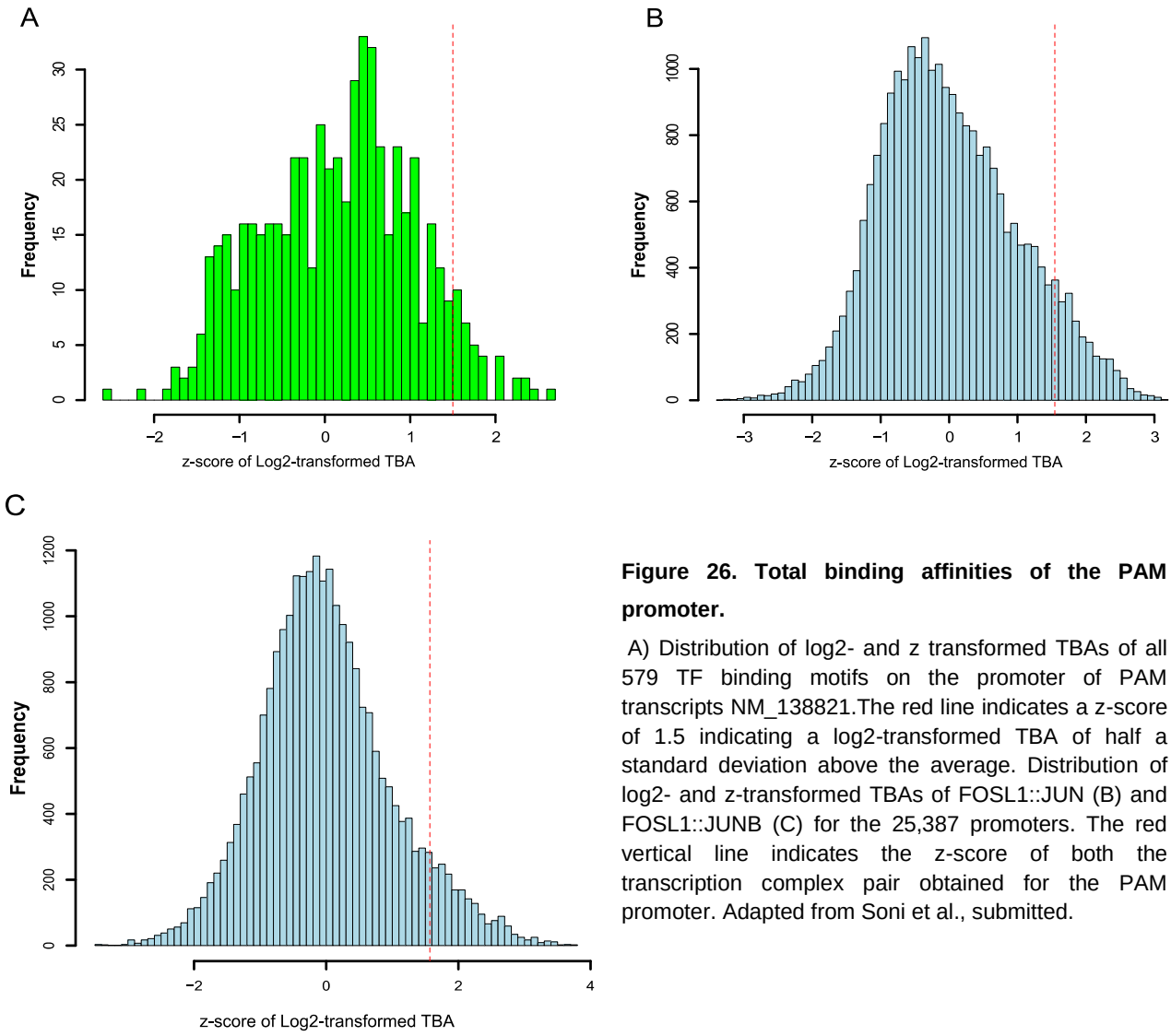

Figure 26. Total binding affinities of the PAM promoter.

A) Distribution of log2- and z transformed TBAs of all 579 TF binding motifs on the promoter of PAM transcripts NM_138821.The red line indicates a z-score of 1.5 indicating a log2-transformed TBA of half a standard deviation above the average. Distribution of log2- and z-transformed TBAs of FOSL1::JUN (B) and FOSL1::JUNB (C) for the 25,387 promoters. The red vertical line indicates the z-score of both the transcription complex pair obtained for the PAM promoter. Adapted from Soni et al., submitted.

3.3.7 Differential expression of PAM in glioblastoma subtypes and its relation to AP-1 transcription factor.

In order to determine whether AP-1 regulates the increase of *PAM* mRNA in glioblastoma, we inhibited AP-1 in LN308 cells using the specific inhibitor SR11302 (AP-1i) under hypoxia. The AP-1i reduced *PAM* mRNA levels suggesting a putative role of AP-1 in driving PAM expression (Figure 27A). Gene expression-based molecular classification has divided glioblastoma into three main subtypes namely, classical (CL), proneural (PN) and mesenchymal (MS). To find out whether PAM expression is glioblastoma subtype-specific, we checked *PAM* mRNA and protein levels in mesenchymal-subtype glioma-stem like cells (GSCs; NCH705 & NCH711) and pro-neural GSCs (NCH644 and NCH421K) under

hypoxia (Figure 27B and C). Surprisingly, PAM expression was found only in mesenchymal subtype GSCs at both protein and mRNA levels.

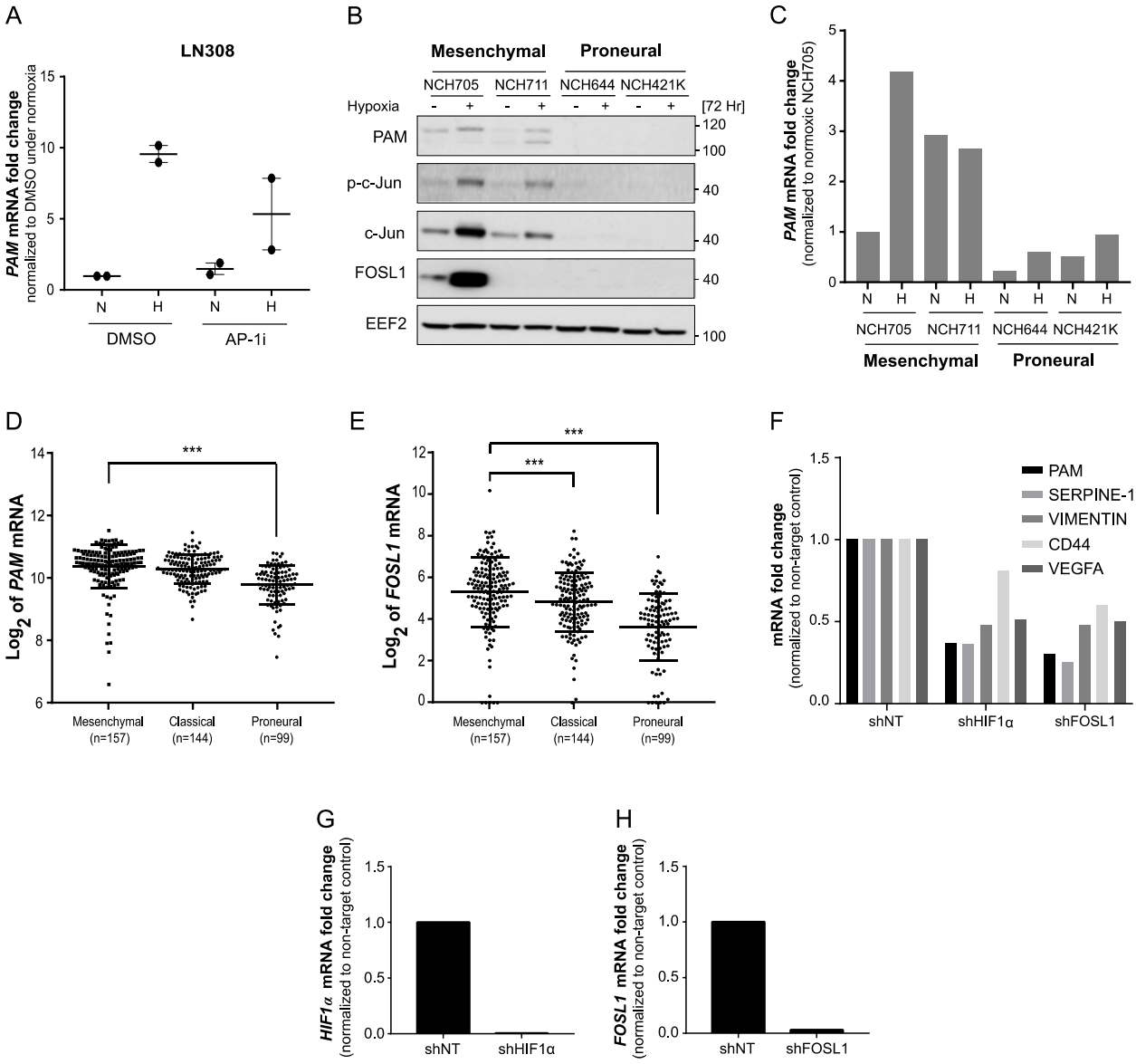

Figure 27. Differential expression of PAM in glioblastoma subtypes and its relation to AP-1 transcription factor.

A) PAM mRNA regulation in the presence of AP-1i (SR11302) in LN308 cells under 24 hours of hypoxia. The data is represented as a mean of two independent biological replicates. PAM protein (B) and mRNA (C) levels in glioblastoma subtypes when treated with hypoxia for 72 hours. The data is represented as single biological replicate. mRNA levels are normalized to normoxic NCH705. *RPS13* was used as housekeeper. Box plot showing the expression levels of *PAM* (D) and *FOSL1* (E) mRNA in glioblastoma patients classified into different subtypes (data retrieved from https://www.cancer.gov/tcga; error bars depict standard deviation in the expression values (t-test with p-value <0.001***)). F) mRNA fold change in expression of target genes under *HIF1α* and *FOSL1* knockdown in NCH705 GSCs. *RPS13* was used as housekeeper. The data is representation of a single biological replicate. Knockdown efficiency of (G) *HIF1α* and (H) *FOSL1* for the experiment in (F). *RPS13* was used as housekeeper. N-Normoxia, H-Hypoxia. Adapted from Soni et al., submitted.

Mesenchymal GSCs also showed increased expression of AP-1 components FOSL1 and c-JUN supporting the involvement of AP-1 transcription factor in regulating the expression of *PAM* mRNA. Clinical data also shows a high expression of *PAM* and *FOSL1* mRNA in mesenchymal subtype of glioblastoma (Figure 27D and E)[233]. Furthermore, knocking down both *HIF1α* and *FOSL1* reduced *PAM* mRNA levels in NCH705 GSCs confirming the previous finding that FOSL1 mediates the expression of PAM in glioblastoma (Figure 27F-H). In that respect, the AP-1 complex, particularly FOSL1, seems to be an important transcription factor in the regulation of PAM expression in glioblastoma. Although, whether PERK regulates *PAM* mRNA expression in glioblastoma via AP-1 is still a question to be answered.

3.3.8 PAM regulates angiogenesis *in vitro*

PAM monooxygenase activity is the rate-limiting step for the activation of several neuropeptides like oxytocin, vasopressin and adrenomedullin (ADM). As ADM is a known for its role in regulating angiogenesis, we wanted to observe whether PAM also plays a pro-angiogenic role in glioblastoma. The two ways with which we could have checked the contribution of PAM towards angiogenesis was either by inhibiting its activity with known inhibitor 4P3BA or knocking down its expression using shRNA. We first opted to examine the effect of 4P3BA on the expression and activity of PAM. For this, we treated LN308 cells with 4P3BA and observed only a slight reduction in the PHM activity (Figure 28A). On the other hand, 4P3BA enhanced PAM expression in LN308 cells which might be the reason of a positive feedback mechanism thereby showing little effect of 4P3BA on PHM activity of the cells (Figure 28B). As the inhibition of PHM activity of the cells by 4P3BA was not strong, we decided to check the effect of PAM on angiogenesis by reducing its expression using shRNA-mediated knockdown.

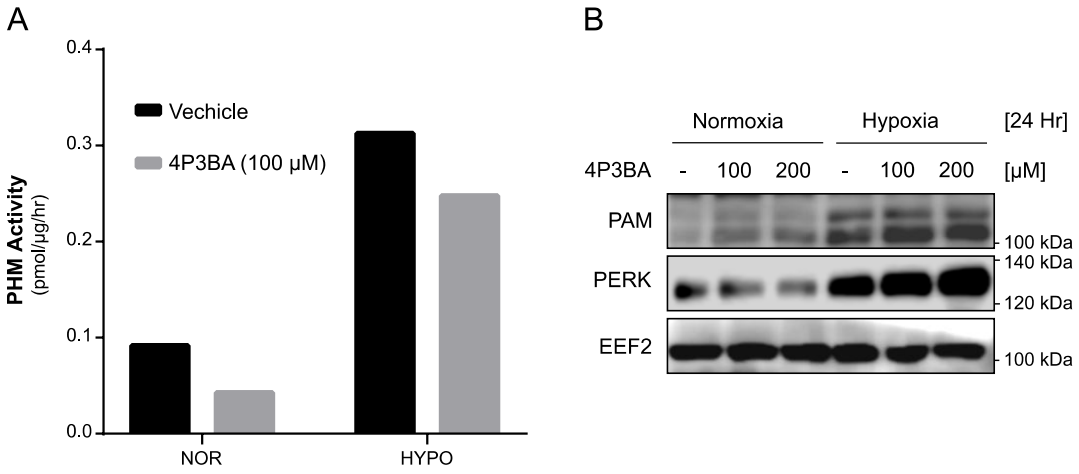

Figure 28. 4P3BA does not effectively reduce PHM activity in LN308 glioblastoma cells.
PAM PHM activity (A) and protein levels (B) in LN308 cells under hypoxia with PAM inhibitor 4P3BA. NOR-Normoxia, HYPO-Hypoxia.

We performed the standard tube formation assay where we subjected HUVECs with conditioned media from non-target and *PERK* or *PAM* knockdown LN229 cells treated under hypoxia and allowed them to form tubes on growth factor-reduced matrigel within 24 hours. The number of junctions and tube meshes formed by HUVECs significantly decreased when nourished with conditioned media from shPERK and shPAM LN229 cells in comparison to non-target control (Figure 29A and B).

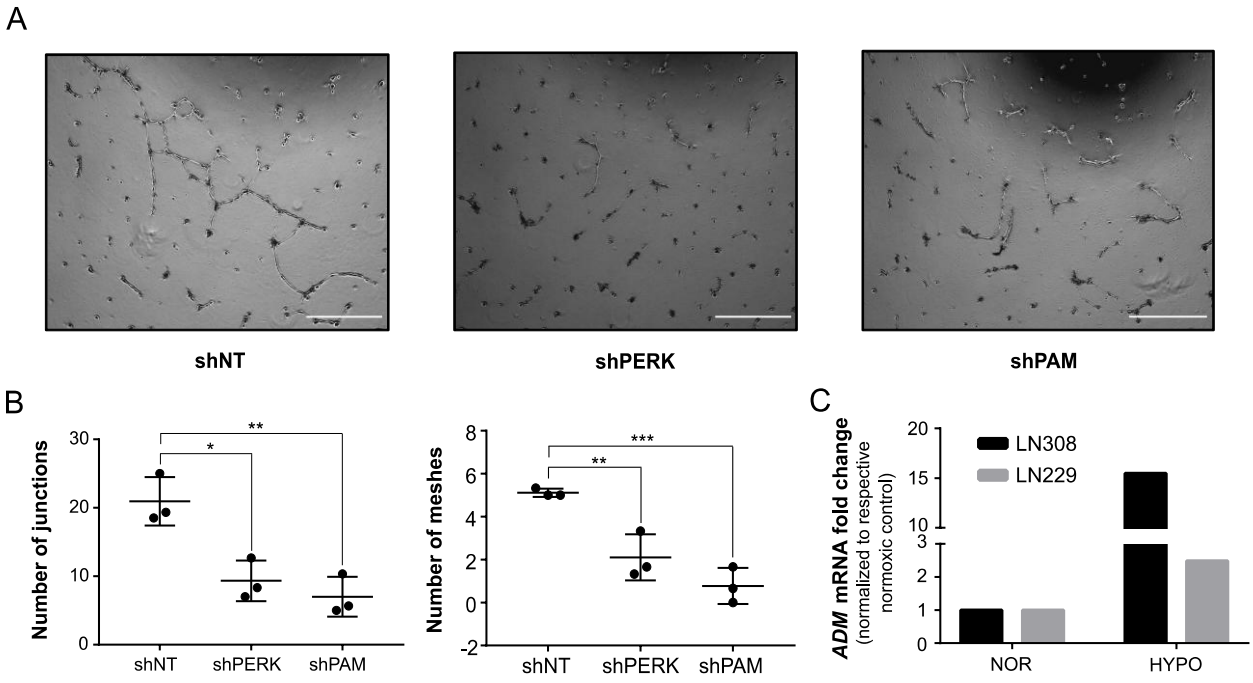

Figure 29. PERK and PAM support blood vessel formation in glioblastoma *in vitro*.
A) Tubes formed by HUVECs when treated with conditioned media from *PERK* and *PAM* knockdown LN229 cells along with non-target control. Scale bars: 500 µm. B) Plots showing number of junctions and meshes formed by HUVECs when treated with conditioned media from shPERK and shPAM LN229 cells. The data is normalized to the shNT control and is represented as a mean of three independent biological replicates ± SEM (t-test with p-value < 0.05*, <0.01** and < 0.001***). C) *ADM* mRNA expression in LN308 and LN229 glioblastoma cells. The data is represented as a single biological replicate. *EEF2* was used as housekeeper. NOR-Normoxia, HYPO-Hypoxia. Adapted from Soni et al., submitted.

We also confirmed the expression of *ADM* mRNA in LN308 and LN229 cells (Figure 29C) and observed an increase in the number of junctions and tube meshes formed by HUVECs when treated with active-ADM (ADM-NH_2; Figure 30A and B). Thus, in light of these results we propose a pro-angiogenic role of PAM in glioblastoma.

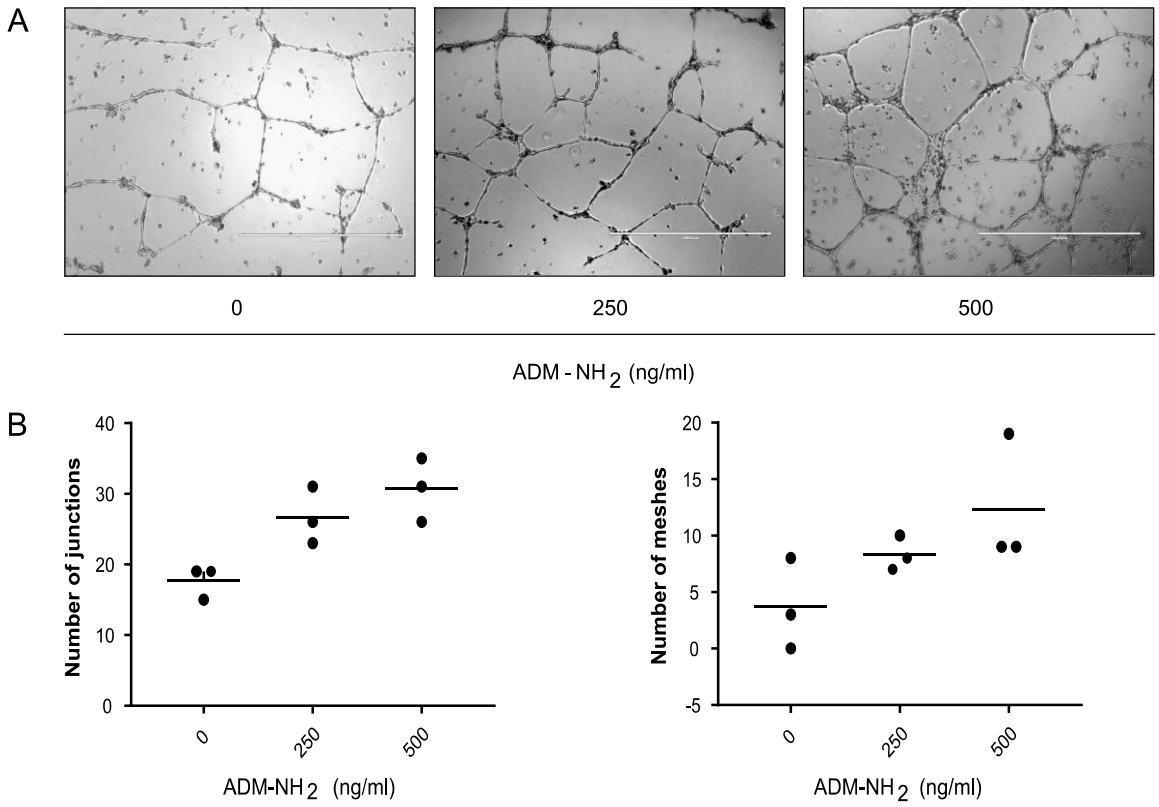

Figure 30. Active ADM increases number of junctions and meshes formed by HUVECs *in vitro*.
A) Images showing tubes formed by HUVECs over reduced-matrigel for 18 hours in the presence of different concentrations of active adrenomedullin active. The data are represented as mean of three technical replicates. Scale bars: 1000 µm. B) Corresponding numbers of junctions and meshes formed by HUVECs under adrenomedullin treatment. Adapted from Soni et al., submitted.

3.3.9 PAM regulates tumor progression *in vivo*.

Literature evidence shows that PERK expression affects the tumor growth kinetics. To observe the same and determine whether PAM reduction can also affect glioblastoma proliferation, we knockdown *PAM* and *PERK* using shRNA and analyzed cell proliferation in glioblastoma cells. The data (Figure 31A and B) suggests more than 50% reduction in the viability of LN229 cells upon *PERK* knockdown whereas no effect of *PAM* knockdown was observed on proliferation of LN229 cells. As *PERK* knockdown would have completely reduced the chances of tumor engraftment *in vivo*, we planned to not go further with analyzing the effect of *PERK* knockdown but rather observe the effect of *PAM* knockdown on tumor growth kinetics. To determine the effect of *PAM* knockdown on glioblastoma progression and overall survival of mice, we implanted LN229 cells expressing GFP-2A-luciferase in immuno-compromised NSG mice and recorded total flux (photons/sec) 7 and 14 days after implantation. Reduced PAM expression decreases tumor growth kinetics and increased the overall survival in the glioblastoma model (Figure 31C-E). Interestingly *PAM* mRNA expression is also increased in glioblastoma patients as compared to normal brain and high expression correlates with poor prognosis (Figure 31F and G). Altogether, we propose that PAM expression supports the growth of glioblastoma *in vivo* and acts as one of the important factor responsible for poor prognosis in glioblastoma patients.

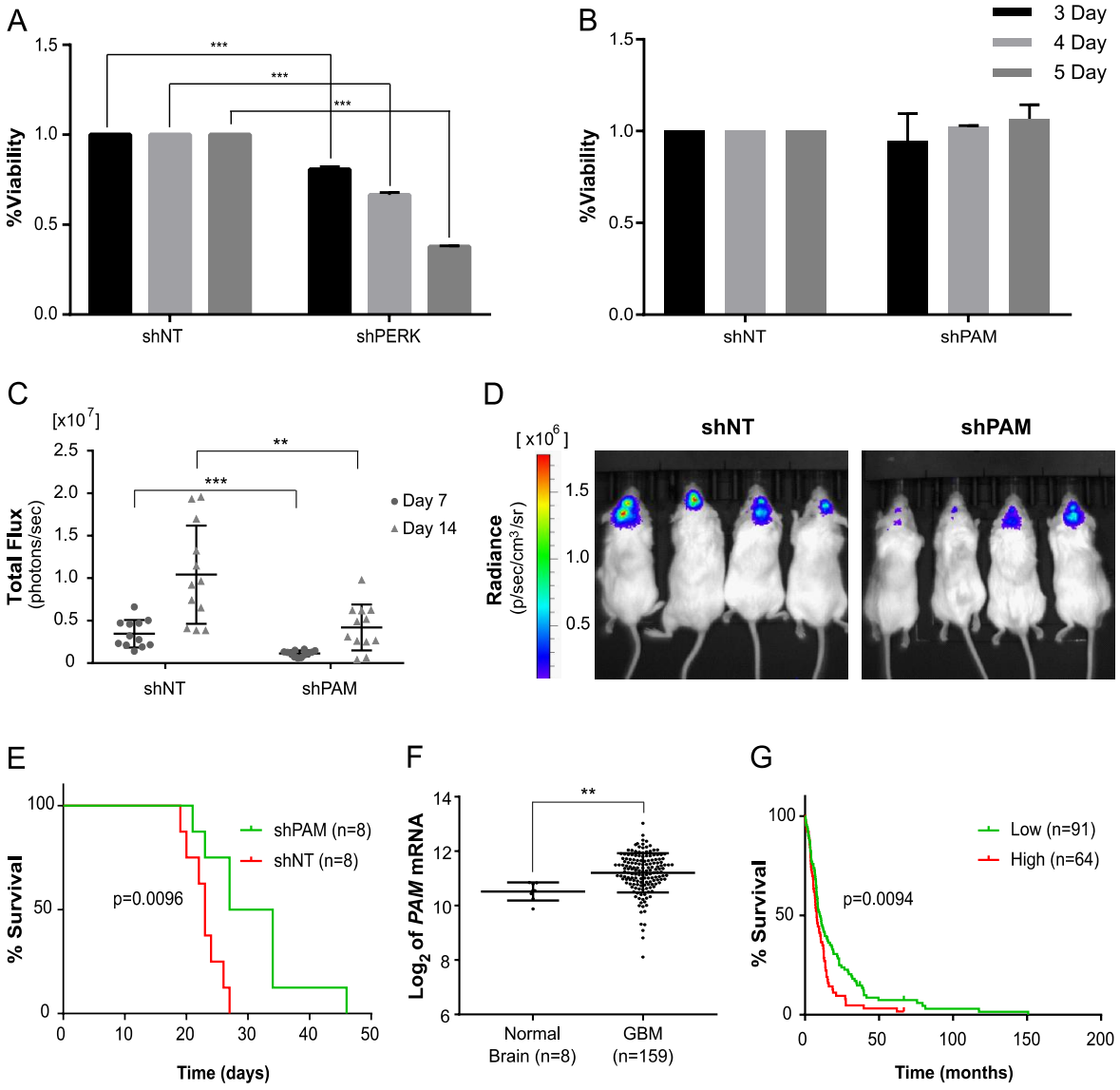

Figure 31. PAM expression is necessary for progression of glioblastoma *in vivo*.
A) Cell Titer-Glo® luminescent cell viability assay showing the effect of PERK on LN229 cell viability determined 3, 4, and 5 days post virus infection. The values correspond to the three biological replicates normalized to the respective shNT control ± SEM (t-test with p-value < 0.05*, <0.01** and < 0.001***). B) Cell Titer-Glo® luminescent cell viability assay showing the effect of PAM on LN229 cell viability determined 3, 4, and 5 days post virus infection. The values correspond to the two biological replicates normalized to the respective shNT control. C) Tumor growth kinetics on the basis of total flux calculated for mice implanted with LN229 cells having either shNT or shPAM for the indicated time-points. The data is normalized to respective shNT control and contains 12 mice per cohort ± SD (t-test with p-value < 0.05*, <0.01** and < 0.001***). D) Representative bio-luminescence images of mice 14 days after implantation with LN229 glioma having expression of either shNT or shPAM for the indicated time-points. E) Overall survival of mice with shNT and shPAM LN229 glioblastoma using Kaplan Meier survival analysis. Significance was calculated using Log-rank method. F) Scatter dot plot showing the expression levels of *PAM* in glioblastoma patients versus the normal brain control (data retrieved from Gravendeel et al. 2009; error bars depict standard deviation in the expression values (t-test with p-value <0.01**)). G) Kaplan Meier survival analysis representing percentage survival of patients with low (green) and high (red) PAM expression from Gravendeel et al. 2009. Most significant expression cutoff was used for survival analysis. Significance was calculated using Log-rank method. Adapted from Soni et al., submitted.

4. Discussion

(The text in this section has been adapted from Soni et al., submitted, which corresponds to my PhD research project.)

PERK has been previously showed to sustain tumor growth by regulating the expression of angiogenic factors like VEGF which in turn provides nutrients and oxygen to proliferating cancer cells. Many studies have reported the activation of UPR under stressful hypoxic condition in order to enhance their survival[234–237]. Targeting VEGF using the monoclonal antibody Bevacizumab has shown variable clinical outcomes with respect to the type of cancer, wherein patients with metastatic colorectal cancer and non-small cell lung cancer has seen significant increase in overall survival (OS) but patients with metastatic breast cancer and glioblastoma have shown improvement of the progression-free survival (PFS) rate[238–241]. The reasons behind the unfavorable outcome from these clinical trials may include insensitivity of anti-VEGF therapy towards tumor blood vessel[242], alternative angiogenic growth factor expression[243,244], increased recruitment of myeloid cells supporting tumor angiogenesis[245,246], pericytes-mediated protection of endothelial cells and therapy-induced mesenchymal phenotype of tumor cells[247,248]. As current angiogenic therapies have failed to provide any benefit to the glioblastoma patients, there is an urgent need to identify other angiogenic factors in glioblastoma and possibly the mechanism behind their expression to effectively target them. Here, we aimed to determine which secretory factors might be responsible in mediating PERK-induced angiogenesis in glioblastoma. We conducted a mass spectrometry screening of the secretome of LN308 glioblastoma cell line under hypoxic stress and identified PAM to be regulated by PERK under these conditions. We found a HIF1α-dependent increase of *PAM* mRNA expression under hypoxia. We also provide evidence of a transcription-independent regulation of PAM sfCD under the influence of active PERK which might be an effect of formation of a complex between PERK and PAM. Our *in vitro* study confirmed PAM-mediated induction of tube formation by HUVECs whereas our *in vivo* data suggests PAM-led progression of glioblastoma in xenograft mice.

Initially, we characterized UPR pathway in glioblastoma cells and analyzed whether these cells are better adapted to endoplasmic reticulum (ER) stress condition in comparison to a non-glioblastoma cell model (HEK293). IRE1α is a dual activity protein that maintains cellular proteostasis. Upon sensing miss-folded proteins in the lumen of the ER, IRE1α gets dimerized and auto-phosphorylates its kinase domain thereby activating it's RNase activity[249,250]. It's RNase domain-mediated generation of *XBP1s* acts as a pro-survival factor for tumor growth whereas it's RIDD activity has been found responsible for regulating the expression of different invasive and angiogenic factors for example SPARC, CTGF, etc[251–253]. However, prolonged ER stress leads to IRE1α-mediated activation of apoptosis via IRE1α kinase-JNK-ASK1 pathway[254]. To avoid such situations during the initial phase of ER stress, UPR activation also leads to the generation of a negative feedback loop. PP2A and PPM are the two phosphatases which

dephosphorylate and thus inactivate IRE1α[65,255]. Stimulation of UPR by tunicamycin, an ER stress inducer, led to the phosphorylation of IRE1α at Ser724 residue in LN308 glioblastoma cells. The treatment also activated IRE1α and generated *XBP1s* in both glioblastoma cells as well as HEK293, however glioblastoma cells were found to have a better adaptation to chronic ER stress condition as observed by a reduced amount of *XBP1s* generation during second cycle (24 hours) of IRE1α RNase activity. This difference between glioblastoma and HEK cells could be due to differentially enhanced expression of factors responsible to maintain proteostasis for example, chaperons, etc, or high expression of proteins responsible for inhibition of IRE1α enzymatic activity, such as phosphatases. We also observed IRE1α-mediated regulation of invasive and angiogenic factors, like HEVIN, CYR61 and CTGF in LN308 glioblastoma cell lines. Inhibition of IRE1α endoribonuclease activity by STF083010 led to the stabilization of HEVIN and CTGF whereas IRE1α activation using APY29, an IRE1α-specific activator, led to reduction of their expression. PERK also gets dimerized and auto-phosphorylates itself upon accumulation of miss-folded protein within the ER and reduces overall translation of the cell by phosphorylating and inactivating eIF2α[256]. Phosphorylation of eIF2α leads to the disruption of the translation initiation complex which reduces the translation of regular proteins but enhances the expression of stress-induced proteins including ATF4 and CHOP[75]. Like, IRE1α, PERK activity can also be affected by a negative feedback loop where expression of GADD34 and PPP1R15B downstream of ATF4 leads to dephoshorylation of eIF2α thereby activating cellular translation machinery[78,257,258]. Treatment of LN308 glioblastoma cells with tunicamycin for 6 hours also led the activation of PERK branch of the UPR as could be observed by phosphorylation status of PERK, eIF2α and generation of ATF4. A reduction of P-eIF2α and ATF4 expression after 16 hours of tunicamycin treatment was also observed which might have happened because of feedback inhibition by expression of GADD34 and PPP1R15B.

Decades of research has shown involvement of UPR in tumor development although there is still little information known regarding branch-specific regulation of tumor development in glioblastoma[44,45,247].By investigating the secretome of glioblastoma, we have identified a new function of the UPR sensor PERK mediating the expression and cleavage of PAM. The UPR plays a major role in cancer progression being involved in the activation or repression of oncogenes and tumor-suppressor genes such as *BRAFv600E*[149] and *H-RAS*[151], respectively, regulating proliferation and angiogenesis[154], as well as invasion and tumor metastasis via the regulation of transcription factors such as SNAIL1, SNAIL2, ZEB2 and TCF3[165]. Most importantly, the UPR is among the main mechanisms involved in the adaptation of glioblastoma to the hypoxic stress, inducing its aggressive phenotype[236,237].When characterizing the activation of different UPR branches in low oxygen conditions, we found activation of PERK and ATF6α only, and a reduction in the activity of both domains of IRE1α. This could be a consequence of better adaptation of these cells to the hypoxic stress conditions avoiding the activation of pro-apoptotic mechanisms downstream of UPR signaling such as CHOP production or IRE1α-mediated activation of TRAF2-JNK-ASK1 signaling[66,259]. Unlike previous studies, our data suggest a selective activation of

different UPR branches under 1% O_2 in glioblastoma, a phenomenon that could be explained by the different levels of oxygen to which the tumor cells are exposed in the different tissues.[260,261]

Confrontation of cancer cells with both intrinsic metabolic burdens like nutrient deprivation, and simultaneous exposure to external environmental stresses including chemotherapeutic drugs, drives them towards activating the UPR in order to cope up with the increasing demand of protein synthesis. UPR thus, not just helps in maintaining protein homeostasis within the cell but also alerts the neighboring cells of the spawning tension in the microenvironment.[262–264] External transfer of stress signaling by UPR has recently come out to be an important phenomenon to induce immunogenicity against cancer cells which is most significantly being driven by PERK by a phenomenon known as DAMPs (Damage Associated Molecular Patterns)[265]. However, literature suggests that this extrinsic signaling via UPR can activate both pro- or anti-tumor inflammatory respons.[266,267]

As PERK is known to regulate the expression of several angiogenic factors such as VEGF-A, IL6 and FGF[236,268], we aimed to identify secreted factors that might be involved in PERK-mediated angiogenesis in glioblastoma. By proteomic screening of the secretome of the LN308 glioblastoma cell line under hypoxic stress, we identified PAM to be regulated by PERK. Among the identified hits, PAM is the only protein known to be either present on the plasma membrane, exosomal vesicles or secreted out as a cleaved product[199]. In that respect, we concluded that expression of PAM is significantly increased with reduced oxygen levels in glioblastoma cell lines only and shows an important regulation by HIF1α at the transcriptional level. Our data also suggested the presence of PAM expression on crude exosomal fraction from glioblastoma cells treated with hypoxia. As exosomes have been suggested to be a major tool with which cancer cells communicate with their microenvironment, presence of PAM on glioblastoma exosomes also implies the importance of PAM for the aggressiveness of glioblastoma. PAM has been shown previously to induce cytoskeleton rearrangements as well as the production and secretion of neuro-peptides[269,270]. It is composed of several luminal domains, a transmembrane domain and an unstructured cytosolic domain (PAM-CD), which facilitates its ability to interact with different proteins. The multiple phosphorylation sites among the 86 amino acid residues in this unstructured domain determine endocytic trafficking and proteolytic cleavage of PAM and influence the generation of PAM soluble fragment cytosolic domain (sfCD)[271,272]. Like other membrane proteins, such as SREBP (Sterol-regulatory element-binding protein) or ICA512 (an autoantigen of type I diabetes), PAM sfCD was also shown to transfer signals to the nuclei as a feedback mechanism[273,274]. Indeed, gene expression profiling of AtT-20 cells (mouse corticotrope tumor cells) overexpressing PAM showed increased expression of Aquaporin 1 (*Aqp1*) and secretory leukocyte peptidase inhibitor (*Slpi*), affecting formation and proteome content of secretory granules[275–277], both of which were validated to be regulated by PAM sfCD[209]. Moreover, *Aqp1* was also described to be involved in tumor migration, invasion and angiogenesis in glioblastoma[278,279]. By treating glioblastoma cells with a PERK activator, we show that its kinase activity is involved in the generation of the PAM sfCD, which might occur via a direct interaction between the proteins as

suggested by our findings. Recently published RNA-seq data showed many different pathways to be affected by PAM. Atf3, one of the major repressor transcription factor of UPR genes, was down-regulated upon PAM overexpression while Fkbp2, a peptidyl prolyl isomerases (PPIase) from FK506 binding proteins (FKBPs) family responsible for rate-limiting step in protein folding, was up-regulated highlighting the role of PAM in influencing ER protein folding capacity[280]. On the other hand, we were not able to observe any effect of PERK kinase activity on phosphorylation status of PAM suggesting an indirect effect of PERK kinase on generation of PAM sfCD. Our results, in the light of these studies, provide a strong hint towards the involvement of PAM in regulating essential pathways in glioblastoma including protein folding capacity of the ER, endocytic trafficking and secretion of factors necessary for tumor growth and angiogenesis.

PERK reduces the ER stress by inhibiting protein translation and reducing oxidative stress. In order to do so, PERK phosphorylates eukaryotic initiation factor 2α (eIF2α) and NRF2, respectively[82,281]. Upstream open reading frames (uORFs) in the 5' untranslated region (5'UTR) act as regulatory elements responsible for the inhibition of translation of the primary ORFs. In general, these regulatory uORFs are composed of short sequences and their translation lead to a frameshift which inhibits the translation of primary ORFs. Upon phosphorylation of eIF2α, the process of formation of translation initiation complex gets delayed which inhibits the translation of uORFs and lead to the expression of the primary ORF, for example, ATF4 expression. ATF4 regulates the transcription of many different mRNAs including chaperones responsible for the maintenance of protein homeostasis within the cell. ER stress can also be induced by other factors like amino acid deficiency, virus infection or reduced heme levels leading to the activation of GCN2, PKR or HRI, respectively, where these kinases also reduce the overall translation by phosphorylating eIF2α at serine-51 residue[282]. On the other hand, PERK-regulated stabilization of NRF2 transcription factor leads to expression of anti-oxidative proteins like NQO-1, HO-1, etc[283,284]. Interestingly, although our data showed that PERK kinase activity has a major impact on PAM protein, only PERK silencing showed a very strong effect on *PAM* mRNA levels, a phenomenon that seemed to be HIF1α-dependent. Through our experiments we could also show that among all eIF2α kinases, PERK is the only kinase which can regulate the expression of *PAM* mRNA. Moreover, we could not find any significant role of NRF2 in regulating *PAM* mRNA expression downstream of PERK in glioblastoma. As PERK has also been previously shown to bear kinase-independent roles, for example, in attenuating mitochondrial oxidative stress by regulating the formation of MAMs (Mitochondrial associated membranes) at ER-mitochondria contact sites [285], we postulated that PAM regulation by PERK is another non-canonical kinase-independent signaling paradigm with which PERK regulates glioblastoma angiogenesis.

Among the different glioblastoma subtypes, the mesenchymal (MES) one shows highly invasive growth, infiltration of microglia and thus poor prognosis of the glioblastoma patients[11]. NF1 loss of function and enhanced expression of AP-1 transcription factors are among the major genetic aberrations found in this

subtype of glioblastoma[11,286]. *In silico* analysis of the PAM promoter region revealed several putative transcription factors that might be involved in the regulation of *PAM* mRNA expression level, among which FOSL1, a component of the AP-1 complex. AP-1 consists of homo- or heterodimers of JUN and FOS family proteins and has been linked to EMT, invasion and metastasis in different cancer types including glioblastoma, and colorectal cancer, and has been found massively expressed in mesenchymal subtype of glioblastoma[287,288]. Moreover, HIF1α is an important regulator of AP-1, driving the nuclear localization of c-JUN[289]. Our data suggest that FOSL1-mediatedregulation of *PAM* mRNA expression as shown by AP-1 inhibition, under hypoxic conditions, might be due to an indirect effect of HIF1α stabilization. We found higher expression of PAM in MES-subtype of GSCs in comparison to the PN-subtypes *in vitro* which is also supported by the clinical data provided by TCGA of subtype-stratified glioblastoma patients. However, how PERK regulates PAM mRNA levels still remains to be elucidated.

PAM is a bi-functional type I membrane protein having a monooxygenase and lyase enzymatic units located on its luminal domains. Loss of PAM functionality has been implicated in various neuronal diseases, like, Menkes disease, multiple sclerosis and post-polio syndrome patients, thereby making it an important biomarker candidate [290,291]. Several studies have also shown the importance of PAM in the activation of adrenomedullin (ADM), a neuro-peptide involved in angiogenesis and invasion, as well as in reducing pro-inflammatory phenotype of microglia[217,292,293], and which occurred to induce tube formation in our glioblastoma cellular model. PAM homozygous knockout mice did not show any activation of ADM and die during embryogenesis due to severe edema, thinning of the aorta and carotid arteries depicting the importance of PAM in supporting ADM-mediated angiogenesis[294].Our data highlighted the role of PERK and thereby PAM in regulating angiogenesis in glioblastoma.

Aberrant angiogenesis is a fundamental process in tumor development and is partly responsible for the poor prognosis of glioblastoma patients. Although they have been targeted therapeutically, inhibition of angiogenic pathways in glioblastoma has only led to marginal success in reducing tumor burden. Indeed, Bevacizumab, a monoclonal antibody targeting the proangiogenic signaling molecule VEGFA, did not show promising results in glioblastoma, improving only the progression-free survival (PFS) in patients[241]. The reasons behind the outcome from these clinical trials may include insensitivity of anti-VEGF therapy towards tumor blood vessels[242] and alternative angiogenic growth factor expression[243], highlighting the importance identifying new angiogenic factors to be targeted. Determining the role of PERK in regulating PAM expression in xenograft mouse models would have been really challenging, as PERK knockdown reduced the survival of glioblastoma cells which might cause problems in engraftment of the tumor. On the other hand, recently published data shows that both PERK kinase inhibitors, GSK2606414 and GSK2656157 can inhibit RIPK1 with even higher efficacy thus providing misleading conclusions if used in *in vivo*[295]. Thus we chose to study only the effect of PAM expression on the growth of the tumor and survival of the mouse model. Silencing PAM in glioblastoma cells reduced tumor growth kinetics *in vivo* and thus increased overall survival of mice, demonstrating its importance for the tumor. Interestingly,

PAM mRNA expression level is significantly higher in glioblastoma patients as compared to normal brain samples and higher expression of PAM is an indicator of poor prognosis among glioblastoma patients[296].

Our study provides evidence of a new mechanism by which PERK regulates the expression and function of the proangiogenic factor PAM and highlights its potential to be considered as a therapeutic target for glioblastoma.

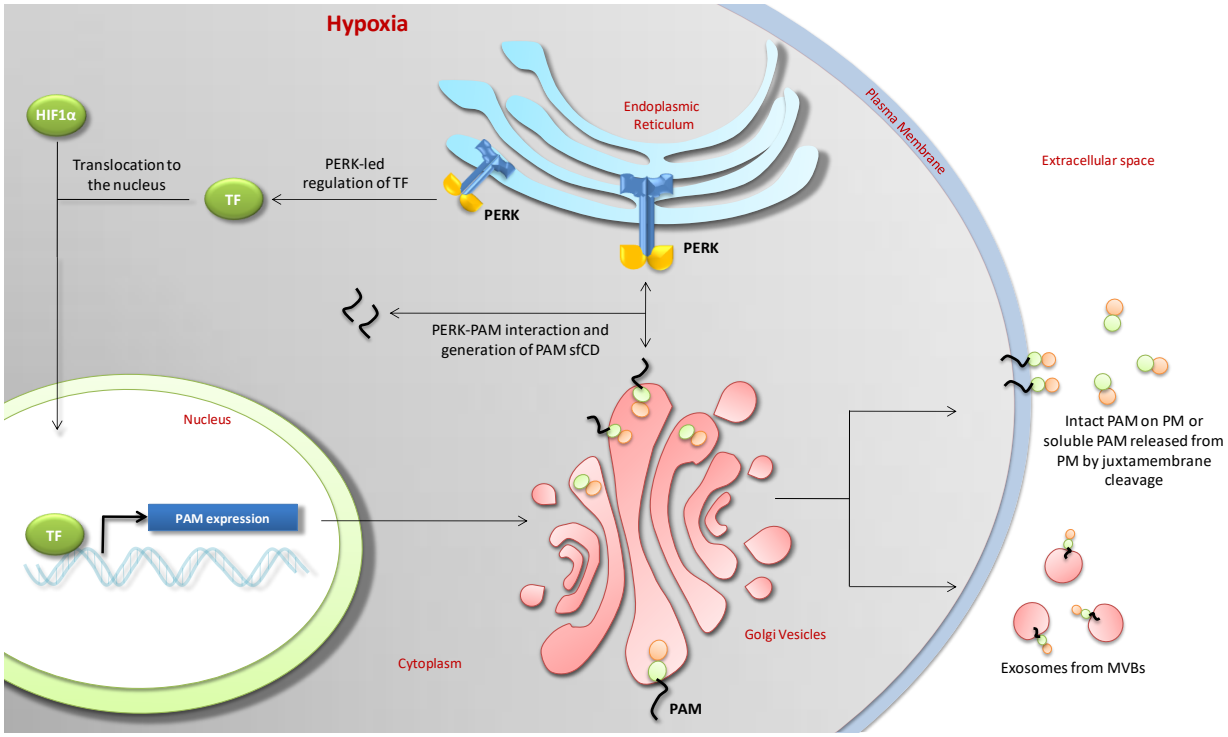

Figure 32. PERK is necessary for the expression of PAM in glioblastoma.
PERK (independent of its kinase activity) regulates the expression of PAM whereas its kinase activity mediates the generation of PAM sfCD. PAM can either be expressed on the plasma membrane or secreted out of the cells on exosomal membrane to induce microenvironment changes supporting tumor growth. TF, Transcription factor.

Outlook

The key objective of the PhD thesis was to investigate the involvement of UPR in glioblastoma secretome modulation under physiological hypoxic condition. In that respect, we opted for a proteomic approach and conducted mass spectrometry on the conditioned media of glioblastoma cell model. PAM was the most promising hit as it was known to be located on the membrane of exosomal vesicles and thereby acting as messenger influencing the tumor microenvironment. In order to uncover the regulatory role of PERK on PAM protein level, we characterized its involvement in PAM transcriptional and post-translational regulation, and studied its importance for tumor angiogenesis *in vitro*. PERK protein was found essential

for the expression of *PAM* mRNA level in glioblastoma under hypoxic condition, a phenomenon that was independent from its kinase activity, suggesting that a non-canonical signaling is responsible for this effect. The *in silico* TBA prediction provided a list of potentialtranscription factors binding to the PAM promoter region, particularly members of the AP-1 transcription complex such as FOSL1, FOS, c-JUN and JUNB. Interestingly, AP-1 inhibition reduced the level of *PAM* mRNA supporting the *in silico* prediction and suggesting an AP-1-mediated regulation of*PAM* mRNA expression. As AP-1 transcription factor is known to be involved in tumor progression, it is crucial to verify the binding of the AP-1 complex to the PAM promoter region by using CHIP sequencing.

Although PERK kinase activity was not regulating PAM at the mRNA level, our study confirmed the involvement of this enzymatic function for the generation of PAM sfCD, using the PERK selective activator CCT020312. In order to verify those results, we will overexpress a PERK kinase-dead mutant and investigate the level of PAM sfCD.

Interestingly, previous studies have highlighted the role of PAM sfCD in regulating gene expression sustaining tumor progression. In order to address it in glioblastoma, the next step would be to perform gene expression profiling of glioblastoma cells treated with hypoxia, with or without PERK activator CCT020312. To ensure that the changes are specific to the sfCD domain, an additional control with PAM knockdown should be included. In addition, it will also be interesting to determine whether PAM sfCD directly regulates gene expression changes by binding to particular gene promoter regions or acts as a part of a transcription factor complex.

Phenotypic characterization of PAM clearly highlighted its role in angiogenesis. This effect could be due to reduced ADM activation upon PAM knockdown, which could be verified by performing a HUVECs tube formation assay and determine whether administration of ADM-NH2 (active PAM product) can induce tube formation when treated with conditioned media from *PAM* knockdown glioblastoma cells.

Our pre-clinical study suggests a prominent role of PAM in supporting tumor growth, as the silencing of PAM in orthotopically transplanted glioblastoma cells increased the overall survival of mice as compared to glioblastoma cells expressing endogenous PAM. The fact that PAM is not the only regulator of angiogenesis in glioblastoma and VEGFA, a well studied and therapeutically intervened angiogenic factor is also expressed in our glioblastoma model, there is a need to determine that the reduced angiogenesis leading to decrease in tumor growth is specifically because of PAM and ADM-NH2. This can be achieved by performing VEGFA immunohistochemistry on the tumor sections from the *in vivo* experiment and determine whether *PAM* knockdown changes VEGFA expression in the xenograft model. As *PAM* knockdown in LN229 cells did not reduce the growth of the tumor completely, further pre-clinical studies need to be performed in combination with current chemotherapeutics and observe whether a combinatorial therapy including PAM inhibitors can be used to drastically improve glioblastoma patient survival.

This will help us to further characterize the significance of PAM in glioblastoma and determine whether it can be used as a potential therapeutic target for clinical studies. PAM-specific small molecule inhibitor screen can be performed to identify drug that targets PAM activity and the identified hit can later be assessed for its clinical efficacy. The identified drug can also be analyzed for its usage in combination with other anti-angiogenic therapeutics for effectively targeting glioblastoma thereby reducing the tumor growth and increasing the prognosis of patients.

5. References

1. Bray F, Ferlay J, Soerjomataram I, Siegel RL, Torre LA, Jemal A. Global cancer statistics 2018: GLOBOCAN estimates of incidence and mortality worldwide for 36 cancers in 185 countries. *CA Cancer J Clin*. 2018;68(6):394-424.

2. Bray F, Ferlay J, Soerjomataram I, Siegel RL, Torre LA, Jemal A. Global cancer statistics 2018: GLOBOCAN estimates of incidence and mortality worldwide for 36 cancers in 185 countries. *CA Cancer J Clin*. 2018;68(6):394-424.

3. Louis DN, Ohgaki H, Wiestler OD, Cavenee WK, Burger PC, Jouvet A, et al. The 2007 WHO classification of tumours of the central nervous system. *Acta Neuropathol*. 2007;114(2):97-109.

4. Louis DN, Perry A, Reifenberger G, von Deimling A, Figarella-Branger D, Cavenee WK, et al. The 2016 World Health Organization Classification of Tumors of the Central Nervous System: a summary. *Acta Neuropathol*. 2016;131(6):803-820.

5. van den Bent MJ, Weller M, Wen PY, Kros JM, Aldape K, Chang S. A clinical perspective on the 2016 WHO brain tumor classification and routine molecular diagnostics. *Neuro Oncol*. 2017;19(5):614-624.

6. Crespo I, Vital AL, Gonzalez-Tablas M, Patino M del C, Otero A, Lopes MC, et al. Molecular and Genomic Alterations in Glioblastoma Multiforme. *Am J Pathol*. 2015;185(7):1820-1833.

7. Aldape K, Zadeh G, Mansouri S, Reifenberger G, von Deimling A. Glioblastoma: pathology, molecular mechanisms and markers. *Acta Neuropathol*. 2015;129(6):829-848.

8. Hegi ME, Diserens A-C, Gorlia T, Hamou M-F, de Tribolet N, Weller M, et al. *MGMT* Gene Silencing and Benefit from Temozolomide in Glioblastoma. *N Engl J Med*. 2005;352(10):997-1003.

9. Stupp R, Mason WP, van den Bent MJ, Weller M, Fisher B, Taphoorn MJB, et al. Radiotherapy plus Concomitant and Adjuvant Temozolomide for Glioblastoma. *N Engl J Med*. 2005;352(10):987-996.

10. Cancer Genome Atlas Research Network TCGA (TCGA) R. Comprehensive genomic characterization defines human glioblastoma genes and core pathways. *Nature*. 2008;455(7216):1061-1068.

11. Wang Q, Hu B, Hu X, Kim H, Squatrito M, Scarpace L, et al. Tumor Evolution of Glioma-Intrinsic Gene Expression Subtypes Associates with Immunological Changes in the Microenvironment.

Cancer Cell. 2017;32(1):42-56.e6.

12. Phillips HS, Kharbanda S, Chen R, Forrest WF, Soriano RH, Wu TD, et al. Molecular subclasses of high-grade glioma predict prognosis, delineate a pattern of disease progression, and resemble stages in neurogenesis. *Cancer Cell*. 2006;9(3):157-173.

13. Huse JT, Phillips HS, Brennan CW. Molecular subclassification of diffuse gliomas: Seeing order in the chaos. *Glia*. 2011;59(8):1190-1199.

14. Zheng S, Chheda MG, Verhaak RGW. Studying a complex tumor: potential and pitfalls. *Cancer J*. 2012;18(1):107-114.

15. Ozawa T, Riester M, Cheng Y-K, Huse JT, Squatrito M, Helmy K, et al. Most Human Non-GCIMP Glioblastoma Subtypes Evolve from a Common Proneural-like Precursor Glioma. *Cancer Cell*. 2014;26(2):288-300.

16. Bhat KPL, Balasubramaniyan V, Vaillant B, Ezhilarasan R, Hummelink K, Hollingsworth F, et al. Mesenchymal differentiation mediated by NF-κB promotes radiation resistance in glioblastoma. *Cancer Cell*. 2013;24(3):331-346.

17. Noushmehr H, Weisenberger DJ, Diefes K, Phillips HS, Pujara K, Berman BP, et al. Identification of a CpG Island Methylator Phenotype that Defines a Distinct Subgroup of Glioma. *Cancer Cell*. 2010;17(5):510-522.

18. Sturm D, Witt H, Hovestadt V, Khuong-Quang D-A, Jones DTW, Konermann C, et al. Hotspot Mutations in H3F3A and IDH1 Define Distinct Epigenetic and Biological Subgroups of Glioblastoma. *Cancer Cell*. 2012;22(4):425-437.

19. Ann N, Bush O, Chang SM, Berger MS. Current and future strategies for treatment of glioma.

20. Winkler F, Kozin S V., Tong RT, Chae S-S, Booth MF, Garkavtsev I, et al. Kinetics of vascular normalization by VEGFR2 blockade governs brain tumor response to radiation: Role of oxygenation, angiopoietin-1, and matrix metalloproteinases. *Cancer Cell*. 2004;6(6):553-563.

21. Batchelor TT, Reardon DA, de Groot JF, Wick W, Weller M. Antiangiogenic therapy for glioblastoma: current status and future prospects. *Clin Cancer Res*. 2014;20(22):5612-5619.

22. Kreisl TN, Kim L, Moore K, Duic P, Royce C, Stroud I, et al. Phase II trial of single-agent bevacizumab followed by bevacizumab plus irinotecan at tumor progression in recurrent glioblastoma. *J Clin Oncol*. 2009;27(5):740-745.

23. Friedman HS, Prados MD, Wen PY, Mikkelsen T, Schiff D, Abrey LE, et al. Bevacizumab Alone and in Combination With Irinotecan in Recurrent Glioblastoma. *J Clin Oncol*. 27:4733-4740.

24. Chinot OL, Wick W, Mason W, Henriksson R, Saran F, Nishikawa R, et al. Bevacizumab plus Radiotherapy–Temozolomide for Newly Diagnosed Glioblastoma. *N Engl J Med*. 2014;370(8):709-722.

25. Gilbert MR, Dignam JJ, Armstrong TS, Wefel JS, Blumenthal DT, Vogelbaum MA, et al. A Randomized Trial of Bevacizumab for Newly Diagnosed Glioblastoma. *N Engl J Med*. 2014;370(8):699-708.

26. Franz DN, Belousova E, Sparagana S, Bebin EM, Frost M, Kuperman R, et al. Efficacy and safety of everolimus for subependymal giant cell astrocytomas associated with tuberous sclerosis complex (EXIST-1): a multicentre, randomised, placebo-controlled phase 3 trial. *Lancet*. 2013;381(9861):125-132.

27. Franz DN, Belousova E, Sparagana S, Bebin EM, Frost M, Kuperman R, et al. Everolimus for subependymal giant cell astrocytoma in patients with tuberous sclerosis complex: 2-year open-label extension of the randomised EXIST-1 study. *Lancet Oncol*. 2014;15(13):1513-1520.

28. Chow KK, Naik S, Kakarla S, Brawley VS, Shaffer DR, Yi Z, et al. T Cells Redirected to EphA2 for the Immunotherapy of Glioblastoma. *Mol Ther*. 2013;21(3):629-637.

29. Nam J, Joo KM, Lee SJ, Jo M-Y, Kim Y, Jin Y, et al. Synergistic therapeutic effects of cytokine-induced killer cells and temozolomide against glioblastoma. *Oncol Rep*. 2010;25(1):33-39.

30. Reardon DA, Freeman G, Wu C, Chiocca EA, Wucherpfennig KW, Wen PY, et al. Immunotherapy advances for glioblastoma. *Neuro Oncol*. 2014;16(11):1441-1458.

31. Brown CE, Starr R, Aguilar B, Shami AF, Martinez C, D'Apuzzo M, et al. Stem-like tumor-initiating cells isolated from IL13Rα2 expressing gliomas are targeted and killed by IL13-zetakine-redirected T Cells. *Clin Cancer Res*. 2012;18(8):2199-2209.

32. Fagone P, Jackowski S. Membrane phospholipid synthesis and endoplasmic reticulum function. *J Lipid Res*. 2009;50 Suppl(Supplement):S311-6.

33. Berridge MJ. The endoplasmic reticulum: a multifunctional signaling organelle. *Cell Calcium*. 2002;32(5-6):235-249.

34. Coe H, Michalak M. *R e v i e w Calcium Binding Chaperones of the Endoplasmic Reticulum*. Vol 28.; 2009. http://www.gpb.sav.sk/FI-2009/F96.pdf. Accessed April 6, 2019.

35. Filadi R, Theurey P, Pizzo P. The endoplasmic reticulum-mitochondria coupling in health and disease: Molecules, functions and significance. *Cell Calcium*. 2017;62:1-15.

36. Walter P, Ron D. The unfolded protein response: from stress pathway to homeostatic regulation. *Science*. 2011;334(6059):1081-1086.

37. Tabas I, Ron D. Integrating the mechanisms of apoptosis induced by endoplasmic reticulum stress. *Nat Cell Biol*. 2011;13(3):184-190.

38. Bertolotti A, Zhang Y, Hendershot LM, Harding HP, Ron D. Dynamic interaction of BiP and ER stress transducers in the unfolded-protein response. *Nat Cell Biol*. 2000;2(6):326-332.

39. Xiang C, Wang Y, Zhang H, Han F. The role of endoplasmic reticulum stress in neurodegenerative disease. *Apoptosis*. 2017;22(1):1-26.

40. Cao SS, Luo KL, Shi L. Endoplasmic Reticulum Stress Interacts With Inflammation in Human Diseases. *J Cell Physiol*. 2016;231(2):288-294.

41. Engin F. ER stress and development of type 1 diabetes. *J Investig Med*. 2016;64(1):2-6.

42. Gregor MF, Hotamisligil GS. *Thematic review series: Adipocyte Biology.* Adipocyte stress: the endoplasmic reticulum and metabolic disease. *J Lipid Res*. 2007;48(9):1905-1914.

43. Hazari YM, Bashir A, Haq E ul, Fazili KM. Emerging tale of UPR and cancer: an essentiality for malignancy. *Tumor Biol*. 2016;37(11):14381-14390.

44. Le Reste P-J, Avril T, Quillien V, Morandi X, Chevet E. Reprint of: Signaling the Unfolded Protein Response in primary brain cancers. *Brain Res*. 2016;1648:542-552.

45. Peñaranda Fajardo NM, Meijer C, Kruyt FAE. The endoplasmic reticulum stress/unfolded protein response in gliomagenesis, tumor progression and as a therapeutic target in glioblastoma. *Biochem Pharmacol*. 2016;118:1-8.

46. Gardner BM, Walter P. Unfolded proteins are Ire1-activating ligands that directly induce the unfolded protein response. *Science*. 2011;333(6051):1891-1894.

47. Credle JJ, Finer-Moore JS, Papa FR, Stroud RM, Walter P. On the mechanism of sensing unfolded protein in the endoplasmic reticulum. *Proc Natl Acad Sci U S A*. 2005;102(52):18773-18784.

48. Lu Y, Liang F-X, Wang X. A Synthetic Biology Approach Identifies the Mammalian UPR RNA

Ligase RtcB. *Mol Cell*. 2014;55(5):758-770.

49. Yanagitani K, Imagawa Y, Iwawaki T, Hosoda A, Saito M, Kimata Y, et al. Cotranslational Targeting of XBP1 Protein to the Membrane Promotes Cytoplasmic Splicing of Its Own mRNA. *Mol Cell*. 2009;34(2):191-200.

50. Yanagitani K, Kimata Y, Kadokura H, Kohno K. Translational pausing ensures membrane targeting and cytoplasmic splicing of XBP1u mRNA. *Science*. 2011;331(6017):586-589.

51. Yoshida H, Oku M, Suzuki M, Mori K. pXBP1(U) encoded in XBP1 pre-mRNA negatively regulates unfolded protein response activator pXBP1(S) in mammalian ER stress response. *J Cell Biol*. 2006;172(4):565-575.

52. Han D, Lerner AG, Vande Walle L, Upton J-P, Xu W, Hagen A, et al. IRE1α Kinase Activation Modes Control Alternate Endoribonuclease Outputs to Determine Divergent Cell Fates. *Cell*. 2009;138(3):562-575.

53. Maurel M, Chevet E, Tavernier J, Gerlo S. Getting RIDD of RNA: IRE1 in cell fate regulation. *Trends Biochem Sci*. 2014;39(5):245-254.

54. Hollien J, Weissman JS. Decay of endoplasmic reticulum-localized mRNAs during the unfolded protein response. *Science*. 2006;313(5783):104-107.

55. Hollien J, Lin JH, Li H, Stevens N, Walter P, Weissman JS. Regulated Ire1-dependent decay of messenger RNAs in mammalian cells. *J Cell Biol*. 2009;186(3):323-331.

56. Shoulders MD, Ryno LM, Genereux JC, Moresco JJ, Tu PG, Wu C, et al. Stress-Independent Activation of XBP1s and/or ATF6 Reveals Three Functionally Diverse ER Proteostasis Environments. *Cell Rep*. 2013;3(4):1279-1292.

57. Kanemoto S, Kondo S, Ogata M, Murakami T, Urano F, Imaizumi K. XBP1 activates the transcription of its target genes via an ACGT core sequence under ER stress. *Biochem Biophys Res Commun*. 2005;331(4):1146-1153.

58. Genereux JC, Qu S, Zhou M, Ryno LM, Wang S, Shoulders MD, et al. Unfolded protein response-induced ERdj3 secretion links ER stress to extracellular proteostasis. *EMBO J*. 2015;34(1):4-19.

59. Yoshida H, Matsui T, Hosokawa N, Kaufman RJ, Nagata K, Mori K. A Time-Dependent Phase Shift in the Mammalian Unfolded Protein Response. *Dev Cell*. 2003;4(2):265-271.

60. Acosta-Alvear D, Zhou Y, Blais A, Tsikitis M, Lents NH, Arias C, et al. XBP1 Controls Diverse Cell

Type- and Condition-Specific Transcriptional Regulatory Networks. *Mol Cell*. 2007;27(1):53-66.

61. Calfon M, Zeng H, Urano F, Till JH, Hubbard SR, Harding HP, et al. IRE1 couples endoplasmic reticulum load to secretory capacity by processing the XBP-1 mRNA. *Nature*. 2002;415(6867):92-96.

62. Yoshida H, Matsui T, Yamamoto A, Okada T, Mori K. XBP1 mRNA Is Induced by ATF6 and Spliced by IRE1 in Response to ER Stress to Produce a Highly Active Transcription Factor. *Cell*. 2001;107(7):881-891.

63. Lee K, Tirasophon W, Shen X, Michalak M, Prywes R, Okada T, et al. IRE1-mediated unconventional mRNA splicing and S2P-mediated ATF6 cleavage merge to regulate XBP1 in signaling the unfolded protein response. *Genes Dev*. 2002;16(4):452-466.

64. Lu G, Ota A, Ren S, Franklin S, Rau CD, Ping P, et al. PPM1l encodes an inositol requiring-protein 1 (IRE1) specific phosphatase that regulates the functional outcome of the ER stress response. *Mol Metab*. 2013;2(4):405-416.

65. Qiu Y, Mao T, Zhang Y, Shao M, You J, Ding Q, et al. A crucial role for RACK1 in the regulation of glucose-stimulated IRE1alpha activation in pancreatic beta cells. *Sci Signal*. 2010;3(106):ra7.

66. Urano F, Wang X, Bertolotti A, Zhang Y, Chung P, Harding HP, et al. Coupling of stress in the ER to activation of JNK protein kinases by transmembrane protein kinase IRE1. *Science*. 2000;287(5453):664-666.

67. Harding HP, Zhang Y, Ron D. Protein translation and folding are coupled by an endoplasmic-reticulum-resident kinase. *Nature*. 1999;397(6716):271-274.

68. Harding HP, Zhang Y, Bertolotti A, Zeng H, Ron D. Perk Is Essential for Translational Regulation and Cell Survival during the Unfolded Protein Response. *Mol Cell*. 2000;5(5):897-904.

69. Krishnan N, Fu C, Pappin DJ, Tonks NK. H2S-Induced sulfhydration of the phosphatase PTP1B and its role in the endoplasmic reticulum stress response. *Sci Signal*. 2011;4(203):ra86.

70. Huber A-L, Lebeau J, Guillaumot P, Pétrilli V, Malek M, Chilloux J, et al. p58IPK-Mediated Attenuation of the Proapoptotic PERK-CHOP Pathway Allows Malignant Progression upon Low Glucose. *Mol Cell*. 2013;49(6):1049-1059.

71. Yan W, Frank CL, Korth MJ, Sopher BL, Novoa I, Ron D, et al. Control of PERK eIF2alpha kinase activity by the endoplasmic reticulum stress-induced molecular chaperone P58IPK. *Proc Natl Acad Sci U S A*. 2002;99(25):15920-15925.

72. Yamani L, Latreille M, Larose L. Interaction of Nck1 and PERK phosphorylated at Y ^{561} negatively modulates PERK activity and PERK regulation of pancreatic β-cell proinsulin content. Luo K, ed. *Mol Biol Cell*. 2014;25(5):702-711.

73. Harding HP, Zhang Y, Bertolotti A, Zeng H, Ron D. Perk Is Essential for Translational Regulation and Cell Survival during the Unfolded Protein Response. *Mol Cell*. 2000;5(5):897-904.

74. HARBOR AH-CS, 2000 undefined. Mechanism and regulation of initiator methionyl-tRNA binding to ribosomes. *CSH COLD SPRING Harb*. https://scholar.google.com/scholar?hl=en&as_sdt=0%2C5&q=Mechanism+and+regulation+of+initiator+methionyl-tRNA+binding+to+ribosomes%2C+in+Translational+Control+of+Gene+Expression%2C&btnG=. Accessed April 6, 2019.

75. Vattem KM, Wek RC. Reinitiation involving upstream ORFs regulates ATF4 mRNA translation in mammalian cells. *Proc Natl Acad Sci U S A*. 2004;101(31):11269-11274.

76. Zhou D, Palam LR, Jiang L, Narasimhan J, Staschke KA, Wek RC. Phosphorylation of eIF2 Directs ATF5 Translational Control in Response to Diverse Stress Conditions. *J Biol Chem*. 2008;283(11):7064-7073.

77. Palam LR, Baird TD, Wek RC. Phosphorylation of eIF2 facilitates ribosomal bypass of an inhibitory upstream ORF to enhance CHOP translation. *J Biol Chem*. 2011;286(13):10939-10949.

78. Lee Y-Y, Cevallos RC, Jan E. An upstream open reading frame regulates translation of GADD34 during cellular stresses that induce eIF2alpha phosphorylation. *J Biol Chem*. 2009;284(11):6661-6673.

79. Shi Y, Vattem KM, Sood R, An J, Liang J, Stramm L, et al. Identification and characterization of pancreatic eukaryotic initiation factor 2 alpha-subunit kinase, PEK, involved in translational control. *Mol Cell Biol*. 1998;18(12):7499-7509. http://www.ncbi.nlm.nih.gov/pubmed/9819435. Accessed August 23, 2018.

80. Cullinan SB, Diehl JA. *PERK-Dependent Activation of Nrf2 Contributes to Redox Homeostasis and Cell Survival Following ER Stress*. JBC Papers in Press; 2004. http://www.jbc.org/. Accessed August 23, 2018.

81. Cullinan SB, Zhang D, Hannink M, Arvisais E, Kaufman RJ, Diehl JA. Nrf2 is a direct PERK substrate and effector of PERK-dependent cell survival. *Mol Cell Biol*. 2003;23(20):7198-7209.

82. Cullinan SB, Diehl JA. Coordination of ER and oxidative stress signaling: The PERK/Nrf2 signaling pathway. *Int J Biochem Cell Biol*. 2006;38(3):317-332.

83. Bobrovnikova-Marjon E, Pytel D, Riese MJ, Vaites LP, Singh N, Koretzky GA, et al. PERK utilizes intrinsic lipid kinase activity to generate phosphatidic acid, mediate Akt activation, and promote adipocyte differentiation. *Mol Cell Biol*. 2012;32(12):2268-2278.

84. Thuerauf DJ, Morrison L, Glembotski CC. Opposing roles for ATF6alpha and ATF6beta in endoplasmic reticulum stress response gene induction. *J Biol Chem*. 2004;279(20):21078-21084.

85. Thuerauf DJ, Marcinko M, Belmont PJ, Glembotski CC. Effects of the isoform-specific characteristics of ATF6 alpha and ATF6 beta on endoplasmic reticulum stress response gene expression and cell viability. *J Biol Chem*. 2007;282(31):22865-22878.

86. Haze K, Yoshida H, Yanagi H, Yura T, Mori K. Mammalian Transcription Factor ATF6 Is Synthesized as a Transmembrane Protein and Activated by Proteolysis in Response to Endoplasmic Reticulum Stress. Silver P, ed. *Mol Biol Cell*. 1999;10(11):3787-3799.

87. Nadanaka S, Okada T, Yoshida H, Mori K. Role of disulfide bridges formed in the luminal domain of ATF6 in sensing endoplasmic reticulum stress. *Mol Cell Biol*. 2007;27(3):1027-1043.

88. Higa A, Taouji S, Lhomond S, Jensen D, Fernandez-Zapico ME, Simpson JC, et al. Endoplasmic Reticulum Stress-Activated Transcription Factor ATF6α Requires the Disulfide Isomerase PDIA5 To Modulate Chemoresistance. *Mol Cell Biol*. 2014;34(10):1839-1849.

89. Lynch JM, Maillet M, Vanhoutte D, Schloemer A, Sargent MA, Blair NS, et al. A Thrombospondin-Dependent Pathway for a Protective ER Stress Response. *Cell*. 2012;149(6):1257-1268.

90. Schewe DM, Aguirre-Ghiso JA. ATF6alpha-Rheb-mTOR signaling promotes survival of dormant tumor cells in vivo. *Proc Natl Acad Sci U S A*. 2008;105(30):10519-10524.

91. Schindler AJ, Schekman R. In vitro reconstitution of ER-stress induced ATF6 transport in COPII vesicles. *Proc Natl Acad Sci U S A*. 2009;106(42):17775-17780.

92. Fonseca SG, Ishigaki S, Oslowski CM, Lu S, Lipson KL, Ghosh R, et al. Wolfram syndrome 1 gene negatively regulates ER stress signaling in rodent and human cells. *J Clin Invest*. 2010;120(3):744-755.

93. Ye J, Rawson RB, Komuro R, Chen X, Davé UP, Prywes R, et al. ER Stress Induces Cleavage of Membrane-Bound ATF6 by the Same Proteases that Process SREBPs. *Mol Cell*. 2000;6(6):1355-1364.

94. Roy B, Lee AS. Transduction of calcium stress through interaction of the human transcription factor CBF with the proximal CCAAT regulatory element of the grp78/BiP promoter. *Mol Cell Biol*. 1995;15(4):2263-2274.

95. Roy B, Li WW, Lee AS. Calcium-sensitive transcriptional activation of the proximal CCAAT regulatory element of the grp78/BiP promoter by the human nuclear factor CBF/NF-Y. *J Biol Chem*. 1996;271(46):28995-29002.

96. Thuerauf DJ, Morrison LE, Hoover H, Glembotski CC. Coordination of ATF6-mediated transcription and ATF6 degradation by a domain that is shared with the viral transcription factor, VP16. *J Biol Chem*. 2002;277(23):20734-20739.

97. Yoshida H, Okada T, Haze K, Yanagi H, Yura T, Negishi M, et al. ATF6 Activated by Proteolysis Binds in the Presence of NF-Y (CBF) Directly to the cis-Acting Element Responsible for the Mammalian Unfolded Protein Response. *Mol Cell Biol*. 2000;20(18):6755-6767.

98. Shkoda A, Ruiz PA, Daniel H, Kim SC, Rogler G, Sartor RB, et al. Interleukin-10 Blocked Endoplasmic Reticulum Stress in Intestinal Epithelial Cells: Impact on Chronic Inflammation. *Gastroenterology*. 2007;132(1):190-207.

99. Odisho T, Zhang L, Volchuk A. ATF6β regulates the Wfs1 gene and has a cell survival role in the ER stress response in pancreatic β-cells. *Exp Cell Res*. 2015;330(1):111-122.

100. Lee A-H, Heidtman K, Hotamisligil GS, Glimcher LH. Dual and opposing roles of the unfolded protein response regulated by IRE1alpha and XBP1 in proinsulin processing and insulin secretion. *Proc Natl Acad Sci U S A*. 2011;108(21):8885-8890.

101. Rutkowski DT, Kang S-W, Goodman AG, Garrison JL, Taunton J, Katze MG, et al. The Role of p58 ^{IPK} in Protecting the Stressed Endoplasmic Reticulum. Gilmore R, ed. *Mol Biol Cell*. 2007;18(9):3681-3691.

102. Howarth DL, Lindtner C, Vacaru AM, Sachidanandam R, Tsedensodnom O, Vasilkova T, et al. Activating Transcription Factor 6 Is Necessary and Sufficient for Alcoholic Fatty Liver Disease in Zebrafish. Mullins MC, ed. *PLoS Genet*. 2014;10(5):e1004335.

103. Nakanishi K, Sudo T, Morishima N. Endoplasmic reticulum stress signaling transmitted by ATF6 mediates apoptosis during muscle development. *J Cell Biol*. 2005;169(4):555-560.

104. Thuerauf DJ, Hoover H, Meller J, Hernandez J, Su L, Andrews C, et al. Sarco/endoplasmic reticulum calcium ATPase-2 expression is regulated by ATF6 during the endoplasmic reticulum

stress response: intracellular signaling of calcium stress in a cardiac myocyte model system. *J Biol Chem*. 2001;276(51):48309-48317.

105. Pandey VK, Mathur A, Kakkar P. Emerging role of Unfolded Protein Response (UPR) mediated proteotoxic apoptosis in diabetes. *Life Sci*. 2019;216:246-258.

106. Schönenberger MJ, Kovacs WJ. Hypoxia signaling pathways: modulators of oxygen-related organelles. *Front cell Dev Biol*. 2015;3:42.

107. Kim LC, Cook RS, Chen J. mTORC1 and mTORC2 in cancer and the tumor microenvironment.

108. Laplante M, Sabatini DM. mTOR Signaling in Growth Control and Disease. *Cell*. 2012;149(2):274-293.

109. Saxton RA, Sabatini DM. mTOR Signaling in Growth, Metabolism, and Disease. *Cell*. 2017;168(6):960-976.

110. Connolly E, Braunstein S, Formenti S, Schneider RJ. Hypoxia inhibits protein synthesis through a 4E-BP1 and elongation factor 2 kinase pathway controlled by mTOR and uncoupled in breast cancer cells. *Mol Cell Biol*. 2006;26(10):3955-3965.

111. Wang S, Kaufman RJ. The impact of the unfolded protein response on human disease. *J Cell Biol*. 2012;197(7):857-867.

112. Hipp MS, Park S-H, Hartl FU. Proteostasis impairment in protein-misfolding and -aggregation diseases. *Trends Cell Biol*. 2014;24(9):506-514.

113. Ji C, Kaplowitz N. ER stress: Can the liver cope? *J Hepatol*. 2006;45(2):321-333.

114. Sozen E, Ozer NK. Impact of high cholesterol and endoplasmic reticulum stress on metabolic diseases: An updated mini-review. *Redox Biol*. 2017;12:456-461.

115. Koeberle A, Pergola C, Shindou H, Koeberle SC, Shimizu T, Laufer SA, et al. Role of p38 mitogen-activated protein kinase in linking stearoyl-CoA desaturase-1 activity with endoplasmic reticulum homeostasis. *FASEB J*. 2015;29(6):2439-2449.

116. Khan MM, Yang W-L, Brenner M, Bolognese AC, Wang P. Cold-inducible RNA-binding protein (CIRP) causes sepsis-associated acute lung injury via induction of endoplasmic reticulum stress. *Sci Rep*. 2017;7:41363.

117. Zeng M, Sang W, Chen S, Chen R, Zhang H, Xue F, et al. 4-PBA inhibits LPS-induced

inflammation through regulating ER stress and autophagy in acute lung injury models. *Toxicol Lett*. 2017;271:26-37.

118. Shah D, Romero F, Guo Z, Sun J, Li J, Kallen CB, et al. Obesity-Induced Endoplasmic Reticulum Stress Causes Lung Endothelial Dysfunction and Promotes Acute Lung Injury. *Am J Respir Cell Mol Biol*. 2017;57(2):204-215.

119. Zhang L, Wang Y, Pandupuspitasari NS, Wu G, Xiang X, Gong Q, et al. Endoplasmic reticulum stress, a new wrestler, in the pathogenesis of idiopathic pulmonary fibrosis. *Am J Transl Res*. 2017;9(2):722-735. http://www.ncbi.nlm.nih.gov/pubmed/28337301. Accessed May 1, 2018.

120. Maekawa H, Inagi R. Stress Signal Network between Hypoxia and ER Stress in Chronic Kidney Disease. *Front Physiol*. 2017;8:74.

121. Zhuang A, Forbes JM. Stress in the kidney is the road to pERdition: is endoplasmic reticulum stress a pathogenic mediator of diabetic nephropathy? *J Endocrinol*. 2014;222(3):R97-R111.

122. Fan Y, Zhang J, Xiao W, Lee K, Li Z, Wen J, et al. Rtn1a-Mediated Endoplasmic Reticulum Stress in Podocyte Injury and Diabetic Nephropathy. *Sci Rep*. 2017;7(1):323.

123. Sano R, Reed JC. ER stress-induced cell death mechanisms. *Biochim Biophys Acta - Mol Cell Res*. 2013;1833(12):3460-3470.

124. Tabas I, Ron D. Integrating the mechanisms of apoptosis induced by endoplasmic reticulum stress. *Nat Cell Biol*. 2011;13(3):184-190.

125. EBSCOhost | 85860044 | Inositol-requiring protein 1α signaling pathway is activated in the temporal cortex of patients with mesial temporal lobe epilepsy. http://web.a.ebscohost.com/abstract?site=ehost&scope=site&jrnl=15901874&AN=85860044&h=wg%2FNWsTEfqO7Lq9kMrad%2BocujV%2FQVUWzJhFgL0St3tggl1HPdZ1%2Fk2yt5VxZ6ixE%2Bep5nMZKE%2BFrXED03MnwpA%3D%3D&crl=c&resultLocal=ErrCrlNoResults&resultNs=Ehost&crlhashurl=logi. Accessed May 1, 2018.

126. Wang J, Cazzato E, Ladewig E, Frattini V, Rosenbloom DIS, Zairis S, et al. Clonal evolution of glioblastoma under therapy. *Nat Genet*. 2016.

127. Hetz C, Thielen P, Matus S, Nassif M, Court F, Kiffin R, et al. XBP-1 deficiency in the nervous system protects against amyotrophic lateral sclerosis by increasing autophagy. *Genes Dev*. 2009;23(19):2294-2306.

128. Vidal RL, Figueroa A, Court FA, Thielen P, Molina C, Wirth C, et al. Targeting the UPR

transcription factor XBP1 protects against Huntington's disease through the regulation of FoxO1 and autophagy. *Hum Mol Genet*. 2012;21(10):2245-2262.

129. Valenzuela V, Collyer E, Armentano D, Parsons GB, Court FA, Hetz C. Activation of the unfolded protein response enhances motor recovery after spinal cord injury. *Cell Death Dis*. 2012;3(2):272.

130. Gerakis Y, Hetz C. A decay of the adaptive capacity of the unfolded protein response exacerbates Alzheimer's disease. *Neurobiol Aging*. 2018;63:162-164.

131. Valdés P, Mercado G, Vidal RL, Molina C, Parsons G, Court FA, et al. Control of dopaminergic neuron survival by the unfolded protein response transcription factor XBP1. *Proc Natl Acad Sci U S A*. 2014;111(18):6804-6809.

132. Placzek AN, Prisco GV Di, Khatiwada S, Sgritta M, Huang W, Krnjević K, et al. eIF2α-mediated translational control regulates the persistence of cocaine-induced LTP in midbrain dopamine neurons. *Elife*. 2016;5:e17517.

133. Tsaytler P, Harding HP, Ron D, Bertolotti A. Selective Inhibition of a Regulatory Subunit of Protein Phosphatase 1 Restores Proteostasis. *Science (80-)*. 2011;332(6025):91-94.

134. Das I, Krzyzosiak A, Schneider K, Wrabetz L, D'Antonio M, Barry N, et al. Preventing proteostasis diseases by selective inhibition of a phosphatase regulatory subunit. *Science (80-)*. 2015;348(6231):239-242.

135. Ma T, Trinh MA, Wexler AJ, Bourbon C, Gatti E, Pierre P, et al. Suppression of eIF2α kinases alleviates Alzheimer's disease–related plasticity and memory deficits. *Nat Neurosci*. 2013;16(9):1299-1305.

136. Moreno JA, Radford H, Peretti D, Steinert JR, Verity N, Martin MG, et al. Sustained translational repression by eIF2α-P mediates prion neurodegeneration. *Nature*. 2012;485(7399):507-511.

137. Moreno JA, Halliday M, Molloy C, Radford H, Verity N, Axten JM, et al. Oral Treatment Targeting the Unfolded Protein Response Prevents Neurodegeneration and Clinical Disease in Prion-Infected Mice. *Sci Transl Med*. 2013;5(206):206ra138-206ra138.

138. Eizirik DL, Cardozo AK, Cnop M. The Role for Endoplasmic Reticulum Stress in Diabetes Mellitus. *Endocr Rev*. 2008;29(1):42-61.

139. Salvadó L, Palomer X, Barroso E, Vázquez-Carrera M. Targeting endoplasmic reticulum stress in insulin resistance. *Trends Endocrinol Metab*. 2015;26(8):438-448.

140. Sommerweiss D, Gorski T, Richter S, Garten A, Kiess W. Oleate rescues INS-1E β-cells from palmitate-induced apoptosis by preventing activation of the unfolded protein response. *Biochem Biophys Res Commun*. 2013;441(4):770-776.

141. Sha H, He Y, Yang L, Qi L. Stressed out about obesity: IRE1α-XBP1 in metabolic disorders. *Trends Endocrinol Metab*. 2011;22(9):374-381.

142. Jiang D, Niwa M, Koong AC. Targeting the IRE1α-XBP1 branch of the unfolded protein response in human diseases. *Semin Cancer Biol*. 2015;33:48-56.

143. Maron BJ, Ferrans VJ, Roberts WC. Ultrastructural features of degenerated cardiac muscle cells in patients with cardiac hypertrophy. *Am J Pathol*. 1975;79(3):387-434. http://www.ncbi.nlm.nih.gov/pubmed/124533. Accessed May 1, 2018.

144. Okada K -i., Minamino T, Tsukamoto Y, Liao Y, Tsukamoto O, Takashima S, et al. Prolonged Endoplasmic Reticulum Stress in Hypertrophic and Failing Heart After Aortic Constriction: Possible Contribution of Endoplasmic Reticulum Stress to Cardiac Myocyte Apoptosis. *Circulation*. 2004;110(6):705-712.

145. Minamino T, Komuro I, Kitakaze M. Endoplasmic Reticulum Stress As a Therapeutic Target in Cardiovascular Disease. *Circ Res*. 2010;107(9):1071-1082.

146. Duan Q, Ni L, Wang P, Chen C, Yang L, Ma B, et al. Deregulation of XBP1 expression contributes to myocardial vascular endothelial growth factor-A expression and angiogenesis during cardiac hypertrophy *in vivo*. *Aging Cell*. 2016;15(4):625-633.

147. Jin J-K, Blackwood EA, Azizi K, Thuerauf DJ, Fahem AG, Hofmann C, et al. ATF6 Decreases Myocardial Ischemia/Reperfusion Damage and Links ER Stress and Oxidative Stress Signaling Pathways in the HeartNovelty and Significance. *Circ Res*. 2017;120(5):862-875.

148. Prola A, Pires Da Silva J, Guilbert A, Lecru L, Piquereau J, Ribeiro M, et al. SIRT1 protects the heart from ER stress-induced cell death through eIF2α deacetylation. *Cell Death Differ*. 2017;24(2):343-356.

149. Croft A, Tay KH, Boyd SC, Guo ST, Jiang CC, Lai F, et al. Oncogenic Activation of MEK/ERK Primes Melanoma Cells for Adaptation to Endoplasmic Reticulum Stress. *J Invest Dermatol*. 2014;134(2):488-497.

150. Hart LS, Cunningham JT, Datta T, Dey S, Tameire F, Lehman SL, et al. ER stress-mediated autophagy promotes Myc-dependent transformation and tumor growth. *J Clin Invest*.

2012;122(12):4621-4634.

151. Blazanin N, Son J, Craig-Lucas AB, John CL, Breech KJ, Podolsky MA, et al. ER stress and distinct outputs of the IRE1α RNase control proliferation and senescence in response to oncogenic Ras. *Proc Natl Acad Sci U S A*. 2017;114(37):9900-9905.

152. Li X-X, Zhang H-S, Xu Y-M, Zhang R-J, Chen Y, Fan L, et al. Knockdown of IRE1α inhibits colonic tumorigenesis through decreasing β-catenin and IRE1α targeting suppresses colon cancer cells. *Oncogene*. 2017;36(48):6738-6746.

153. Logue SE, McGrath EP, Cleary P, Greene S, Mnich K, Almanza A, et al. Inhibition of IRE1 RNase activity modulates the tumor cell secretome and enhances response to chemotherapy. *Nat Commun*. 2018;9(1):3267.

154. Malzer E, Daly M-L, Moloney A, Sendall TJ, Thomas SE, Ryder E, et al. Impaired tissue growth is mediated by checkpoint kinase 1 (CHK1) in the integrated stress response. *J Cell Sci*. 2010;123(Pt 17):2892-2900.

155. Chen X, Iliopoulos D, Zhang Q, Tang Q, Greenblatt MB, Hatziapostolou M, et al. XBP1 promotes triple-negative breast cancer by controlling the HIF1α pathway. *Nature*. 2014;508(7494):103-107.

156. Rouschop KMA, van den Beucken T, Dubois L, Niessen H, Bussink J, Savelkouls K, et al. The unfolded protein response protects human tumor cells during hypoxia through regulation of the autophagy genes MAP1LC3B and ATG5. *J Clin Invest*. 2010;120(1):127-141.

157. Mahadevan NR, Rodvold J, Sepulveda H, Rossi S, Drew AF, Zanetti M. Transmission of endoplasmic reticulum stress and pro-inflammation from tumor cells to myeloid cells. *Proc Natl Acad Sci U S A*. 2011;108(16):6561-6566.

158. Cullen SJ, Fatemie S, Ladiges W. Breast tumor cells primed by endoplasmic reticulum stress remodel macrophage phenotype. *Am J Cancer Res*. 2013;3(2):196-210. http://www.ncbi.nlm.nih.gov/pubmed/23593541. Accessed November 17, 2018.

159. de Almeida SF, Fleming J V, Azevedo JE, Carmo-Fonseca M, de Sousa M. Stimulation of an unfolded protein response impairs MHC class I expression. *J Immunol*. 2007;178(6):3612-3619.

160. Granados DP, Tanguay P-L, Hardy M-P, Caron É, de Verteuil D, Meloche S, et al. ER stress affects processing of MHC class I-associated peptides. *BMC Immunol*. 2009;10(1):10.

161. Fang L, Gong J, Wang Y, Liu R, Li Z, Wang Z, et al. MICA/B expression is inhibited by unfolded protein response and associated with poor prognosis in human hepatocellular carcinoma. *J Exp*

Clin Cancer Res. 2014;33(1):76.

162. Blais JD, Addison CL, Edge R, Falls T, Zhao H, Wary K, et al. Perk-Dependent Translational Regulation Promotes Tumor Cell Adaptation and Angiogenesis in Response to Hypoxic Stress †. *Mol Cell Biol*. 2006;26(24):9517-9532.

163. Wang Y, Alam GN, Ning Y, Visioli F, Dong Z, Nör JE, et al. The Unfolded Protein Response Induces the Angiogenic Switch in Human Tumor Cells through the PERK/ATF4 Pathway. 2012.

164. Ghosh R, Lipson KL, Sargent KE, Mercurio AM, Hunt JS, Ron D, et al. Transcriptional Regulation of VEGF-A by the Unfolded Protein Response Pathway. Blagosklonny M V., ed. *PLoS One*. 2010;5(3):e9575.

165. Cuevas EP, Eraso P, Mazón MJ, Santos V, Moreno-Bueno G, Cano A, et al. LOXL2 drives epithelial-mesenchymal transition via activation of IRE1-XBP1 signalling pathway. *Sci Rep*. 2017;7(1):44988.

166. Feng Y-X, Sokol ES, Del Vecchio CA, Sanduja S, Claessen JHL, Proia TA, et al. Epithelial-to-mesenchymal transition activates PERK-eIF2α and sensitizes cells to endoplasmic reticulum stress. *Cancer Discov*. 2014;4(6):702-715.

167. Fujimoto A, Kawana K, Taguchi A, Adachi K, Sato M, Nakamura H, et al. Inhibition of endoplasmic reticulum (ER) stress sensors sensitizes cancer stem-like cells to ER stress-mediated apoptosis. *Oncotarget*. 2016;7(32):51854-51864.

168. Hanahan D, Weinberg RA. The hallmarks of cancer. *Cell*. 2000;100(1):57-70.

169. Hanahan D, Weinberg RA. Hallmarks of Cancer: The Next Generation. *Cell*. 2011;144(5):646-674.

170. Hanahan D, Folkman J. Patterns and emerging mechanisms of the angiogenic switch during tumorigenesis. *Cell*. 1996;86(3):353-364.

171. Baeriswyl V, Christofori G. The angiogenic switch in carcinogenesis. *Semin Cancer Biol*. 2009;19(5):329-337.

172. Raza A, Franklin MJ, Dudek AZ. Pericytes and vessel maturation during tumor angiogenesis and metastasis. *Am J Hematol*. 2010;85(8):593-598.

173. Zumsteg A, Christofori G. Corrupt policemen: inflammatory cells promote tumor angiogenesis. *Curr Opin Oncol*. 2009;21(1):60-70.

174. Francescone RA, Scully S, Faibish M, Taylor SL, Oh D, Moral L, et al. Role of YKL-40 in the angiogenesis, radioresistance, and progression of glioblastoma. *J Biol Chem*. 2011;286(17):15332-15343.

175. Chen Y, Gou X, Ke X, Cui H, Chen Z. Human Tumor Cells Induce Angiogenesis through Positive Feedback between CD147 and Insulin-Like Growth Factor-I. Lee T, ed. *PLoS One*. 2012;7(7):e40965.

176. Wang C, Yao H, Chen L, Jia J, Wang L, Dai J, et al. CD147 induces angiogenesis through a vascular endothelial growth factor and hypoxia-inducible transcription factor 1α-mediated pathway in rheumatoid arthritis. *Arthritis Rheum*. 2012;64(6):1818-1827.

177. Wu M, Huang C, Li X, Li X, Gan K, Chen Q, et al. LRRC4 inhibits glioblastoma cell proliferation, migration, and angiogenesis by downregulating pleiotropic cytokine expression and responses. *J Cell Physiol*. 2008;214(1):65-74.

178. Xu Y, Yuan F-E, Chen Q-X, Liu B-H. Molecular mechanisms involved in angiogenesis and potential target of antiangiogenesis in human glioblastomas. *Glioma*. 2018;1(2):35.

179. Ferrara N. Vascular Endothelial Growth Factor. *Arterioscler Thromb Vasc Biol*. 2009;29(6):789-791.

180. Gabhann F Mac, Popel AS. Systems Biology of Vascular Endothelial Growth Factors. *Microcirculation*. 2008;15(8):715-738.

181. Nagy JA, Dvorak HF. Heterogeneity of the tumor vasculature: the need for new tumor blood vessel type-specific targets. *Clin Exp Metastasis*. 2012;29(7):657-662.

182. Raica M, Cimpean AM, Ribatti D. Angiogenesis in pre-malignant conditions. *Eur J Cancer*. 2009;45(11):1924-1934.

183. Wang R, Chadalavada K, Wilshire J, Kowalik U, Hovinga KE, Geber A, et al. Glioblastoma stem-like cells give rise to tumour endothelium. *Nature*. 2010;468(7325):829-833.

184. Ricci-Vitiani L, Pallini R, Biffoni M, Todaro M, Invernici G, Cenci T, et al. Tumour vascularization via endothelial differentiation of glioblastoma stem-like cells. *Nature*. 2010;468(7325):824-828.

185. Chang YS, di Tomaso E, McDonald DM, Jones R, Jain RK, Munn LL, et al. Mosaic blood vessels in tumors: frequency of cancer cells in contact with flowing blood. *Proc Natl Acad Sci U S A*. 2000;97(26):14608-14613.

186. Das S, Marsden PA. Angiogenesis in Glioblastoma. Phimister EG, ed. *N Engl J Med*. 2013;369(16):1561-1563.

187. Wang N, Jain RK, Batchelor TT. New Directions in Anti-Angiogenic Therapy for Glioblastoma. *Neurotherapeutics*. 2017;14(2):321-332.

188. Huang X, Wong MK, Yi H, Watkins S, Laird AD, Wolf SF, et al. Combined therapy of local and metastatic 4T1 breast tumor in mice using SU6668, an inhibitor of angiogenic receptor tyrosine kinases, and the immunostimulator B7.2-IgG fusion protein. *Cancer Res*. 2002;62(20):5727-5735.

189. Shojaei F, Wu X, Qu X, Kowanetz M, Yu L, Tan M, et al. G-CSF-initiated myeloid cell mobilization and angiogenesis mediate tumor refractoriness to anti-VEGF therapy in mouse models. *Proc Natl Acad Sci U S A*. 2009;106(16):6742-6747.

190. Chung AS, Wu X, Zhuang G, Ngu H, Kasman I, Zhang J, et al. An interleukin-17–mediated paracrine network promotes tumor resistance to anti-angiogenic therapy. *Nat Med*. 2013;19(9):1114-1123.

191. Young SD, Tamburini PP. Enzymatic peptidyl .alpha.-amidation proceeds through formation of an .alpha.-hydroxyglycine intermediate. *J Am Chem Soc*. 1989;111(5):1933-1934.

192. Katopodis AG, Ping D, May SW. *Biochemistry © A Novel Enzyme from Bovine Neurointermediate Pituitary Catalyzes Dealkylation of A-Hydroxyglycine Derivatives, Thereby Functioning Sequentially with Peptidylglycine-Amidating Monooxygenase in Peptide Amidation*. https://pubs.acs.org/sharingguidelines. Accessed November 6, 2018.

193. Perkins SN, Husten EJ, Eipper BA. The 108-kDa peptidylglycine α-amidating monooxygenase precursor contains two separable enzymatic activities involved in peptide amidation. *Biochem Biophys Res Commun*. 1990;171(3):926-932.

194. Bundgaard H, Kahns AH. Chemical stability and plasma-catalyzed dealkylation of peptidyl-α-hydroxyglycine derivatives—Intermediates in peptide α-amidation. *Peptides*. 1991;12(4):745-748.

195. Eippers BA, Perkinsg SN, Husten EJ, Johnson RC, Keutmannll HT, Mains RE. *THE JOURNAL OF BIOLOGICAL CHEMISTRY Peptidyl-a-Hydroxyglycine a-Amidating Lyase PURIFICATION, CHARACTERIZATION, AND EXPRESSION**. Vol 266.; 1991. http://www.jbc.org/content/266/12/7827.full.pdf. Accessed November 19, 2018.

196. Prigge ST, Kolhekar AS, Eipper BA, Mains RE, Amzel LM. Amidation of bioactive peptides: the structure of peptidylglycine alpha-hydroxylating monooxygenase. *Science*. 1997;278(5341):1300-

1305.

197. Prigge ST. Dioxygen Binds End-On to Mononuclear Copper in a Precatalytic Enzyme Complex. *Science (80-)*. 2004;304(5672):864-867.

198. Chufán EE, De M, Eipper BA, Mains RE, Amzel LM. Amidation of Bioactive Peptides: The Structure of the Lyase Domain of the Amidating Enzyme. *Structure*. 2009;17(7):965-973.

199. Kumar D, Mains RE, Eipper BA. 60 YEARS OF POMC: From POMC and α-MSH to PAM, molecular oxygen, copper, and vitamin C. *J Mol Endocrinol*. 2016;56(4):T63-76.

200. Schafer MK, Stoffers DA, Eipper BA, Watson SJ. Expression of peptidylglycine alpha-amidating monooxygenase (EC 1.14.17.3) in the rat central nervous system. *J Neurosci*. 1992;12(1):222-234.

201. Oldham CD, Li C, Girard PR, Nerem RM, May SW. Peptide amidating enzymes are present in cultured endothelial cells. *Biochem Biophys Res Commun*. 1992;184(1):323-329.

202. MAINS RE, MYERS AC, EIPPER BA. Hormonal, Drug, and Dietary Factors Affecting Peptidyl Glycine *α* -Amidating Monooxygenase Activity in Various Tissues of the Adult Male Rat*. *Endocrinology*. 1985;116(6):2505-2515.

203. Wand GS, Ney RL, Mains RE, Eipper BA. Characterization of peptide alpha-amidation activity in human cerebrospinal fluid and central nervous system tissue. *Neuroendocrinology*. 1985;41(6):482-489.

204. Rajagopal C, Stone KL, Francone VP, Mains RE, Eipper BA. Secretory granule to the nucleus: role of a multiply phosphorylated intrinsically unstructured domain. *J Biol Chem*. 2009;284(38):25723-25734.

205. Alam MR, Caldwell BD, Johnson RC, Darlington DN, Mains RE, Eipper BA. Novel proteins that interact with the COOH-terminal cytosolic routing determinants of an integral membrane peptide-processing enzyme. *J Biol Chem*. 1996;271(45):28636-28640.

206. Lee C-M, Yang P, Chen L-C, Chen C-C, Wu S-C, Cheng H-Y, et al. A Novel Role of RASSF9 in Maintaining Epidermal Homeostasis. Beier F, ed. *PLoS One*. 2011;6(3):e17867.

207. Bonnemaison ML, Bäck N, Duffy ME, Ralle M, Mains RE, Eipper BA. Adaptor Protein-1 Complex Affects the Endocytic Trafficking and Function of Peptidylglycine α-Amidating Monooxygenase, a Luminal Cuproenzyme. *J Biol Chem*. 2015;290(35):21264-21279.

208. Rajagopal C, Mains RE, Eipper BA. Signaling from the secretory granule to the nucleus. *Crit Rev Biochem Mol Biol*. 2012;47(4):391-406.

209. Francone VP, Ifrim MF, Rajagopal C, Leddy CJ, Wang Y, Carson JH, et al. Signaling from the Secretory Granule to the Nucleus: Uhmk1 and PAM. *Mol Endocrinol*. 2010;24(8):1543-1558.

210. Czyzyk TA, Ning Y, Hsu M-S, Peng B, Mains RE, Eipper BA, et al. Deletion of peptide amidation enzymatic activity leads to edema and embryonic lethality in the mouse. *Dev Biol*. 2005;287(2):301-313.

211. Bousquet-Moore D, Prohaska JR, Nillni EA, Czyzyk T, Wetsel WC, Mains RE, et al. Interactions of peptide amidation and copper: Novel biomarkers and mechanisms of neural dysfunction. *Neurobiol Dis*. 2010;37(1):130-140.

212. Bousquet-Moore D, Ma XM, Nillni EA, Czyzyk TA, Pintar JE, Eipper BA, et al. Reversal of Physiological Deficits Caused by Diminished Levels of Peptidylglycine α-Amidating Monooxygenase by Dietary Copper. *Endocrinology*. 2009;150(4):1739-1747.

213. Simpson PD, Eipper BA, Katz MJ, Gandara L, Wappner P, Fischer R, et al. Striking Oxygen Sensitivity of the Peptidylglycine α-Amidating Monooxygenase (PAM) in Neuroendocrine Cells. *J Biol Chem*. 2015;290(41):24891-24901.

214. Vishwanatha K, Bäck N, Mains RE, Eipper BA. A histidine-rich linker region in peptidylglycine α-amidating monooxygenase has the properties of a pH sensor. *J Biol Chem*. 2014;289(18):12404-12420.

215. Trendel JA, Ellis N, Sarver JG, Klis WA, Dhananjeyan M, Bykowski CA, et al. Catalytically Active Peptidylglycine α-Amidating Monooxygenase in the Media of Androgen-Independent Prostate Cancer Cell Lines. *J Biomol Screen*. 2008;13(8):804-809.

216. Du J, Keegan BP, North WG. Key peptide processing enzymes are expressed by breast cancer cells. *Cancer Lett*. 2001;165(2):211-218.

217. Ouafik L, Sauze S, Boudouresque F, Chinot O, Delfino C, Fina F, et al. Neutralization of Adrenomedullin Inhibits the Growth of Human Glioblastoma Cell Lines in Vitro and Suppresses Tumor Xenograft Growth in Vivo. *Am J Pathol*. 2002;160(4):1279-1292.

218. Vos MD, Scott FM, Iwai N, Treston AM. Expression in human lung cancer cell lines of genes of prohormone processing and the neuroendocine phenotype. *J Cell Biochem*. 1996;63(S24):257-268.

219. Stepan VM, Sawada M, Todisco A, Dickinson CJ. Glycine-extended gastrin exerts growth-promoting effects on human colon cancer cells. *Mol Med*. 1999;5(3):147-159. http://www.ncbi.nlm.nih.gov/pubmed/10404512. Accessed November 19, 2018.

220. Singh P, Xu Z, Dai B, Rajaraman S, Rubin N, Dhruva B. Incomplete processing of progastrin expressed by human colon cancer cells: role of noncarboxyamidated gastrins. *Am J Physiol*. 1994;266(3 Pt 1):G459-68.

221. Smith AM, Watson SA. Gastrin and Colorectal Cancer. *Aliment Pharmacol Ther*. 2000;14(10):1231-1247.

222. Steel JH, Mart[illegible]nez A, Springall DR, Treston AM, Cuttitta F, Polak JM. Peptidylglycine ?-amidating monooxygenase (PAM) immunoreactivity and messenger RNA in human pituitary and increased expression in pituitary tumours. *Cell Tissue Res*. 1994;276(1):197-207.

223. Burkhart JM, Schumbrutzki C, Wortelkamp S, Sickmann A, Zahedi RP. Systematic and quantitative comparison of digest efficiency and specificity reveals the impact of trypsin quality on MS-based proteomics. *J Proteomics*. 2012;75(4):1454-1462.

224. Craig R, Beavis RC. TANDEM: matching proteins with tandem mass spectra. *Bioinformatics*. 2004;20(9):1466-1467.

225. Vaudel M, Barsnes H, Berven FS, Sickmann A, Martens L. SearchGUI: An open-source graphical user interface for simultaneous OMSSA and X!Tandem searches. *Proteomics*. 2011;11(5):996-999.

226. Vaudel M, Burkhart JM, Zahedi RP, Oveland E, Berven FS, Sickmann A, et al. PeptideShaker enables reanalysis of MS-derived proteomics data sets. *Nat Biotechnol*. 2015;33(1):22-24.

227. Perez-Riverol Y, Csordas A, Bai J, Bernal-Llinares M, Hewapathirana S, Kundu DJ, et al. The PRIDE database and related tools and resources in 2019: improving support for quantification data. *Nucleic Acids Res*. 2019;47(D1):D442-D450.

228. Kolhekar AS, Mains RE, Eipper BA. [5] Peptidylglycine α-amidating monooxygenase: An ascorbate-requiring enzyme. *Methods Enzymol*. 1997;279:35-43.

229. Kent WJ, Sugnet CW, Furey TS, Roskin KM, Pringle TH, Zahler AM, et al. The human genome browser at UCSC. *Genome Res*. 2002;12(6):996-1006.

230. Khan A, Fornes O, Stigliani A, Gheorghe M, Castro-Mondragon JA, van der Lee R, et al. JASPAR 2018: update of the open-access database of transcription factor binding profiles and its web

framework. *Nucleic Acids Res*. 2018;46(D1):D260-D266.

231. Grassi E, Zapparoli E, Molineris I, Provero P. Total Binding Affinity Profiles of Regulatory Regions Predict Transcription Factor Binding and Gene Expression in Human Cells. Aerts S, ed. *PLoS One*. 2015;10(11):e0143627.

232. DeCicco-Skinner KL, Henry GH, Cataisson C, Tabib T, Gwilliam JC, Watson NJ, et al. Endothelial cell tube formation assay for the in vitro study of angiogenesis. *J Vis Exp*. 2014;(91):e51312.

233. Brennan CW, Verhaak RGW, McKenna A, Campos B, Noushmehr H, Salama SR, et al. The Somatic Genomic Landscape of Glioblastoma. *Cell*. 2013;155(2):462-477.

234. Kim H, Bhattacharya A, Qi L. Endoplasmic reticulum quality control in cancer: Friend or foe. *Semin Cancer Biol*. 2015;33:25-33.

235. Sandoval MV, Fluegen G, Staschke KA, Calvo-Vidal V, Aguirre-Ghiso JA. Abstract A45: PERK-Inhibition as a possible therapy for hypoxia-induced solitary dormant tumor cells. *Cancer Res*. 2016;76(7 Supplement):A45-A45.

236. Karali E, Bellou S, Stellas D, Klinakis A, Murphy C, Fotsis T. Article VEGF Signals through ATF6 and PERK to Promote Endothelial Cell Survival and Angiogenesis in the Absence of ER Stress. 2014.

237. Zong Z-H, Du Z-X, Zhang H-Y, Li C, An M-X, Li S, et al. Involvement of Nrf2 in proteasome inhibition-mediated induction of ORP150 in thyroid cancer cells. *Oncotarget*. 2016;7(3):3416-3426.

238. Hurwitz H, Fehrenbacher L, Novotny W, Cartwright T, Hainsworth J, Heim W, et al. Bevacizumab plus Irinotecan, Fluorouracil, and Leucovorin for Metastatic Colorectal Cancer. *N Engl J Med*. 2004;350(23):2335-2342.

239. Sandler A, Gray R, Perry MC, Brahmer J, Schiller JH, Dowlati A, et al. Paclitaxel–Carboplatin Alone or with Bevacizumab for Non–Small-Cell Lung Cancer. *N Engl J Med*. 2006;355(24):2542-2550.

240. Miller K, Wang M, Gralow J, Dickler M, Cobleigh M, Perez EA, et al. Paclitaxel plus Bevacizumab versus Paclitaxel Alone for Metastatic Breast Cancer. *N Engl J Med*. 2007;357(26):2666-2676.

241. Taal W, Oosterkamp HM, Walenkamp AME, Dubbink HJ, Beerepoot L V, Hanse MCJ, et al. Single-agent bevacizumab or lomustine versus a combination of bevacizumab plus lomustine in patients with recurrent glioblastoma (BELOB trial): a randomised controlled phase 2 trial. *Lancet Oncol*. 2014;15(9):943-953.

242. Sitohy B, Nagy JA, Jaminet S-CS, Dvorak HF. Tumor-Surrogate Blood Vessel Subtypes Exhibit Differential Susceptibility to Anti-VEGF Therapy. *Cancer Res*. 2011;71(22):7021-7028.

243. Shojaei F, Wu X, Zhong C, Yu L, Liang X-H, Yao J, et al. Bv8 regulates myeloid-cell-dependent tumour angiogenesis. *Nature*. 2007;450(7171):825-831.

244. Casanovas O, Hicklin DJ, Bergers G, Hanahan D. Drug resistance by evasion of antiangiogenic targeting of VEGF signaling in late-stage pancreatic islet tumors. *Cancer Cell*. 2005;8(4):299-309.

245. De Groot JF, Piao Y, Tran H, Gilbert M, Wu H-K, Liu J, et al. Myeloid Biomarkers Associated with Glioblastoma Response to Anti-Vascular Endothelial Growth Factor Therapy with Aflibercept. 2011.

246. Yang L, DeBusk LM, Fukuda K, Fingleton B, Green-Jarvis B, Shyr Y, et al. Expansion of myeloid immune suppressor Gr+CD11b+ cells in tumor-bearing host directly promotes tumor angiogenesis. *Cancer Cell*. 2004;6(4):409-421.

247. Piao Y, Liang J, Holmes L, Henry V, Sulman E, de Groot JF. Acquired resistance to anti-VEGF therapy in glioblastoma is associated with a mesenchymal transition. *Clin Cancer Res*. 2013;19(16):4392-4403.

248. Du R, Lu K V., Petritsch C, Liu P, Ganss R, Passegué E, et al. HIF1α Induces the Recruitment of Bone Marrow-Derived Vascular Modulatory Cells to Regulate Tumor Angiogenesis and Invasion. *Cancer Cell*. 2008;13(3):206-220.

249. Walter P, Ron D. The unfolded protein response: from stress pathway to homeostatic regulation. *Science*. 2011;334(6059):1081-1086.

250. Korennykh A V, Egea PF, Korostelev AA, Finer-Moore J, Zhang C, Shokat KM, et al. The unfolded protein response signals through high-order assembly of Ire1. *Nature*. 2009;457(7230):687-693.

251. Romero-Ramirez L, Cao H, Nelson D, Hammond E, Lee A-H, Yoshida H, et al. XBP1 is essential for survival under hypoxic conditions and is required for tumor growth. *Cancer Res*. 2004;64(17):5943-5947.

252. Tam AB, Koong AC, Niwa M. Ire1 Has Distinct Catalytic Mechanisms for XBP1/HAC1 Splicing and RIDD. *Cell Rep*. 2014;9(3):850-858.

253. Auf G, Jabouille A, Guérit S, Pineau R, Delugin M, Bouchecareilh M, et al. Inositol-requiring enzyme 1alpha is a key regulator of angiogenesis and invasion in malignant glioma. *Proc Natl Acad Sci U S A*. 2010;107(35):15553-15558.

254. Nishitoh H, Matsuzawa A, Tobiume K, Saegusa K, Takeda K, Inoue K, et al. ASK1 is essential for endoplasmic reticulum stress-induced neuronal cell death triggered by expanded polyglutamine repeats. *Genes Dev*. 2002;16(11):1345-1355.

255. Lu G, Ota A, Ren S, Franklin S, Rau CD, Ping P, et al. PPM1l encodes an inositol requiring-protein 1 (IRE1) specific phosphatase that regulates the functional outcome of the ER stress response. *Mol Metab*. 2013;2(4):405-416.

256. Wu J, Kaufman RJ. From acute ER stress to physiological roles of the Unfolded Protein Response. *Cell Death Differ*. 2006;13(3):374-384.

257. Novoa I, Zeng H, Harding HP, Ron D. Feedback inhibition of the unfolded protein response by GADD34-mediated dephosphorylation of eIF2alpha. *J Cell Biol*. 2001;153(5):1011-1022.

258. So J-S, Cho S, Min S-H, Kimball SR, Lee A-H. lRE1α-Dependent Decay of CReP/Ppp1r15b mRNA Increases Eukaryotic Initiation Factor 2α Phosphorylation and Suppresses Protein Synthesis. *Mol Cell Biol*. 2015;35(16):2761-2770.

259. Rutkowski DT, Arnold SM, Miller CN, Wu J, Li J, Gunnison KM, et al. Adaptation to ER Stress Is Mediated by Differential Stabilities of Pro-Survival and Pro-Apoptotic mRNAs and Proteins. Weissman JS, ed. *PLoS Biol*. 2006;4(11):e374.

260. Minchenko DO, Danilovskyi S V., Kryvdiuk I V., Bakalets T V., Lypova NM, Karbovskyi LL, et al. Inhibition of ERN1 modifies the hypoxic regulation of the expression of TP53-related genes in U87 glioma cells. *Endoplasmic Reticulum Stress Dis*. 2014;1(1):18-26.

261. Auf G, Jabouille A, Guerit S, Pineau R, Delugin M, Bouchecareilh M, et al. Inositol-requiring enzyme 1 is a key regulator of angiogenesis and invasion in malignant glioma. *Proc Natl Acad Sci*. 2010;107(35):15553-15558.

262. Dejeans N, Manié S, Hetz C, Bard F, Hupp T, Agostinis P, et al. Addicted to secrete – novel concepts and targets in cancer therapy. *Trends Mol Med*. 2014;20(5):242-250.

263. Garg AD, Krysko D V, Verfaillie T, Kaczmarek A, Ferreira GB, Marysael T, et al. A novel pathway combining calreticulin exposure and ATP secretion in immunogenic cancer cell death. *EMBO J*. 2012;31:1062-1079.

264. Luo B, Lee AS. The critical roles of endoplasmic reticulum chaperones and unfolded protein response in tumorigenesis and anticancer therapies. *Oncogene*. 2013;32(7):805-818.

265. Panaretakis T, Kepp O, Brockmeier U, Tesniere A, Bjorklund A-C, Chapman DC, et al.

Mechanisms of pre-apoptotic calreticulin exposure in immunogenic cell death. *EMBO J*. 2009;28(5):578-590.

266. Nakagawa H, Umemura A, Taniguchi K, Font-Burgada J, Dhar D, Ogata H, et al. ER Stress Cooperates with Hypernutrition to Trigger TNF-Dependent Spontaneous HCC Development. *Cancer Cell*. 2014;26(3):331-343.

267. Kroemer G, Galluzzi L, Kepp O, Zitvogel L. Immunogenic Cell Death in Cancer Therapy. *Annu Rev Immunol*. 2013;31(1):51-72.

268. Wang Y, Alam GN, Ning Y, Visioli F, Dong Z, Nor JE, et al. The Unfolded Protein Response Induces the Angiogenic Switch in Human Tumor Cells through the PERK/ATF4 Pathway. *Cancer Res*. 2012;72(20):5396-5406.

269. Ciccotosto GD, Schiller MR, Eipper BA, Mains RE. Induction of integral membrane PAM expression in AtT-20 cells alters the storage and trafficking of POMC and PC1. *J Cell Biol*. 1999;144(3):459-471.

270. Schiller MR, Mains RE, Eipper BA. A Novel Neuroendocrine Intracellular Signaling Pathway. *Mol Endocrinol*. 1997;11(12):1846-1857.

271. Francone VP, Ifrim MF, Rajagopal C, Leddy CJ, Wang Y, Carson JH, et al. Signaling from the Secretory Granule to the Nucleus: Uhmk1 and PAM. *Mol Endocrinol*. 2010;24(8):1543-1558.

272. Mains RE, Alam MR, Johnson RC, Darlington DN, Bäck N, Hand TA, et al. Kalirin, a multifunctional PAM COOH-terminal domain interactor protein, affects cytoskeletal organization and ACTH secretion from AtT-20 cells. *J Biol Chem*. 1999;274(5):2929-2937.

273. Rajagopal C, Stone KL, Francone VP, Mains RE, Eipper BA. Secretory granule to the nucleus: role of a multiply phosphorylated intrinsically unstructured domain. *J Biol Chem*. 2009;284(38):25723-25734.

274. Steveson TC, Zhao GC, Keutmann HT, Mains RE, Eipper BA. Access of a membrane protein to secretory granules is facilitated by phosphorylation. *J Biol Chem*. 2001;276(43):40326-40337.

275. Arnaoutova I, Cawley NX, Patel N, Kim T, Rathod T, Loh YP. Aquaporin 1 Is Important for Maintaining Secretory Granule Biogenesis in Endocrine Cells. *Mol Endocrinol*. 2008;22(8):1924-1934.

276. Bäck N, Litonius E, Mains RE, Eipper BA. Fluoride causes reversible dispersal of Golgi cisternae and matrix in neuroendocrine cells. *Eur J Cell Biol*. 2004;83(8):389-402.

277. Mains RE, Bloomquist BT, Eipper BA. Manipulation of Neuropeptide Biosynthesis through the Expression of Antisense RNA for Peptidylglycine α-Amidating Monooxygenase. *Mol Endocrinol*. 1991;5(2):187-193.

278. Tomita Y, Dorward H, Yool A, Smith E, Townsend A, Price T, et al. Role of Aquaporin 1 Signalling in Cancer Development and Progression. *Int J Mol Sci*. 2017;18(2):299.

279. Yao Z, Yang C, Ma L, Tan Y. Abstract 5075: Hedgehog Pathway Transcription Factor Gli1 Promotes Glioma Invasiveness through Up-regulating Aquaporin 1. *Cancer Res*. 2016;76(14 Supplement):5075-5075.

280. Mains RE, Blaby-Haas C, Rheaume BA, Eipper BA. Changes in Corticotrope Gene Expression Upon Increased Expression of Peptidylglycine α-Amidating Monooxygenase. *Endocrinology*. 2018;159(7):2621-2639.

281. Harding HP, Zhang Y, Ron D. Protein translation and folding are coupled by an endoplasmic-reticulum-resident kinase. *Nature*. 1999;397(6716):271-274.

282. Sonenberg N, Hinnebusch AG. Regulation of Translation Initiation in Eukaryotes: Mechanisms and Biological Targets. *Cell*. 2009;136(4):731-745.

283. Zimmermann K, Baldinger J, Mayerhofer B, Atanasov AG, Dirsch VM, Heiss EH. Activated AMPK boosts the Nrf2/HO-1 signaling axis—A role for the unfolded protein response. *Free Radic Biol Med*. 2015;88:417-426.

284. Machida K, Kalra VK, Yeligar SM. ETHANOL INDUCED HO-1 AND NQO1 ARE DIFFERENTIALLY REGULATED BY HIF-1α AND NRF2 TO ATTENUATE INFLAMMATORY CYTOKINES EXPRESSION* Yeligar. 2010.

285. Verfaillie T, Rubio N, Garg AD, Bultynck G, Rizzuto R, Decuypere J-P, et al. PERK is required at the ER-mitochondrial contact sites to convey apoptosis after ROS-based ER stress. *Cell Death Differ*. 2012;19(11):1880-1891.

286. Verhaak RGW, Hoadley KA, Purdom E, Wang V, Qi Y, Wilkerson MD, et al. Integrated Genomic Analysis Identifies Clinically Relevant Subtypes of Glioblastoma Characterized by Abnormalities in PDGFRA, IDH1, EGFR, and NF1. *Cancer Cell*. 2010;17(1):98-110.

287. Ahn S-H, Park H, Ahn Y-H, Kim S, Cho M-S, Kang JL, et al. Necrotic cells influence migration and invasion of glioblastoma via NF-κB/AP-1-mediated IL-8 regulation. *Sci Rep*. 2016;6(1):24552.

288. Lu J, Zhang ZL, Huang D, Tang N, Li Y, Peng Z, et al. Cdk3-promoted epithelial-mesenchymal

transition through activating AP-1 is involved in colorectal cancer metastasis. *Oncotarget*. 2016;7(6):7012-7028.

289. Laderoute KR, Calaoagan JM, Gustafson-Brown C, Knapp AM, Li G-C, Mendonca HL, et al. The response of c-jun/AP-1 to chronic hypoxia is hypoxia-inducible factor 1 alpha dependent. *Mol Cell Biol*. 2002;22(8):2515-2523.

290. Steveson TC, Ciccotosto GD, Ma X-M, Mueller GP, Mains RE, Eipper BA. Menkes Protein Contributes to the Function of Peptidylglycine α-Amidating Monooxygenase. *Endocrinology*. 2003;144(1):188-200.

291. Gonzalez H, Ottervald J, Nilsson KC, Sjögren N, Miliotis T, Von Bahr H, et al. Identification of novel candidate protein biomarkers for the post-polio syndrome — Implications for diagnosis, neurodegeneration and neuroinflammation. *J Proteomics*. 2009;71(6):670-681.

292. Deville J-L, Salas S, Figarella-Branger D, Ouafik L, Daniel L. Adrenomedullin as a therapeutic target in angiogenesis. *Expert Opin Ther Targets*. 2010;14(10):1059-1072.

293. Consonni A, Morara S, Codazzi F, Grohovaz F, Zacchetti D. Inhibition of lipopolysaccharide-induced microglia activation by calcitonin gene related peptide and adrenomedullin. *Mol Cell Neurosci*. 2011;48(2):151-160.

294. Czyzyk TA, Ning Y, Hsu M-S, Peng B, Mains RE, Eipper BA, et al. Deletion of peptide amidation enzymatic activity leads to edema and embryonic lethality in the mouse. *Dev Biol*. 2005;287(2):301-313.

295. Rojas-Rivera D, Delvaeye T, Roelandt R, Nerinckx W, Augustyns K, Vandenabeele P, et al. When PERK inhibitors turn out to be new potent RIPK1 inhibitors: critical issues on the specificity and use of GSK2606414 and GSK2656157. *Cell Death Differ*. 2017;24(6):1100-1110.

296. Gravendeel LAM, Kouwenhoven MCM, Gevaert O, de Rooi JJ, Stubbs AP, Duijm JE, et al. Intrinsic gene expression profiles of gliomas are a better predictor of survival than histology. *Cancer Res*. 2009;69(23):9065-9072.

297. Dong X, Stothard P, Forsythe IJ, Wishart DS. PlasMapper: a web server for drawing and auto-annotating plasmid maps. *Nucleic Acids Res*. 2004;32(Web Server):W660-W664.

6. Publications

1. PERK-mediated expression of peptidylglycine α-amidating monooxygenase supports angiogenesis in glioblastoma. **Himanshu Soni**, Julia Bode, Chi D L Nguyen, Laura Puccio, Michelle Neßling, Rosario M. Piro, Jonas Bub, Emma Phillips, Robert Ahrends, Betty A. Eipper, Björn Tews & Violaine Goidts. *Oncogene*, 2019, **Under submission**

2. RhoA regulates translation of the Nogo-A decoy SPARC in white matter-invading glioblastomas. Peter Wirthschaft, Julia Bode*, **Himanshu Soni***, Fabio Dietrich, Thomas Krüwel, Christiane B. Knobbe-Thomsen, Giulia Rossetti, Andreas Hentschel, Norman Mack, Kai Schönig, Michael O. Breckwoldt, André Schmandke, Stefan Pusch, Jan Medenbach, Martin Bendszus, Martin E. Schwab, Andreas von Deimling, Marcel Kool, Christel Herold-Mende, Guido Reifenberger, Robert Ahrends, Bjoern Tews. *Acta Neuropathologica* 2019*,* **Accepted**. *Shared Authorship

3. Induction of ER and mitochondrial stress by the alkylphosphocholine erufosine in oral squamous cell carcinoma cells. Ansari, Shariq S., Ashwini K. Sharma, **Himanshu Soni**, Doaa M. Ali, Björn Tews, Rainer König, Hansjörg Eibl, and Martin R. Berger. *Cell death & disease* 9, no. 3 (2018): 296.

4. Anti-folate resistance induced by unfolded protein response mediated metabolic reprogramming. Stefan Reich, Chi DL Nguyen, Canan Has, Dominik Conrad, Sascha Steltgens, **Himanshu Soni**, Christiane B Knobbe-Thomsen, Björn Tews, Grischa Toedt, Robert Ahrends, and Jan Medenbach. *Cell Metabolism*, 2019, **Under submission**

7. Appendix

Plasmid maps (mapped using PlasMapper Version 2.0[297])

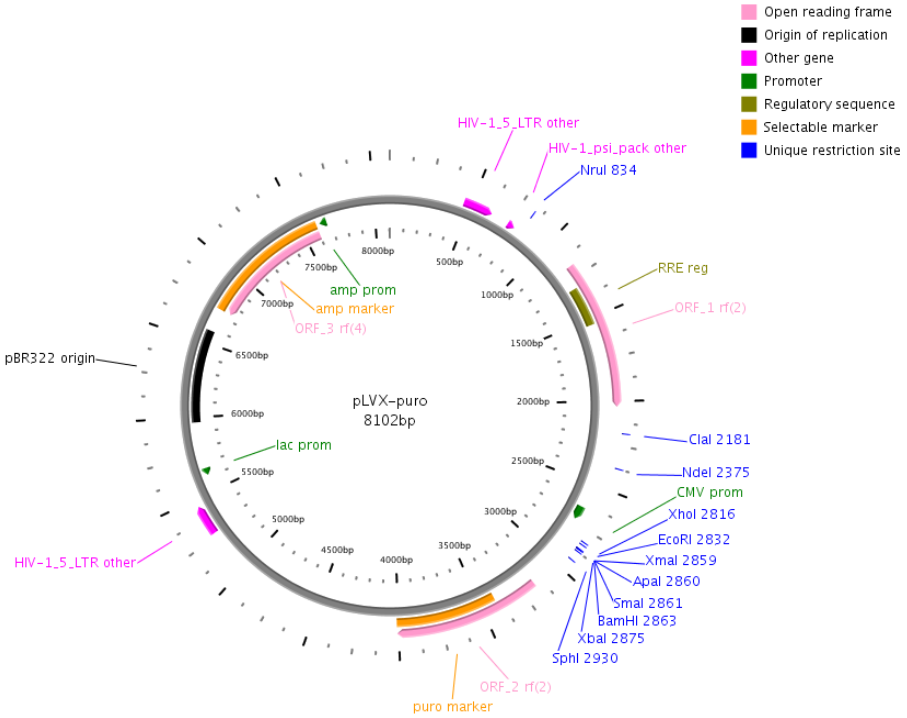

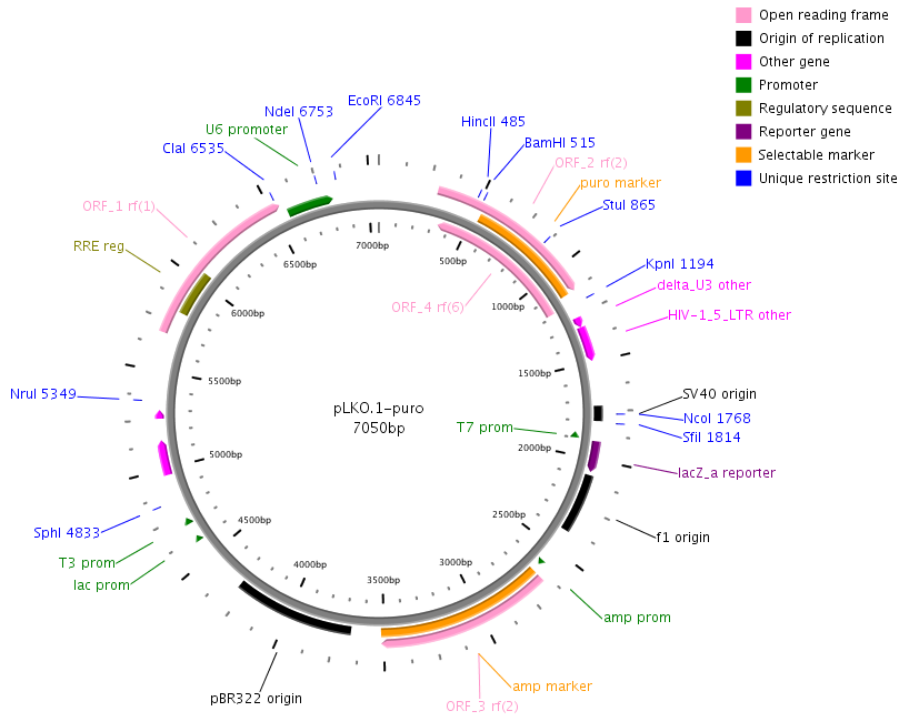

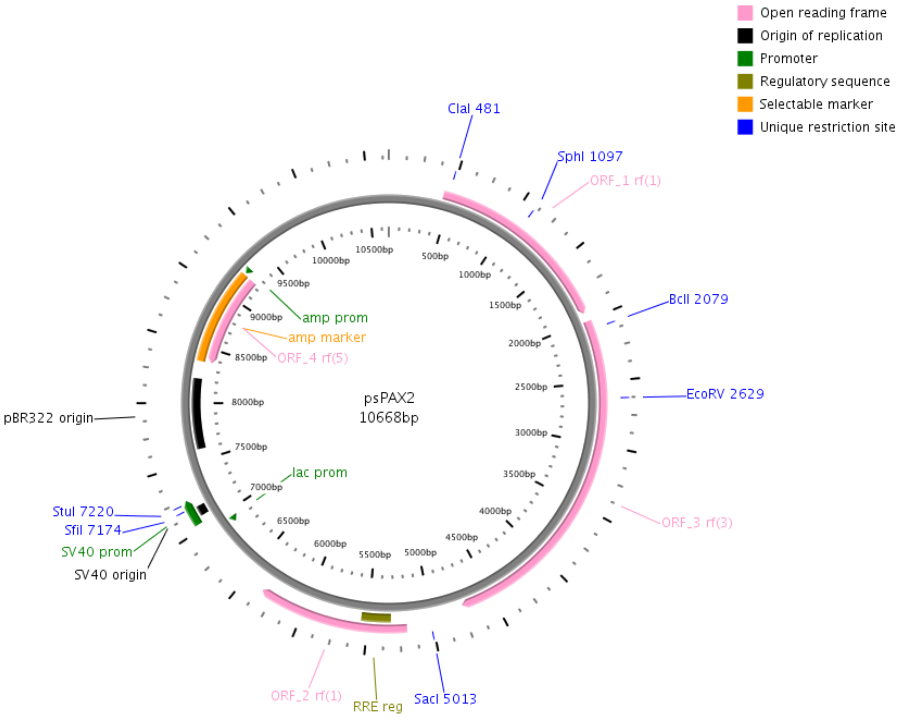
Open reading frame
Origin of replication
Promoter
Regulatory sequence
Selectable marker
Unique restriction site
ClaI 481
SphI 1097
ORF_1 rf(1)
BclI 2079
EcoRV 2629
ORF_3 rf(3)
SacI 5013
RRE reg
ORF_2 rf(1)
pBR322 origin
StuI 7220
SfiI 7174
SV40 prom
SV40 origin
amp prom
amp marker
ORF_4 rf(5)
lac prom
psPAX2
10668bp

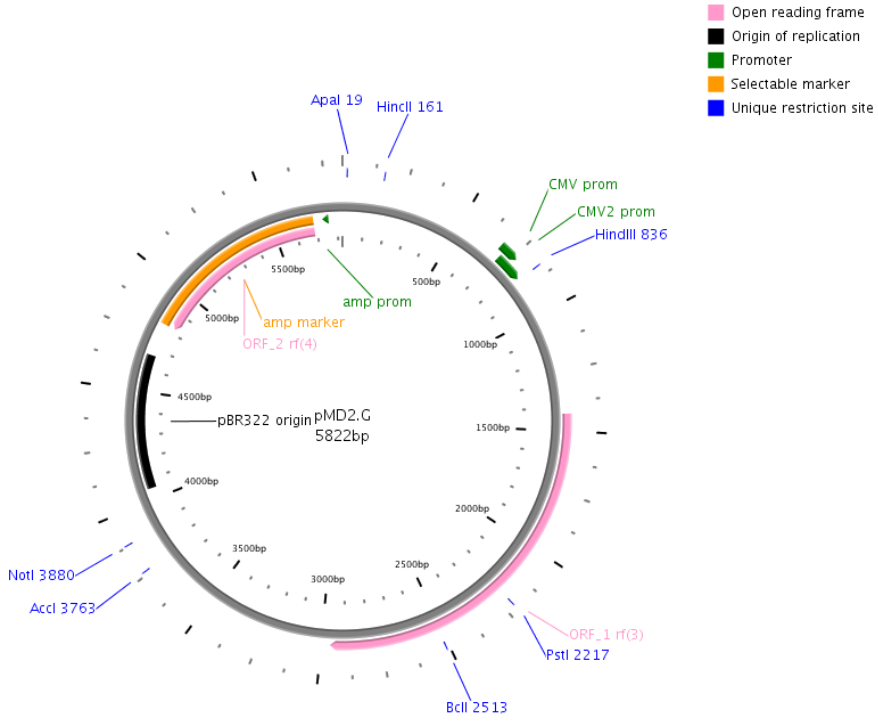
Open reading frame
Origin of replication
Promoter
Selectable marker
Unique restriction site
ApaI 19
HincII 161
CMV prom
CMV2 prom
HindIII 836
ORF_1 rf(3)
PstI 2217
BclI 2513
NotI 3880
AccI 3763
pBR322 origin
amp prom
amp marker
ORF_2 rf(4)
pMD2.G
5822bp

8. Acknowledgements

First, I would like to thank Dr. Björn Tews for providing me the opportunity to follow the project, all the fruitful discussions, supervision and opportunity to have collaborations throughout the PhD duration.

I would like to express my uttermost gratitude to Dr. Violaine Goidts for accepting me and this project. I also appreciate her guidance, continuous motivation and scientific mentorship during this period. I can't thank her enough for the tremendous support and help. I would like to thank Dr. Lindsay Murrells and the DKFZ Graduate School for their constant help, concern and support, especially during the final phase of the thesis.

I would like to thank Dr. Betty A. Eipper for providing scientific insights regarding PAM, and collaborative work for the project. I would like to thank Dr. Robert Ahrends and Chi D. L. Nguyen, for the great collaboration and assistance for the PERK-PAM project and for the SUPR-G consortium. I would also like to thank Dr. Michelle Neßling and the EM core facility for providing electron microscopy support and Dr. Rosario M. Piro for guiding me through the bioinformatics part of the thesis.

I would like to express my gratitude to Prof. Karsten Rippe for being my first supervisor and part of my Thesis Advisory Committee (TAC). I would also like to express my gratitude to Prof. Alwin Kramer, Dr. Jan Medenbach for guiding me through my PhD thesis with scientific advice.

I would like to acknowledge the TCGA Research Network (https://www.cancer.gov/tcga) for providing clinical data to support the PhD project.

I would like to appreciate the effort of Dr. Julia Bode in performing the *in vivo* part of the project. I would like to thank both Laura Puccio and Frederic Bethke for providing highly supportive technical assistance.

The thesis duration also included amazing fruitful scientific discussions with Peter Wirthschaft, Aishwarya Iyer Bierhoff, Rakesh Sharma and Emma Phillips for which I am very grateful.

I would like thank Ashik Ahmed Abdul Pari and Shariq Ansari for the scientific help and nice times. I would like to appreciate Tolga Lokumcu, Mona Göttmann, Obada Alhalabi as well as members of V077, B060/B062 divisions for all the nice times we had together.

Importantly, my time at the DKFZ has been even more fun with Marta Fratini, Lavinia Arseni, Deepti Talwar, Rakesh Sharma, Pranav Shah, Markus Mukenhirn, Marie Groth, Britta Stolze. I would like to thank them for letting me have some of the best moments from this whole phase.

Last but not least, my family has always been there to provide me with emotional support through all ups and downs during this time. I would like to thank them for being there for me.